



Pacific Northwest
NATIONAL LABORATORY

Proudly Operated by Battelle Since 1965

Effluent Management Facility Evaporator Bottoms: Waste Streams Formulation and Waste Form Qualification Testing

July 2018

SA Saslow
W Um
RL Russell
B Williams
RM Asmussen

T Varga
O Qafoku
B Riley
A Lawter
M Snyder

S Baum
I Leavy

DISCLAIMER

This report was prepared as an account of work sponsored by an agency of the United States Government. Neither the United States Government nor any agency thereof, nor Battelle Memorial Institute, nor any of their employees, makes **any warranty, express or implied, or assumes any legal liability or responsibility for the accuracy, completeness, or usefulness of any information, apparatus, product, or process disclosed, or represents that its use would not infringe privately owned rights.** Reference herein to any specific commercial product, process, or service by trade name, trademark, manufacturer, or otherwise does not necessarily constitute or imply its endorsement, recommendation, or favoring by the United States Government or any agency thereof, or Battelle Memorial Institute. The views and opinions of authors expressed herein do not necessarily state or reflect those of the United States Government or any agency thereof.

PACIFIC NORTHWEST NATIONAL LABORATORY
operated by
BATTELLE
for the
UNITED STATES DEPARTMENT OF ENERGY
under Contract DE-AC05-76RL01830

Printed in the United States of America

Available to DOE and DOE contractors from the
Office of Scientific and Technical Information,
P.O. Box 62, Oak Ridge, TN 37831-0062;
ph: (865) 576-8401
fax: (865) 576-5728
email: reports@adonis.osti.gov

Available to the public from the National Technical Information Service
5301 Shawnee Rd., Alexandria, VA 22312
ph: (800) 553-NTIS (6847)
email: orders@ntis.gov <<http://www.ntis.gov/about/form.aspx>>
Online ordering: <http://www.ntis.gov>



This document was printed on recycled paper.

(8/2010)

Effluent Management Facility Evaporator Bottoms: Waste Streams Formulation and Waste Form Qualification Testing

July 2018

SA Saslow
W Um
RL Russell
B Williams
RM Asmussen

T Varga
O Qafoku
B Riley
A Lawter
M Snyder

S Baum
I Leavy

Prepared for
the U.S. Department of Energy
under Contract DE-AC05-76RL01830

Pacific Northwest National Laboratory
Richland, Washington 99352

Executive Summary

This report describes the results from grout formulation and cementitious waste form testing performed by Pacific Northwest National Laboratory for Washington River Protection Solutions, LLC (WRPS). These results are part of a screening test that investigates grout formulations proposed for encapsulating a wide range of compositions predicted to be present in evaporator bottoms wastes from the Hanford Effluent Management Facility (EMF). This work supports the technical development need for alternative treatment and disposition paths for the EMF evaporator bottoms waste and future direct-feed low-activity waste (DFLAW) operations at the Hanford Site. High-priority activities included simulant production, grout formulation, and cementitious waste form testing. The work contained within this report relates to waste form development and testing, but does not directly support the 2017 Integrated Disposal Facility (IDF) performance assessment (PA). However, this work contains information useful for future PA updates [beyond fiscal year (FY) 2017] and future waste form development efforts. These analytical results can be used by (i) cementitious waste form scientists to further the understanding of cementitious leach behavior of contaminants of concern (COCs), (ii) decision makers interested in off-site waste form disposal, and (iii) the U.S. Department of Energy, their Hanford Site contractors, and stakeholders as they continue to assess the IDF PA program at the Hanford Site. The reported results help fill existing data gaps, support final selection of a cementitious waste form for the EMF evaporator bottoms waste, and improve the technical defensibility of long-term waste form risk estimates.

Specific grout formulation and waste form testing efforts described in this report include

- preparation of eight EMF evaporator bottoms waste simulants containing a range of major salt species concentrations (boron, chloride, nitrite, and sulfate) and one average EMF evaporator bottoms waste simulant;
- formulation and characterization of cementitious waste forms for treatment of the eight EMF Composition Screening (ECS) simulants and/or average simulant used for Extended Qualification Tests (EQT) using four final dry ingredient recipes: the original Cast Stone recipe [8% type I/II ordinary portland cement (OPC), 45% class C/F fly ash (FA), and 47% class 100 blast furnace slag (BFS)], 20% Aquaset II-GH®/80% BFS, 20% OPC/80% BFS, and 10% hydrated lime (HL)/18% OPC/72% BFS;
- physical property measurements for formulations used to immobilize the average simulant, including set time, moisture content, density, compressive strength, and saturated hydraulic conductivity, to confirm developed waste forms meet physical criteria for disposal;
- solid phase characterization to assess changes in mineralogy, morphology, and areas concentrated in radionuclides, e.g., ⁹⁹Tc, to understand how immobilization and leaching of contaminants of primary concern is dependent on the chemical processes that occur during waste form formation and leaching;
- residual free liquid observations of the cementitious waste forms, for up to 30 days, to assess the storage time necessary for residual free liquids to drop below 1 volumetric percent (vol%) prior to disposal according to Hanford Site solid waste acceptance criteria, HNF-EP-0063, Rev. 14¹;

¹ Ramirez AJ. 2008. Hanford Site Solid Waste Acceptance Criteria. HNF-EP-0063, Rev. 14, Fluor Federal Services, Inc., Richland, WA. Accessed May 31, 2017, at http://www.hanford.gov/files.cfm/WAC_HNF-EP-0063_%20CurrentRv.pdf.

- Toxicity Characteristic Leaching Procedure (TCLP)¹ testing to demonstrate that these cementitious waste form(s) will meet Resource Conservation and Recovery Act (RCRA)² land disposal restrictions (LDRs) for hazardous wastes when compared to the Universal Treatment Standards (40 CFR 268)³;
- determination of effective diffusivity (D_{eff})⁴ values for ⁹⁹Tc, ¹²⁷I, and Na⁺ in deionized water leach solutions to assess the long-term immobilization potential of the waste form under different leach environments; and
- quantification of ⁹⁹Tc desorption K_d (distribution coefficient) values from the cementitious material under oxidizing conditions to support maintenance of the Hanford IDF PA predictions for ⁹⁹Tc transport.

The key findings from this work are listed below and are supported by the details that follow:

1. The Cast Stone formulation was best at re-absorbing residual free liquids to within acceptable criteria for waste form disposal for seven of the eight simulants. For these seven simulants, free liquids were re-absorbed within 3 to 5 days after monolith production. The Aquaset/BFS formulation was successful at treating all eight simulants, but required 10 to 18 days before free liquids were re-absorbed into the grout. For the average simulant, Cast Stone and HL/OPC/BFS (herein abbreviated to simply HL) formulations performed equally for reabsorbing free liquids, doing so within 3 to 8 days.
2. Solid-phase characterization of the waste form monoliths showed **increases in ettringite formation in those formulations containing HL or simulants with high SO₄²⁻ content.**
3. **All test batches passed TCLP testing**, meeting Universal Treatment Standards (40 CFR 268) that are used as LDRs for incoming waste forms at off-site disposal facilities.
4. The range of values reported for ⁹⁹Tc D_{eff} (**$\sim 1 \times 10^{-11}$ to $\sim 5 \times 10^{-11}$ cm²/s**) **determined from 28- to 63-day leaching intervals** represent the effects of diffusion-controlled processes in addition to physical and/or chemical processes that immobilize ⁹⁹Tc, such as the incorporation of ⁹⁹Tc in ettringite formed during later leach periods.
5. ⁹⁹Tc release, measured as **⁹⁹Tc desorption distribution coefficient (K_d)**, under oxidizing conditions was determined to range between **8 and 289 mL/g**. The HL formulation performed better than the original Cast Stone recipe by a factor of ~ 3.7 or greater and K_d values generally increased when the starting solution:solid ratio increased from 10 to 25 mL/g.

Details supporting these conclusions follow:

¹ EPA – U.S. Environmental Protection Agency. 1992. Method 1311, Revision 0 – Toxicity Characteristic Leaching Procedure. In Test Methods for Evaluating Solid Waste: Physical/Chemical Methods. EPA SW 846, U.S. Environmental Protection Agency, Washington, D.C. Accessed May 26, 2017, at <https://www.epa.gov/sites/production/files/2015-12/documents/1311.pdf>.

² Resource Conservation and Recovery Act (RCRA). 1976. Public Law 94-580, as amended, 42 USC 6901 et seq. and 42 USC 6927(c) et seq. Accessed May 31, 2017, at <https://www.epw.senate.gov/rcra.pdf>.

³ 40 CFR 268. 2015. “Land Disposal Restrictions.” Code of Federal Regulations, U.S. Environmental Protection Agency, Washington, DC. Accessed June 1, 2017, at <https://www.gpo.gov/fdsys/pkg/CFR-2012-title40-vol28/xml/CFR-2012-title40-vol28-part268.xml>.

⁴ Effective diffusion coefficients are called observed diffusion coefficients (D_{obs}) in U.S. Environmental Protection Agency (EPA) test methodologies. The two terms are synonymous.

Eight simulant solutions (ECS simulants) were prepared according to a test matrix provided by the client (WRPS) that requires only a small set of simulants to be generated for this screening phase of grout-based waste form development by examining the most extreme ranges in composition. ECS simulants were prepared with varying boron, chloride, nitrite, and sulfate concentrations with a composition range based on wet electrostatic precipitator and submerged bed scrubber condensates estimated by DM10 melter and off-gas system campaigns documented in VSL-12R2640-1, Rev. 0.¹ Additionally, all ECS simulants were spiked with Zn (target 700 ppm) and RCRA metals, As (target 180 ppm), Se (target 180 ppm), Cr (target 300 ppm), and Hg (>30 ppm). All ECS simulant solutions contained variable amounts of visible precipitates at the bottom of their containment vessels when observed several days after preparation. A decrease in soluble Zn was observed to correlate with those ECS simulants containing low initial boron levels, as determined by solution analysis. Due to the presence of precipitates, ECS simulants were continuously mixed immediately before and during grout production to obtain the highest level of homogeneity. In addition to these eight simulants, an average simulant, with a composition equal to the average composition of the eight ECS simulants, was also prepared and spiked with Zn (target 700 ppm), Cr (target 300 ppm), ⁹⁹Tc (target 25 ppm), and ¹²⁷I (target 25 ppm). No precipitates were observed in the average simulant.

Twenty-four grout formulations were prepared using the eight ECS simulant solutions and three dry material recipes: the original Cast Stone recipe (8% OPC, 45% FA, and 47% BFS); 20% Aquaset II-GH®/80% BFS; and 20% OPC/80% BFS. Furthermore, the average simulant and either the original Cast Stone recipe or a 10% HL/18% OPC/72% BFS recipe was used to make four additional formulations that are herein identified as EQT formulations. For all ECS and EQT formulations, a water-to-dry-mix (w/dm) ratio of 0.5 was used and a water-reducing agent (MasterGlenium 3030 from BASF Corp.; Beachwood, Ohio) was added when necessary to reduce viscosity and improve flowability of the mix. Approximately eight monolith specimens were made from each of the 24 grout formulation test batches and were allowed to cure for at least 7 days.

Residual free liquids were monitored for one monolith specimen from each test batch for at least 28 days or until no free liquids (<1% of the total waste volume) were observed. ECS test batches using the original Cast Stone formulation recipe re-absorbed residual free liquid within 3 to 5 days for all simulants except Simulant 7 (low Cl and B, high NO₂ and SO₄), which contained free liquids through the end of the observation period (29 days). Alternatively, the Aquaset (20 wt%) and BFS (80 wt%) formulation was suitable for treating all ECS simulants (i.e., <1% total waste volume), but required 10 to 18 days after monolith production to re-absorb the residual free liquid. ECS simulants immobilization by OPC (20 wt%) and BFS (80 wt%) required 3 to 30 days to reabsorb residual free liquids from the ECS simulants. For EQT treatment of the average simulant, Cast Stone and HL formulations performed equally, reabsorbing free liquids within 3 to 8 days. These results, once confirmed by replicate observations, should guide future formulations for scale-up tests and provide baseline guidance for the storage time required before waste forms may be disposed of in the IDF.

Physical properties measured for EQT non-radiological monoliths during and after curing included monolith set time, moisture content, density, compressive strength, and saturated hydraulic conductivity. Both the Cast Stone and HL formulations performed similarly across most tests, with the exception of compressive strength (see table below). When evaluating compressive strength, the HL monoliths outperformed the Cast Stone monoliths by over double, with an average compressive strength of 3693 ±

¹ Abramowitz H, M Brandys, R Cecil, N D'Angelo, KS Matlack, IS Muller, IL Pegg, RA Callow, and I Joseph. 2012. Technetium Retention in WTP LAW Glass with Recycle Flow-Sheet DM10 Melter Testing. VSL 12R2640-1, Vitreous State Laboratory, Washington, D.C. Accessed June 1, 2017, at <https://digital.library.unt.edu/ark:/67531/metadc842091/m1/>.

785 psi compared to 1751 ± 66 psi, respectively, where the standard deviation of the average is reported to 1σ (and throughout this report).

Physical Property Test	Cast Stone	HL
Set Time	67.3 – 68.7 hours	66.7 – 71.4 hours
Residual Free Liquids	3 – 8 days	3 – 8 days
Moisture Content (MC)	27.32 %	24.24 %
Apparent Density	2.22 ± 0.03 Mg/m ³	2.46 ± 0.15 Mg/m ³
Volume of Permeable Pore Space	42.40 ± 0.03 %	43.95 ± 2.42 %
Compressive Strength	$1,751 \pm 66$ psi	$3,693 \pm 785$ psi
Saturated Hydraulic Conductivity (K_{sat})	1.3×10^{-10} cm/s	1.4×10^{-10} cm/s

Solid phase characterization of ECS and EQT specimens by X-ray diffraction showed that the majority of the waste form is composed of an amorphous phase, likely calcium silicate hydrate (CSH) (~71 – 85 wt%). The remaining material consisted of mineral phases including portlandite [$\text{Ca}(\text{OH})_2$], ettringite [$\text{Ca}_6\text{Al}_2(\text{SO}_4)_3(\text{OH})_{12} \cdot 26\text{H}_2\text{O}$], calcite [CaCO_3], larnite [Ca_2SiO_4], hydrocalumite [$\text{Ca}_4\text{Al}_2(\text{OH})_{12}(\text{OH})_2 \cdot 6\text{H}_2\text{O}$], and quartz [SiO_2]. In monoliths made from high-sulfate simulants or with HL, there was a noticeable increase in ettringite formation. These mineralogical observations may have implications for long-term Tc immobilization, since ettringite is hypothesized to incorporate Tc into its mineral structure, which could increase Tc stability within the waste form. For the EQT monoliths, there is an increase in ettringite present in the material collected from the outer wall of non-leached and post-leached specimens. Based on these findings, elevated regions of ⁹⁹Tc detected on the outer wall of HL-based EQT monoliths before and after leaching as well as the outer wall of Cast Stone samples further supports ⁹⁹Tc association with ettringite formation.

The TCLP test results when compared to Universal Treatment Standards (40 CFR 268) for hazardous wastes show that all ECS and EQT test batches pass LDRs (40 CFR 268) for each COC. An observation worth noting is that all Hg levels were non-detectable in the leachate despite being present in the simulants used to make the ECS cementitious waste forms at elevated concentrations (≥ 38 ppm in each). However, these results are non-conservative for the ECS specimens due to the presence of precipitates in the starting simulants and the fact that COCs immobilized as a solid (precipitate) rather than in the aqueous phase may exhibit different leach behaviors. Furthermore, these initial TCLP trends are based on the analysis of one specimen from each test batch, therefore, replicate specimen analysis by TCLP is recommended for formulations studied in future testing.

EPA Method 1315 leach testing performed on radioactive EQT monoliths formulated with Cast Stone and HL recipes suggests ⁹⁹Tc D_{eff} values (after 28-day leaching) within a range of $\sim 1 \times 10^{-11}$ to 5×10^{-11} cm²/s. However, the HL-based formulation ($\sim 1 \times 10^{-11.0}$ cm²/s) outperforms the Cast Stone recipe ($\sim 5 \times 10^{-11}$ cm²/s) for ⁹⁹Tc during the later leaching period. For ¹²⁷I, the HL-based monoliths also outperform the Cast Stone monoliths, although the ¹²⁷I D_{eff} values (Cast Stone: $\sim 5 \times 10^{-10}$ cm²/s; HL: $\sim 4 \times 10^{-11}$ to 5×10^{-11} cm²/s) were higher compared to ⁹⁹Tc, suggesting that iodine will be more readily released from the waste form. It should be noted that throughout the 63-day leach period, some periods of ⁹⁹Tc and ¹²⁷I release did not follow a pure diffusion trend, suggesting additional chemical reactions may influence contaminant leaching from the waste form. This observation was especially prevalent in the HL formulated specimens. As such, the calculated and reported diffusivity values should be used cautiously since the EPA Method 1315 assumes diffusion-controlled contaminant release.

⁹⁹Tc sorption tests were conducted inside an anoxic chamber to maintain reducing conditions and used size-reduced (0.425 – 2 mm) EQT monolith material from both the Cast Stone and HL non-radiological test batches to initially sorb ~ 1.1 ppb of soluble ⁹⁹Tc for 30 days. Two solution:solid ratios were used (10 mL/g and 25 mL/g) for each formulation. At the end of the sorption period, Cast Stone formulated

monoliths showed minimal and variable ^{99}Tc sorption patterns, with those samples prepared at 10 mL/g sorbing less than ~10% of ^{99}Tc present in the 1.1 ppb solution and the 25 mL/g Cast Stone sorption samples sorbing more ^{99}Tc , but with greater variability. The HL-based samples successfully removed ~80% of ^{99}Tc in solution across all samples. However, the sorption K_d values reported should be used with care due to the unexpected decrease in ^{99}Tc concentration measured in the control samples (~40%), where no solid was present, suggesting that additional chemical reactions (not facilitated by the solid phase) are occurring that influence the ^{99}Tc sorption. After the 30-day sorption period, ^{99}Tc -sorbed material was used to perform ^{99}Tc desorption testing under oxidizing conditions for two reaction times (30 and 44 days). The results showed a significant increase in K_d values across both formulations when increasing the solution:solid ratio from 10 mL/g to 25 mL/g. The average desorption K_d values for Cast Stone samples increased from ~10 mL/g to 45 – 77 mL/g (depending on desorption time) as the solution:solid ratio changed from 10 mL/g to 25 mL/g respectively, and for HL samples the increase was from ~100 mL/g to ~285 mL/g. Based on these ^{99}Tc desorption K_d values and trends, the HL-based material again outperforms the Cast Stone material.

The appendix of this report provides photographic evidence of residual free liquids seen immediately after formulation and at the end of the residual free liquids testing period. Also in the appendix are measured concentrations of major and select trace constituents from individual dry materials used to produce the cementitious waste forms and from the specimens after TCLP analysis, as well as additional data from EPA Method 1315 leach tests.

The results in this report fill existing data gaps, support final selection of cementitious waste forms for EMF evaporator bottoms waste, and improve the technical defensibility of long-term waste form risk estimates. Effective (observed) diffusivity values of ^{99}Tc and ^{129}I using EPA Method 1315 and ^{99}Tc desorption coefficients (K_{dS}) provide additional information that can be used to support future updates of the IDF PA and waste form selection. The data within has also demonstrated that all tested formulations pass LDRs for off-site disposal options based on TCLP testing methods. However, further improvements can be made for on-site disposal performance related to ^{99}Tc and ^{129}I retention within the waste forms. Based on recent advancements controlling natural long-term mineral growth and using material additions (e.g., getters) that stabilize specific COCs within the waste form, effective diffusivity values as low as 10^{-15} cm²/s (reported for ^{99}Tc) are achievable by cementitious waste forms.^{1,2,3} This leaves room for at least three orders of magnitude improvement based on the D_{eff} values reported here ($>10^{-12}$ cm²/s). Optimizing the dry-ingredient formulation for treating EMF evaporator bottoms, through controlling natural mineral growth, incorporating getters, or adjusting the water-to-dry mix ratio, and performing additional qualifying tests under variable cure times and simulated vadose zone pore water conditions would also provide an opportunity to improve the efficiency of transferring waste forms to the IDF (e.g., avoid long hold times due to conservative cure times and reabsorption periods for residual free liquids). Finally, further investigation into the effects of precipitates (as observed in the ECS simulants) is required to diagnose how their presence may affect the chemical and physical properties of the produced cementitious waste forms, and investigations into the low sorption values and reducing environments

¹ Saslow SA, W Um, RL Russell, G Wang, RM Asmussen, and R Sahajpal. 2017. Updated Liquid Secondary Waste Grout Formulation and Preliminary Waste Form Qualification. PNNL-26443, Pacific Northwest National Laboratory, Richland, WA. Accessed April 5, 2018, at https://www.pnnl.gov/main/publications/external/technical_reports/PNNL-26443.pdf.

² Um W, BD Williams, MMV Snyder, and G Wang. 2016. Liquid Secondary Waste Grout Formulation and Waste Form Qualification. PNNL-25129, Pacific Northwest National Laboratory, Richland, WA. Accessed March 21, 2017, at http://www.pnnl.gov/main/publications/external/technical_reports/PNNL-25129.pdf.

³ Asmussen RM, CI Pearce, AR Lawter, RE Clayton, J Stephenson, B Miller, M Bowden, E Buck, N Washton, BD Williams, J Neeway, and NP Qafoku. 2016. Getter Incorporation into Cast Stone and Solid State Characterizations. PNNL-25577, Pacific Northwest National Laboratory, Richland, WA. Accessed April 11, 2018, at https://www.pnnl.gov/main/publications/external/technical_reports/PNNL-25577REV0.pdf.

during sorption testing is recommended to better assess the fate of ^{99}Tc under these conditions. Results from these recommended studies would help support future maintenance of the IDF PA and guide waste form selection to support the implementation of alternative waste pathways for waste streams to be generated at the EMF during DFLAW operations.

Acknowledgments

The authors are grateful to Dave Swanberg and Ridha Mabrouki at Washington River Protection Solutions, LLC, Richland, Washington, for the project funding and programmatic guidance. We also acknowledge Keith Geiszler, Erin McElroy, Amanda Lawter, Ray Clayton, and Guohui Wang in the Subsurface Science and Technology group at Pacific Northwest National Laboratory for their analytical and laboratory support. We would also like to thank Guzel Tartakovsky for calculation reviews and Jeff Serne and Joseph Westsik for their technical reviews. We would like to acknowledge Matthew Wilburn and Maura Zimmerschied for editing this report. Pacific Northwest National Laboratory is a multi-program national laboratory operated by Battelle for the U.S. Department of Energy.

Acronyms and Abbreviations

ANS	American Nuclear Society
ANSI	American National Standards Institute
ASME	American Society of Mechanical Engineers
ASTM	ASTM International (West Conshohocken, PA)
BFS	blast furnace slag
BSE	backscattering electron
COC	contaminant of concern
DFLAW	direct feed low-activity waste
DIW	deionized water
EC	electrical conductivity
ECS	EMF Composition Screening (formerly test group 1 in PNNL-26443, Rev. 0)
EDS	energy dispersive spectroscopy
EMF	Effluent Management Facility
EPA	U.S. Environmental Protection Agency
EQL	estimated quantitation limit
EQT	Extended Qualification Tests (formerly test group 2 in PNNL-26443, Rev. 0)
FA	fly ash
FY	fiscal year
HL	hydrated lime
IC	ion chromatography
ICP-MS	inductively coupled plasma mass spectrometry
ICP-OES	inductively coupled plasma optical emission spectroscopy
IDF	Integrated Disposal Facility
iQID	ionizing-radiation Quantum Imaging Detector
K_d	distribution coefficient
K_{sat}	saturated hydraulic conductivity
LAW	low-activity waste (Hanford)
LDR	land disposal restriction
LI	leachability index
LLC	Limited Liability Company
MC	moisture content
MG 3030	MasterGlenium 3030, water-reducing additive
ND	not detected
NIST	National Institute of Standards and Technology
NQA	Nuclear Quality Assurance
OPC	ordinary portland cement

ORP	oxidation reduction potential (E_h)
PA	performance assessment
PNNL	Pacific Northwest National Laboratory
QA	quality assurance
R&D	research and development
RCRA	Resource Conservation and Recovery Act of 1976
SEM	scanning electron microscopy
SHE	standard hydrogen electrode
SRNL	Savannah River National Laboratory
SwRI	Southwest Research Institute
TCLP	Toxicity Characteristic Leaching Procedure
TDS	total dissolved solids
TS	total solids
UTS	Universal Treatment Standards
VSL	Vitreous State Laboratory
w/dm	free water-to-dry-mix (ratio, g/g)
WESP-SBS	wet electrostatic precipitator–submerged bed scrubber
WRA	water-reducing additive
WRPS	Washington River Protection Solutions, LLC
WTP	Hanford Tank Waste Treatment and Immobilization Plant
WWFTP	WRPS waste form testing program
Z	atomic number

Units of Measure

Å	angstrom(s)
°C	temperature in degree Celsius [$T(^{\circ}\text{C}) = T(\text{K}) - 273.15$]
cm	centimeter(s)
d	day(s)
g	gram(s)
h	hour(s)
keV	kiloelectron volt(s)
kg	kilogram(s)
kV	kilovolt(s)
L	liter(s)
m	meter(s)
M	molarity, mole(s)/liter
mA	milliampere
Mg	megagram(s)
mg	milligram(s)
mL	milliliter(s)
mm	millimeter(s)
MPa	megapascal(s)
mV	millivolt(s)
nA	nanoampere
nm	nanometer(s)
psi	pounds per square inch
ppb	parts per billion
ppm	parts per million
rpm	revolutions per minute
s	second(s)
S	Siemens
vol%	volume percent
wt%	weight percent
vol%	volumetric percent
μ	micro (prefix, 10^{-6})

Contents

Executive Summary	ii
Acknowledgments.....	viii
Acronyms and Abbreviations	ix
Units of Measure.....	xi
Contents	xii
Figures	xv
Tables.....	xvii
1.0 Introduction	1.1
1.1 Objectives.....	1.2
1.2 Report Contents and Organization	1.2
1.3 Quality Assurance	1.3
2.0 Characterization and Analysis Methods	2.1
2.1 Solution Analysis	2.1
2.1.1 pH and Electrical Conductivity (EC) Measurement.....	2.1
2.1.2 Alkalinity Measurement	2.1
2.1.3 Ammonia Analysis.....	2.1
2.1.4 Oxidation Reduction Potential (ORP, E_h) Measurement	2.1
2.1.5 Analysis of Cations, Anions, Hg, ^{99}Tc , and ^{127}I	2.2
2.2 Solid Analysis	2.2
2.2.1 X-Ray Diffraction (XRD) Analysis	2.2
2.2.2 Scanning Electron Microscopy (SEM) and Energy Dispersive Spectroscopy (EDS)....	2.2
2.2.3 Single Particle Digital Autoradiography (iQID)	2.3
3.0 Simulant Preparation and Analysis.....	3.1
3.1 Simulant Composition.....	3.1
3.2 Simulant Preparation	3.2
3.3 Simulant Observations and Analytical Results	3.3
3.4 Simulant Preparation Conclusions	3.10
4.0 Grout Formulation and Sample Preparation.....	4.1
4.1 Preparation of EMF Evaporator Bottoms-Waste Monoliths	4.5
4.1.1 Dry Ingredients.....	4.5
4.1.2 Grout Mixing/Monolith Production	4.5
5.0 Waste Form Physical Properties.....	5.1
5.1 Set Time	5.1
5.1.1 Methods and Materials	5.1
5.1.2 Results and Discussion.....	5.2
5.2 Free Liquids	5.3

5.2.1	Methods and Materials	5.3
5.2.2	Results and Discussion	5.3
5.3	Moisture Content	5.5
5.3.1	Methods and Materials	5.5
5.3.2	Results and Discussion	5.5
5.4	Density	5.6
5.4.1	Methods and Materials	5.6
5.4.2	Results and Discussion	5.6
5.5	Compressive Strength	5.7
5.5.1	Methods and Materials	5.7
5.5.2	Results and Discussion	5.8
5.6	Saturated Hydraulic Conductivity	5.9
5.6.1	Methods and Materials	5.9
5.6.2	Results and Discussion	5.10
6.0	Solid Phase Characterization	6.1
6.1	X-ray Diffraction	6.1
6.2	Scanning Electron Microscopy (SEM) and Energy Dispersive X-Ray Spectroscopy (EDS) ...	6.8
6.2.1	SEM/EDS Results for EQT Average Simulant Cast Stone Specimens	6.9
6.2.2	SEM/EDS Results for EQT Average Simulant HL Specimens	6.11
6.3	Digital Autoradiography	6.13
7.0	TCLP Tests	7.1
7.1	Methods and Materials	7.1
7.2	Results and Discussion	7.3
8.0	EPA Method 1315 Leach Testing	8.1
8.1	Methods and Materials	8.1
8.2	Results and Discussion	8.2
8.2.1	⁹⁹ Tc Leachability in DIW	8.7
8.2.2	¹²⁷ I Leachability in DIW	8.7
8.2.3	Leachability of Na ⁺ in DIW	8.7
8.2.4	Other Measurements in DIW	8.7
9.0	⁹⁹ Tc Desorption Testing	9.1
9.1	Methods and Materials	9.1
9.2	Results and Discussion	9.3
9.2.1	⁹⁹ Tc Sorption on Non- ⁹⁹ Tc-Spiked Monolith Crushed Material	9.3
9.2.2	⁹⁹ Tc Desorption <i>K_d</i> s using ⁹⁹ Tc Sorbed Monolith Powders	9.10
10.0	Summary and Recommendations	10.1
10.1	Conclusions	10.1
10.2	Recommendations	10.5
11.0	References	11.1

Appendix A – Additional Data A.1

Figures

Figure 3.1. Simulant 6 Precipitate after Heating at ~50°C for Several Hours	3.9
Figure 3.2. Precipitate Formation in a 1 L Batch of Simulant 6 as a Function of Time. Photos taken (A) immediately after simulant preparation was complete and (B) 20 hours, (C) 49 hours, and (D) 70 hours after simulant production. After 70 hours (D), 40 ppm of Hg was spiked into the simulant before observation.....	3.10
Figure 4.1. Taking Simulant Subsample while Mixing before Dry Ingredient Addition (left), Mixing Grout after Combining Simulant and Dry Ingredients (middle), and Pouring Grout into Plastic Waste Form Mold (right)	4.7
Figure 5.1. Vicat Needle Apparatus Showing Complete Penetration of the 1 mm Diameter Needle Such That the Rod Has Made an Indentation in the Specimen Surface in Previously Tested Areas. The sample shown is not associated with the samples discussed in this report.	5.2
Figure 5.2. Number of Days after Monolith Production for Free Liquids to Decrease to Less Than 1% of the Total Waste Volume for All ECS and Final EQT Non-Rad Test Batches.....	5.4
Figure 5.3. MTS Model 312.31 Servohydraulic Frame with a 55 kip Actuator and Load Cell Used for Compressive Strength Measurements.	5.8
Figure 6.1. XRD Patterns of Monoliths Formulated Using ECS Simulants and the Original Cast Stone Recipe.....	6.5
Figure 6.2. XRD Patterns of Monoliths Formulated Using ECS Simulants and a Dry Ingredient Recipe of 20% Aquaset II-GH/80% BFS.....	6.6
Figure 6.3. XRD Patterns of Monoliths Formulated Using ECS Simulants and a Dry Ingredient Recipe of 20% OPC/80% BFS.....	6.7
Figure 6.4. EQT XRD Patterns of Monoliths Formulated Using the Avg Simulant and the Cast Stone (TB25 and TB27) or HL (TB26 and TB28) Formulation Recipe	6.8
Figure 6.5. SEM and EDS Element Maps for Specimen Material Collected from Cast Stone Monoliths Cured 28 days. (A) SEM image from material collected from the exterior of a cured EQT non-rad Cast Stone monolith (TB25.1). (Electron Image and Maps) SEM image of material collected from a pre-leached Cast Stone rad monolith (TB27) and element maps for Si, Ca, Tc, S, and Fe, corresponding to the particles imaged in (Electron Image).	6.9
Figure 6.6. The Porous Nature of Spherical Particles Imaged in Cast Stone Based Monoliths Is Illustrated Here with SEM Images Collected for Material Sampled from the Exterior Wall of 63-day Leached Monolith 17-EMF-TB27-1.....	6.10
Figure 6.7. SEM Image and Element Mapping of Exterior EQT Cast Stone Material (rad, leached 63 days in DIW) That Shows the Presence of Particles with No Distinct Morphology or Crystalline Order and a Representative Particle Rich in Fe.....	6.10
Figure 6.8. SEM Electron Images and EDS Analysis for Minor Phases Identified in the Exterior Material of Cast Stone Monolith TB27-1, Leached for 63 Days in DIW. The Top Two Images Show the Platy Particles Containing Enriched Levels of Ba and S, Relative to Other Samples Analyzed. In the bottom two images, the poorly defined morphology of some particles were enriched in Cr or Zr, with elevated levels of Fe.....	6.11
Figure 6.9. Typical SEM Images Collected from HL Specimens. Imaged here is the material collected from the pre-leach, rad TB28-3 specimen.....	6.12
Figure 6.10. Unreacted Large Particles Found in the Exterior Material Collected from HL Based Rad Monolith TB28-1	6.12

Figure 6.11. SEM Image and EDS Element Mapping for a Particle Found in the Exterior Material Collected from 63-day Leached HL Formulated Monolith (TB28-1).....	6.13
Figure 6.12. iQID Image of TB27 (Cast Stone) Both in Its Cured State (top) and Following 63 d Leaching in DIW (bottom). The white arrow is present to highlight a strong signal from the edge of the leached sample.	6.14
Figure 6.13. iQID Image of TB28 (HL) Both in Its Cured State (top) and Following 63 d Leaching in DIW (bottom).....	6.14
Figure 8.1. EQT Specimens Used in EPA Method 1315 Leach Testing Before Leaching (Pre-Leach) and after the 63-day Leach Period Had Elapsed (63-d Leach). Specimens included 17-EMF-TB27-1, 17-EMF-TB27-2, 17-EMF-TB28-1, and 17-EMF-TB28-2. Each 63-day leached specimen is darker in color because it is still damp from the leaching solution.	8.3
Figure 8.2. Effective Diffusivity Values of ^{99}Tc (top, left), ^{127}I (top, right), and Na^+ (bottom) from Avg Simulant (EQT) Radiological Specimens Leached for a Cumulative 63 days in DIW. Monoliths were tested using the original Cast Stone recipe (TB27-1 and TB27-2) and a HL recipe (TB28-1 and TB28-2).	8.5
Figure 9.1. ^{99}Tc Concentrations in the Supernatants after 30-Day Sorption Testing for Cast Stone (TB25.1, black) and HL (TB26.2, red)	9.6
Figure 9.2. ^{99}Tc Concentrations ($\mu\text{g/L}$) Measured in the Filtered Supernatants Collected after Desorption Testing Periods for Cast Stone (TB25.1, black) and HL (TB26.2, red) Samples. Sample names containing D30 and D44 correspond with the desorption testing periods of 30 and 44 days, respectively. SS10 and SS25 correspond with solution:solid ratios of 10 mL/g and 25 mL/g, respectively. Triplicate samples are labelled S1, S2, or S3. The grey line indicates the EQL concentration for ^{99}Tc (0.066 $\mu\text{g/L}$). For those samples with ^{99}Tc concentrations below the EQL, the EQL value was used to calculate ^{99}Tc desorption K_d values in Table 9.2.....	9.11

Tables

Table 3.1. Simulant Design Matrix	3.1
Table 3.2. Target Concentration (g/L) of Variable Simulant Species in the Eight ECS Simulants ^(a)	3.2
Table 3.3. Final Measured Simulant pH, Density, and wt% TS Results	3.5
Table 3.4. Analytical (Measured) Results of Final Simulants	3.6
Table 3.5. Time Between Preparation and Analysis of Simulant Subsamples	3.8
Table 3.6. Solution and Solid Phase Analysis on Simulant 1	3.8
Table 3.7. Acid Digest of Simulant 1 with Hg Spike.....	3.8
Table 4.1. Liquid Secondary Waste Grout Test Matrix for ECS	4.3
Table 4.2. Liquid Secondary Waste Grout Test Matrix for EQT.....	4.4
Table 5.1. EQT Set Time Results using ASTM C191-13	5.3
Table 5.2. Days Required for Free Liquids to Reach Less Than 1% of Total Waste Volume	5.4
Table 5.3. Moisture Content of the Differently Cured Monoliths	5.6
Table 5.4. Density Measurements for EQT Non-Rad Specimens	5.7
Table 5.5. Compressive Strength of Select EQT Non-Rad Specimens	5.9
Table 5.6. Initial and Final Hydraulic Conductivities Measured on Select Samples.....	5.10
Table 6.1. XRD Analysis of ECS and EQT Monoliths.....	6.3
Table 7.1. Specimen Preparation and TCLP Testing Schedule	7.2
Table 7.2. TCLP Results for Simulants Treated with Cast Stone Formulation Recipe	7.4
Table 7.3. TCLP Results for Simulants Treated with Aquaset/BFS Formulation Recipe	7.5
Table 7.4. TCLP Results for Simulants Treated with OPC/BFS Formulation Recipe	7.6
Table 7.5. TCLP Results for EQT Specimens Treating the Avg Simulant with Cast Stone and HL Formulation Recipes	7.7
Table 8.1. Initial Concentrations, C(0), of ⁹⁹ Tc, ¹²⁷ I, and Na ⁺ used in Diffusivity Calculations.....	8.2
Table 8.2. Diffusivity and LI Values of ⁹⁹ Tc, ¹²⁷ I, and Na ⁺ in DIW Leaching Solution.....	8.4
Table 8.3. Calculated Dry Bulk Density of Each Monolith and Averaged <i>D_{eff}</i> Values of ⁹⁹ Tc, I ⁻ , and Na ⁺ from the Cumulative 28-Day to 63-Day Leaching in DIW with Average Fraction of Released Mass in Duplicates of Individual Monolith Batches	8.6
Table 9.1. pH and <i>E_h</i> Results from ⁹⁹ Tc Sorption and Desorption Tests	9.4
Table 9.2. <i>K_d</i> Results from ⁹⁹ Tc Sorption and Desorption Tests.....	9.8
Table 10.1. Summary of Physical Properties for EQT Formulations	10.3

1.0 Introduction

The direct-feed low-activity waste (DFLAW) operations involve concentrating the Hanford low-activity waste (LAW) melter off-gas condensate by evaporation in the Effluent Management Facility (EMF). The concentrated condensate will then be recycled back to the LAW vitrification facility. However, the concentrate is expected to contain high levels of halides and sulfate that require lower waste loading to ensure solubility in the glass melt and minimize potential for corrosion of the melter's refractory lining. Furthermore, recycled radionuclides technetium-99 (^{99}Tc) and iodine-129 (^{129}I) are expected to accumulate in the off-gas treatment waste stream. To this end, the purpose of this research program is to examine alternative disposition paths for the EMF evaporator concentrate waste stream that bypass recycling to the LAW melter (McCabe et al. 2016), thus eliminating recycling of the identified problematic components and decreasing the need for integrated operations with the LAW melter. Technology development and maturation activities conducted within this program will support alternative disposition path investigations for the EMF evaporator bottoms wastes and the results will be used to verify whether developed waste forms can meet off-site disposal acceptance criteria and/or on-site Hanford Integrated Disposal Facility (IDF) waste acceptance criteria.

In fiscal year (FY) 2017, Washington River Protection Solutions, LLC (WRPS) contracted with Pacific Northwest National Laboratory (PNNL) to conduct screening tests to determine whether variation in the bulk EMF evaporator bottoms waste stream composition is a factor in producing an acceptable solidified waste form. High-priority activities include EMF evaporator bottoms waste simulant production, grout-based waste form formulation development, and waste form performance testing. This work supports the WRPS One System Chief Technology Office's Technology Maturation and Analysis Group in identifying options for alternative treatments and dispositions for Hanford Tank Waste Treatment and Immobilization Plant (WTP) secondary liquid wastes from the DFLAW process.

A waste form test matrix for the EMF evaporator bottoms-waste simulants was prepared based on the lessons learned from previous testing programs and results (Westsik et al. 2013; Serne et al. 2015; Um et al. 2016). PNNL's FY 2017 scope of work focused on EMF evaporator bottoms waste simulant production as well as preparation and characterization of cementitious waste forms spiked with selected metals regulated by the Resource Conservation and Recovery Act of 1976 (RCRA 1976) (i.e., Cr, Hg, As, and Se), Zn, ^{99}Tc , and iodine-127 (^{127}I). In addition, PNNL FY 2017 testing has been split into two groups: the EMF Composition Screening (ECS) test group and the Extended Qualification Tests (EQT) test group.¹

For ECS, a total of eight EMF bottoms waste simulants, spiked with Zn and the selected RCRA metals Cr, As, Se, and Hg, were solidified at PNNL using three dry material formulations with baseline dry ingredients, ordinary portland cement (OPC), fly ash (FA), blast furnace slag (BFS), and Aquaset II-GH (Aquaset). This test matrix thus generates a total of 24 grout formulations to be cured as cementitious waste forms. Waste form specimens from each ECS grout formulation were used for two testing procedures: (1) residual free liquid of the freshly prepared waste form paste/slurry, performed at PNNL, and (2) Toxicity Characteristic Leaching Procedure (TCLP, EPA 1992) of the cured waste form specimens, preparation and analysis performed at Southwest Research Institute (SwRI). The results of these tests were used to assess which ECS waste form specimens comply with land disposal restrictions (LDRs) (40 CFR 268, 2015).

¹ In the governing test plan for this report, TP-SWCS-019, Rev 0.1, test group one is referred to as the "off-site" testing group, where "off-site" is meant to indicate that the developed waste forms were tested primarily through a PNNL contract with the U.S. Environmental Protection Agency (EPA)-accredited SwRI. Test group two is referred to as the "on-site" waste forms characterized and tested primarily at PNNL.

Waste form specimens generated as part of the EQT testing group were prepared for use in additional testing procedures (the majority performed at PNNL) that provide qualification information for future IDF performance assessments (PAs) and maintenance. The EQT waste form specimens were generated using a ninth simulant, with a composition matching the average of the eight ECS simulants. Two dry material formulations were tested to solidify the average EMF evaporator bottoms waste simulant: the original Cast Stone dry material formulation and a hydrated lime (HL)/OPC/BFS formulation down-selected from three formulations containing different amounts of HL. The selection of the final HL-containing formulation was based on examination for mixture flow and residual free liquids. Two batches of EQT waste form specimens were generated for each of the two final dry material formulations, one batch with added ^{99}Tc and one without, for a total of four EQT waste form test batches. All EQT specimens were spiked with select RCRA metals, Zn, and ^{127}I (as an analog to ^{129}I). In FY 2017, non- ^{99}Tc specimens were used to assess processing properties of the freshly prepared waste form paste or slurry, including residual free liquids and set time by Vicat needle, which provides an indication of specimen structure development due to hydration reactions (ASTM C191-13). Saturated hydraulic conductivity (K_{sat}) and compressive strength tests were performed at PNNL, and TCLP testing and analysis was performed at SwRI. Solid phase characterization (e.g., mineralogy, morphology, and radionuclide distribution), along with additional tests to determine ^{99}Tc desorption distribution coefficient (K_d) and EPA Method 1315 (EPA 2013) for observed diffusivity of contaminants, were conducted at PNNL in FY 2018 and are discussed in this revision of this report.

1.1 Objectives

The overall objectives of the EMF evaporator bottoms waste form testing program are to

- produce EMF evaporator bottoms-waste simulants based on simulant recipes provided by WRPS that cover the range of expected EMF evaporator waste streams and their average,
- determine a formulation(s) for a grout-based waste form for the EMF evaporator bottoms wastes that meets off-site (e.g., Waste Control Specialists, Texas, USA) and/or on-site Hanford IDF acceptance criteria, and
- provide contaminant release data on the grout-based EMF evaporator bottoms waste form for future PA maintenance and risk assessment evaluations.

1.2 Report Contents and Organization

This report contains 11 sections and an appendix. Section 1 provides an introduction and describes key objectives and quality assurance (QA) procedures of the tests conducted for this study. Section 2 summarizes the characterization and analysis techniques used for solution and solid samples. Section 3 details simulant production and analysis. Section 4 describes grout waste form formulation. Section 5 presents the physical properties of the cementitious waste forms during and after curing for 28 days. Section 6 discusses the results obtained from solid phase characterization methods. Section 7 presents the results of the TCLP tests for both ECS and non-radiological EQT monoliths. Section 8 presents EPA Method 1315 effective (or observed) diffusivity leach tests (EPA 2013) and Section 9 provides measured ^{99}Tc desorption distribution coefficients (K_d s) and discusses their implications. Section 10 provides a summary, including conclusions and recommendations for future work. Finally, Section 11 contains a list of references cited in the report. Photos taken during residual free liquid observations and additional data and information for TCLP and EPA Method 1315 tests are included in Appendix A.

1.3 Quality Assurance

This work was funded by WRPS under contract 36437-161, *Secondary Waste Cast Stone Formulation and Waste Form Qualification*. The work was conducted as part of PNNL Project 68334, Liquid Secondary Waste Formulation Development. SwRI testing is conducted under PNNL contract 348272.

All research and development (R&D) work at PNNL was performed in accordance with PNNL's Laboratory-level Quality Management Program, which is based on a graded application of NQA-1-2000, *Quality Assurance Requirements for Nuclear Facility Applications* (ASME 2000), to R&D activities. In addition to the PNNL-wide QA controls, the QA controls of the WRPS Waste Form Testing Program (WWFTP) QA program were also implemented for the work. The WWFTP QA program consists of the WWFTP Quality Assurance Plan (QA-WWFTP-001) and associated QA-NSLW-numbered procedures that provide detailed instructions for implementing NQA-1 requirements for R&D work. The WWFTP QA program is based on the requirements of NQA-1-2008, *Quality Assurance Requirements for Nuclear Facility Applications*, and NQA-1a-2009, *Addenda to ASME NQA-1-2008 Quality Assurance Requirements for Nuclear Facility Applications*, graded on the approach presented in NQA-1-2008, Part IV, Subpart 4.2, "Guidance on Graded Application of Quality Assurance (QA) for Nuclear-Related Research and Development."

Performance of this work and preparation of this report were assigned the technology level "Applied Research" by PNNL and were conducted in accordance with WWFTP procedure QA-NSLW-1102, *Scientific Investigation for Applied Research*. All staff members contributing to the work have technical expertise in the subject matter and received QA training before performing quality-affecting work. The "Applied Research" technology level provides adequate controls to ensure that the activities were performed correctly. Use of both the PNNL-wide and WWFTP QA controls ensured that all client QA expectations were addressed in performing the work.

2.0 Characterization and Analysis Methods

This section describes the characterization techniques used for solution and solid analyses of samples generated during cementitious waste form formulation and testing activities. All techniques described here are methods and procedures performed at PNNL.

2.1 Solution Analysis

The following instruments were used for analyzing solution samples (simulants and leachates) from the cementitious waste forms to identify and measure the concentration of detectable species or elements.

2.1.1 pH and Electrical Conductivity (EC) Measurement

The pH of the solution samples was measured with a solid-state YSI Inc. pH electrode and a pH meter (YSI MultiLab 4010-3). Before measurement, the pH probe was calibrated with National Institute of Standards and Technology (NIST)-traceable buffers (pH = 7.0, 10.0, and/or 13.0 at 25°C). The precision of each pH measurement was ± 0.10 pH units. A YSI Inc. conductivity sensor was used to measure the EC of leachate solutions. The cell constant of the sensor was calibrated using a 1,413 $\mu\text{S}/\text{cm}$ standard, and then checked with a range of potassium chloride standard solutions, ranging from 100 $\mu\text{S}/\text{cm}$ to 10,000 $\mu\text{S}/\text{cm}$, and a blank containing deionized water (DIW). Calibration checks were repeated after every set of 10 samples analyzed and at the end of analyses performed each day.

2.1.2 Alkalinity Measurement

The alkalinity (mg/L as CaCO_3) was measured using a standard acid titration method (total alkalinity at pH = 4.5). The alkalinity measurement procedure is equivalent to the U.S. Geological Survey method in the National Field Manual for the Collection of Water-Quality Data (USGS 2004).

2.1.3 Ammonia Analysis

An ammonia-specific ion-selective electrode (Cole Parmer) connected to an Oakton meter (Cole Parmer) was used to determine the ammonia concentration in simulants and leachates based on ASTM International standard D1426-15. The ammonia electrode was calibrated in conjunction with the Oakton meter using a pre-developed calibration curve with four standard solutions (0.5, 5.0, 50.0, and 500.0 ppm) prepared quantitatively using NIST-certified ammonia standard solution. An aliquot of leachate of about 50 mL was used for ammonia concentration analysis with a stir bar and plate for continuous, gentle stirring. The ammonia electrode was immersed in the solution being stirred in the beaker and positioned at a 20° angle in order to prevent air bubble formation at the membrane level. The ammonia concentration was directly read as mg/L (or ppm) from the Oakton meter screen as soon as the “stable” prompt appeared on the meter screen.

2.1.4 Oxidation Reduction Potential (ORP, E_h) Measurement

A YSI 4210 ORP probe (connected to a YSI MultiLab 4010-3 meter) or a Hanna HI1313B ORP probe (connected to a Hanna HI5521 meter) was used to measure the ORP of the leachate solutions (Manahan 1994). The calibration of the probe was verified with ZoBell’s ORP/Redox standard solution (Hach, +228.5 mV at 20°C). The E_h values discussed in this report were corrected to E_h standard

hydrogen electrode (SHE) values by adding +211 mV to the value measured by a YSI probe with the 3 M KCl reference, or by adding +208 mV to the value measured by a Hanna probe with the 3.5 M KCl reference (Nordstrom and Wilde 2005).

2.1.5 Analysis of Cations, Anions, Hg, ⁹⁹Tc, and ¹²⁷I

Concentrations of major cations in simulant, leachates, and solids' digests were analyzed using inductively coupled plasma optical emission spectroscopy (ICP-OES), while major anions were analyzed using ion chromatography (IC). Concentrations of Hg, ⁹⁹Tc, and ¹²⁷I were analyzed using inductively coupled plasma mass spectrometry (ICP-MS).

2.2 Solid Analysis

The instruments described below were used for identifying elements, minerals, solid-phase morphology, and chemical composition of bulk solid samples.

2.2.1 X-Ray Diffraction (XRD) Analysis

The mineralogy of solid samples was determined using a Rigaku Miniflex II XRD unit equipped with a Cu K α radiation ($\lambda = 1.5418 \text{ \AA}$ with 30 kV and 15 mA) source. For specimens analyzed by μ -XRD (interior material from EQT samples), a Rigaku D/Max Rapid II instrument with an image plate detector was used and X-rays were produced with a MicroMax 007HF generator fitted with a rotating Cr anode ($\lambda = 2.2897 \text{ \AA}$) and focused on the specimen through a 300 μm diameter collimator. The bulk samples were homogenized by grinding in an agate mortar and pestle, then ~10 wt% TiO₂ standard was mixed in. Samples were then loaded into zero background quartz sample holders, held within custom containers with Kapton windows to prevent dispersion of the radiological powders (when present) before scanning from 3 to 100 degrees 2 θ . Mineral identification was performed using Jade software (Materials Data Incorporated, California) with the International Centre for Diffraction Data XRD database. Quantification was performed by the whole pattern fitting (Rietveld) method using Topas software (v5, Bruker AXS, Germany) with the pattern for each phase calculated from published crystal structures (Inorganic Crystal Structure Database, Fachinformationszentrum Karlsruhe, Germany). For most samples, the phase fractions were scaled to 100% and absolute quantities of minerals, and amorphous material by difference, were determined with reference to the TiO₂ standard.

2.2.2 Scanning Electron Microscopy (SEM) and Energy Dispersive Spectroscopy (EDS)

EQT non-radiological specimens were crushed, mounted on an aluminum stub with double-sided carbon tape, and sputter coated with Pt (Polaron Range SC7640, Quorum Technologies Ltd., East Sussex, England) for scanning electron microscopy/energy dispersive spectrometry (SEM/EDS) analysis. The Pt-coated samples were analyzed using a JSM-7001F field emission gun scanning electron microscope (SEM, JEOL USA, Inc., Peabody, MA), and the EDS analysis was done using a Bruker xFlash 6|60 silicon drift detector (Bruker AXS, Inc., Madison, WI). The acceleration voltage during the analysis was 15 kV. For all of the analyses, K α positions were considered for the calculations. The EDS spectra were collected for 20 s each at 80 k – 100 k counts/s. Background noise subtraction and the estimation of atomic ratios were done using ESPRIT software (v1.9, Bruker AXS, Inc.).

For radiological EQT samples, powdered samples were also mounted with double-sided carbon tape attached to an aluminum stub. The sample was coated with a 10 nm carbon layer to improve sample

conductivity, reduce sample charging, and increase SEM image quality. An FEI Quanta 3D SEM was used to provide images of these samples. Particle morphology was examined using a secondary electron detector at an acceleration voltage of 5 to 10 kV and a current of 0.34 nA. Chemical composition data was collected using a backscattering electron detector (BSE) at an acceleration voltage of 30 keV and a current of 2 to 4 nA. Particles were initially screened using the BSE analysis tool, which allowed for fast identification of solids that have a high atomic number (high Z- contrast), e.g., Tc-99. Tc-containing solids could therefore be identified using this approach. EDS elemental mapping was collected on particles of interest using an acquisition time of 60 seconds.

2.2.3 Single Particle Digital Autoradiography (iQID)

The ionizing-radiation Quantum Imaging Detector (iQID) assesses the spatial distribution of ⁹⁹Tc within cross sectioned monolith pucks. Further information regarding development and use of the technique can be found in Miller et al. (2014, 2015). Horizontal pucks (~1" thickness) sectioned from the TB27 and TB28 monoliths were analyzed using the iQID for 48 h encased in Mylar film.

3.0 Simulant Preparation and Analysis

This section describes the simulant production of the EMF evaporator bottoms waste. Simulant preparation details and solution analyses are included.

3.1 Simulant Composition

A screening test was needed to develop cementitious waste forms for EMF evaporator bottoms slurry waste streams that cover a wide projected compositional range of wet electrostatic precipitator–submerged bed scrubber (WESP-SBS) concentrate compositions and to assess whether cured EMF-based waste forms met LDRs. Eight ECS EMF evaporator bottoms waste simulants were prepared with varying boron, chloride, nitrite, and sulfate concentrations to cover a wide range of major salt compositions projected to be generated by DFLAW operations. The range is based on the WESP-SBS concentrates associated with the Vitreous State Laboratory (VSL) DM10 melter and prototypical off-gas system campaigns documented in VSL-12R2640-1, Rev. 0 (Abramowitz et al. 2012). The matrix was also designed for comparison to simulants developed by Savannah River National Laboratory (SRNL), who also used the DM-10 melter campaign as the basis for their testing campaign (Adamson et al. 2017; Reigel et. al. 2017). In addition to the eight ECS simulants, a ninth simulant for EQT testing was prepared with a composition matching the average of the eight ECS simulants. Mathematical estimates of pH adjustments, to attain a caustic pH (~12.7), and concentrations of the nine simulants to achieve ~15% total dissolved solids (TDS) were made to produce the final projected composition of the EMF evaporator concentrates. The final total solids (TS) (dissolved and precipitated), density, and chemical composition of the nine simulant solutions were measured directly (Table 3.3 and Table 3.4).

WRPS provided a simulant design matrix to allow a small set of simulants to be used for this screening phase of cementitious waste form development. The simulant test matrix was drawn from the NIST website for fractional factorial design (<http://www.itl.nist.gov/div898/handbook/pri/section3/pri334.htm>), and the test matrix for a partial factorial design included nominal high and low ranges in combination with each of the four major salt components. The proposed simulant matrix provided by WRPS for the eight ECS simulants is shown in Table 3.1.

Table 3.1. Simulant Design Matrix

Test	Cl	NO ₂	SO ₄	B
T1	Low	Low	Low	High
T2	High	Low	Low	Low
T3	Low	High	Low	Low
T4	High	High	Low	High
T5	Low	Low	High	High
T6	High	Low	High	Low
T7	Low	High	High	Low
T8	High	High	High	High

The species (Cl, NO₂, SO₄, and B) selected for the ECS simulant matrix are those that are both the most significant contributors to the total salt content and also showed a wide range of concentrations in VSL off-gas results that were projected to be in the EMF evaporator bottoms waste concentrate process. For example, VSL concentrates were observed to contain a range of nitrite levels, from non-detect to 30%.

Variable nitrite is expected due to nitrate reduction by organic reductants (e.g., sucrose) added to the vitrification feed. Because some species were present at relatively consistent low levels, such as fluoride, they were not selected as key factors for simulant testing. Once beyond the screening phase of testing, however, fluoride and other constituents should be included in future simulants.

For this test, it was assumed that the nominal density for the 15% TDS EMF evaporator bottoms-waste concentrate is 1,090 g/L.¹¹ The 15% TDS is the maximum indicated in the Bechtel National, Inc. specification for the EMF evaporator bottoms-waste stream.¹² The major salt portion of this solution is $15\% \times 1,090 = 164$ g/L and divided into fourths. The estimated concentrations of each major salt constituent in the test simulants proposed are shown in Table 3.2. The column labeled “Final B ions, Na⁺ & OH⁻” represents the estimated ionic species present at the final pH condition after boric acid neutralization with sodium hydroxide.

Table 3.2. Target Concentration (g/L) of Variable Simulant Species in the Eight ECS Simulants ^(a)

Test	NaCl	NaNO ₂	Na ₂ SO ₄	Final B Ions, Na ⁺ & OH ⁻	Sum
T1	60	0	15	89	164
T2	119	0	15	30	164
T3	55	68	14	27	164
T4	65	41	8	49	163
T5	41	0	61	61	163
T6	82	0	61	20	163
T7	36	55	55	18	164
T8	41	41	41	41	164

(a) Analytically measured simulant concentrations are provided in Table 3.4.

Since LDR compliance of the final solidified waste forms is a key disposal requirement, the metals of concern identified to-date are Zn, Cr, Hg, As, and Se. The first two of these metals were added as salts to the eight ECS simulants and the average EQT simulant at levels of 0.7 g/L of Zn as Zn(NO₃)₂ and 0.3 g/L of Cr as Na₂CrO₄. The latter three metals, Hg, As, and Se, were also added in solid form as a salt (see next section for details), but only to the eight ECS simulants. The estimated spike levels of Hg (~30 mg/L), As (~180 mg/L), and Se (~180 mg/L) in the simulants are based on calculations of spike levels sufficient to allow sample quantification of the concentrate and the TCLP leachates and may be higher than the concentrations expected in the concentrate waste stream. To the EQT average simulant (Avg), ¹²⁷I and ⁹⁹Tc were also added as NaI and NaTcO₄, respectively, both at levels of ~25 mg/L.

3.2 Simulant Preparation

The simulants described in Section 3.1 were prepared in 5 kg or 10 kg quantities. The target TDS concentration for each of the eight simulants was 15 wt% TDS. Due to precipitation of some simulant constituents with time, the term “total solids” (TS) is used to encompass dissolved and precipitated

¹¹ Target density decided by WRPS and communicated in an email sent on November 17, 2016, between Ridha Mabrouki, David Swanberg, John Mahoney (WRPS), Sarah Saslow, Renee Russell, Wooyong Um, Melanie Chiaradia, and Gary Smith (PNNL).

¹² From WTP report 24590-BOF-3PS-MEVV-T0001, Rev 0, *DFLAW Effluent Management Facility Process System (DEP) Evaporator System*, referenced by WRPS in an email sent on November 28, 2016, between Ridha Mabrouki (WRPS) and Sarah Saslow, Wooyong Um, and Renee Russell (PNNL).

simulant solids. The order of chemical addition was determined to be important in preparing these simulants (Cozzi and McCabe 2016) as explained below.

Zinc nitrate was first dissolved in ~100 mL of DIW. Then the required amount of 50 wt% NaOH solution (120 to 600 g) was heated to 40°C to 50°C (nominal estimated temperature of the EMF evaporator). Once the 50 wt% NaOH solution was at temperature, the zinc nitrate solution was added while stirring.

In another beaker, DIW (600 to 2,900 g) was heated to 50°C and the required amount of H₃BO₃ was dissolved while maintaining temperature and with constant stirring. Once the H₃BO₃ dissolved, this solution was slowly combined over the course of ~10 to 15 minutes with the NaOH solution held at 50°C and with continuous mixing. Once these two solutions were combined and mixed, the resultant solution was transferred to a larger container and ~1 L of DIW was added.

Then NaCl and Na₂SO₄ were added to the solution and mixed until fully dissolved. The pH of the solution was then measured using an ORION Star A215 pH meter to ensure that it was basic, ≥ 12.7 . Once this was confirmed, the Na₂CrO₄, NaNO₂, As₂O₃, SeO₂, Hg(NO₃)₂•H₂O, and/or NaI were added individually to the solution in the order listed and mixed until fully dissolved before adding the next salt. However, the Hg(NO₃)₂•H₂O precipitated almost immediately after addition to the eight ECS simulants. Once all salts (except Hg(NO₃)₂•H₂O) were dissolved, DIW was added to just below the target weight and allowed to cool to room temperature overnight.

Once at room temperature, the pH was measured again to ensure the pH was ≥ 12.7 . DIW was then added to reach the target weight, and the pH checked again to ensure that the pH was still ≥ 12.7 . At this point, the simulant was mixed for several hours before subsamples were taken for analysis by IC, ICP-OES, ICP-MS, and to determine the simulant density and TS. The final simulant was then transferred to a 10 L carboy.

Aliquots of Avg simulant used to produce EQT waste forms were spiked with NaTcO₄ immediately before use. A sub-sample of the ⁹⁹Tc-spiked aliquots was taken for ICP-MS analysis to confirm the initial ⁹⁹Tc concentration in the simulant. Due to the small volume of aqueous NaTcO₄ added to these aliquots, all other constituent concentrations are assumed to be the same as those analyzed in the ⁹⁹Tc-free sub-samples analyzed in the previous step.

3.3 Simulant Observations and Analytical Results

It was noticed during the preparation of the eight ECS simulants that the Hg compound precipitated out of solution almost immediately after addition. This is likely due to the high levels of hydroxide present that are known to precipitate Hg as HgO (Qian et al. 2003), which is resistant to re-dissolution. Furthermore, after allowing the simulants to sit for several days, another dark precipitate began to form at the bottom of each of the eight ECS simulant carboys. Low analytical Zn values in simulants with longer wait times between preparation and analysis suggest that zinc compounds precipitated over this course of time. This suggests that the amount of zinc added to the simulants is above the solubility limit for some Zn compound(s), thus causing it to precipitate. Additionally, Zn precipitation was most evident in simulants with low boron levels. Precipitation of any solid was not observed in the Avg simulant used in EQT formulations.

In Table 3.3, the measured pH, density, and wt% TS for each simulant are provided. Table 3.4. shows the IC and ICP-OES analytical data for the simulants. The measured simulant compositions were all within the expected range and showed no peculiarities. Results are reported as “Batched,” “Initial Analytical,” or “Final Analytical.” The “Batched” concentrations are the expected concentrations for each simulant

according to mass balance calculations. “Initial Analytical” results were determined from simulant aliquots directly, whereas the “Final Analytical” results were determined from acid digested simulant aliquots as described later in this section (ECS simulants only). The final analytical results for constituents Cr, As, and Se were within 15% of the batched values along with the major salt components (B, Cl, SO₄, and NO₂). For the Avg simulant, ¹²⁷I was within 20% of the target concentration and ⁹⁹Tc was within 26% of the target for both aliquots analyzed.

When the ECS simulants had a short wait time (<3 days, Table 3.5) between preparation and the initial analytical measurement, the Zn values were within 10% of the target. However, as this time increased to >3 days, the amount of Zn measured in the supernatant decreased, likely due to Zn precipitation. In some cases this decrease in the initial analytical value was greater than 200 mg/L. However, for the final analytical measurements a decrease in Zn to as low as 132 mg/L was measured (Simulant 7). Low simulant Zn concentrations were observed to correlate with low boron simulants, where the Zn concentration measured in Simulant 7 was 132 mg/L and the boron concentration was 1,612 mg/L. This trend is also observed in Simulants 2, 3, and 6. These four low boron simulants were also observed to contain the most precipitates. One challenge with precipitation is collecting a representative simulant subsample for solution analysis and may contribute to the low concentrations reported in Table 3.4. It is important to note that solids were not observed in the Avg simulant and the final Zn concentration was within 6% of the batched (target) concentration of 700 mg/L.

The initial Hg concentration measured in all eight ECS simulants differed from the target Hg concentration, 30 mg/L, by more than 10% (regarded here as a reasonable uncertainty range) regardless of the time between preparation and analysis. While the exact cause of the low measured Hg concentrations remains unclear, Hg loss could be attributed to adhesion to reaction, containment, and analysis vessels or sampling errors due to the low Hg concentration relative to other constituents and immediate precipitation of Hg.

To determine whether Hg loss was due to precipitation or subsequent inaccurate sampling/analysis, the simulant aqueous phase (filtrate) and solid phase (precipitate) were analyzed separately for the eight ECS simulants. Simulants were thoroughly mixed before a 10 mL slurry aliquot was taken. The slurry aliquot was filtered using pre-weighed filter paper for mass-balance calculations. The supernate was analyzed within 24 h and the solids were dried at room temperature for over 24 h, with the mass checked periodically to make sure drying was complete after the 24 h drying period. The solid (14 – 38 mg) was then digested in 10 mL of concentrated nitric acid and 10 mL of DIW, and analyzed within 24 h. Unfortunately, the calculated Hg concentration was still determined to be very low, as shown in Table 3.6 for Simulant 1. This is likely due to inaccuracy in the testing method, since Zn was also determined to be almost an order of magnitude less than the target concentration (700 mg/L, Table 3.6). Since Zn is not expected to volatilize or react with the containment vessels, all Zn should have been accounted for between the solid and filtrate phases if the mass balance test method was successful.

Table 3.3. Final Measured Simulant pH, Density, and wt% TS Results

Simulant	pH	Density (g/mL)	Wt% TS
	Target pH \geq 12.7	Target = 1.09 g/mL	Target = 15 wt%
Simulant 1	13.55	1.14	16.02
Simulant 2	13.02	1.12	15.70
Simulant 3	13.03	1.12	15.48
Simulant 4	13.27	1.12	15.47
Simulant 5	13.35	1.14	16.07
Simulant 6	12.92	1.12	15.52
Simulant 7	12.82	1.12	15.33
Simulant 8	13.15	1.12	15.30
Avg Simulant	13.19	1.12	15.35

As a second approach for determining the actual concentration of Hg and Zn in the ECS simulants, acid digestion of an aliquot of the total slurry was performed. Three separate, homogeneous slurry aliquots were taken from Simulant 1. Two aliquots were spiked with an additional 21.5 mg/L Hg and 30 mg/L Hg, respectively, from a 1,000 mg/L Hg-spike solution made from $\text{Hg}(\text{NO}_3)_2 \cdot x\text{H}_2\text{O}$ in 2% HNO_3 . The first spike concentration, 21.5 mg/L Hg, was selected to increase the simulant Hg concentration to the target concentration, 30 mg/L Hg, while accounting for the measured Hg already present in Simulant 1, 8.5 mg/L Hg, according to results reported in Table 3.6. The second spike concentration, 30 mg/L Hg, was selected to test the accuracy of the spiking procedure and evaluate possible matrix effects. A third total slurry aliquot did not receive any Hg spike and was used to cross-check the initial Hg concentration in Simulant 1. The slurry samples were directly acid digested with dilute nitric acid, to a final HNO_3 level of ~6% in the subsample, and analyzed for Hg and Zn within 24 to 48 h of preparation (Table 3.7). These results showed that Zn was present within $\pm 10\%$ of the target value, 700 mg/L. For the subsamples spiked with Hg, results show that the final Hg concentration was within $\pm 10\%$ of the spike target (30 mg/L or 38.5 mg/L) and suggest that the Hg-spike method can be used to adjust the simulant Hg concentration as needed. For the subsample analyzed without added Hg spike, Hg was present at 14.7 ppm, slightly higher than originally determined (8.5 ppm).

Based on these results, it is evident that by spiking the simulant with $\text{Hg}(\text{NO}_3)_2 \cdot x\text{H}_2\text{O}$ in 2% HNO_3 immediately before waste form production or analysis, the target Hg concentration can be obtained. Since the direct cause of Hg loss remains unknown, each simulant aliquot prepared for ECS test batches was spiked separately, immediately before adding dry ingredients during waste form formulation. A spike solution of 10,000 mg/L Hg (added as $\text{Hg}(\text{NO}_3)_2 \cdot x\text{H}_2\text{O}$) in 2% HNO_3 was used to decrease the total spike volume added to the ECS simulants and to keep the water/dry mix ratio within the target range. The Hg spike increased the initial Hg concentration in the simulant aliquot by 40 mg/L to account for possible loss during waste form development. The final Hg concentration in the simulant aliquot was determined from a subsample taken while mixing and within 1 minute after adding the Hg spike. Exceeding the target Hg concentration (30 mg/L) helped make sure that the final concentration met the target concentration necessary for TCLP analysis. The final measured compositions of the eight Hg-spiked simulants at the time of grout production are shown in Table 3.4 under “Final Analytical.”

Table 3.4. Analytical (Measured) Results of Final Simulants

Constituent ^(a)	Simulant 1				Simulant 2				Simulant 3			
	Batched (mg/L)	Initial Analytical (mg/L)	Final Analytical (mg/L)	% Difference (Final vs. Batched)	Batched (mg/L)	Initial Analytical (mg/L)	Final Analytical (mg/L)	% Difference (Final vs. Batched)	Batched (mg/L)	Initial Analytical (mg/L)	Final Analytical (mg/L)	% Difference (Final vs. Batched)
B	8,410	7,660	7,838	-7	2,692	2,500	2,506	-7	2,508	2,330	2,495	-1
Na	69,355	68,600	63,664	-8	65,855	62,500	60,720	-8	62,676	62,600 ^(b)	59,248	-5
Zn	732	679	673	-8	718	686	375	-48	718	638	294	-59
Cr	313	302	296	-5	308	289	286	-7	308	278	263	-15
As	188	179	194	3	185	178	191	3	184	187	193	5
Se	189	196	185	-2	185	185	180	-3	184	174	182	-1
Hg	31	18.7	39	27	31	16	38	23	32	9.61	60	86
Cl	38,064	38,300	38,300	0.6	74,091	76,500	76,500	3.3	34,191	34,900	34,900	2.1
NO ₂	0	ND ^(c)	ND ^(c)	-	0	ND ^(c)	ND ^(c)	-	46,459	42,200 ^(b)	42,200	-9.2
SO ₄	10,611	10,600	10,600	-0.1	10,412	10,400	10,400	-0.1	9,702	9,970	9,970	2.8
Constituent ^(a)	Simulant 4				Simulant 5				Simulant 6			
	Batched (mg/L)	Initial Analytical (mg/L)	Final Analytical (mg/L)	% Difference (Final vs. Batched)	Batched (mg/L)	Initial Analytical (mg/L)	Final Analytical (mg/L)	% Difference (Final vs. Batched)	Batched (mg/L)	Initial Analytical (mg/L)	Final Analytical (mg/L)	% Difference (Final vs. Batched)
B	4,500	4,120	4,269	-5	5,650	5,470	5,299	-6	1,797	1,680	1,777	-1
Na	65,855	63,400 ^(b)	61,088	-7	63,848	64,200 ^(b)	59,984	-6	62,802	58,100 ^(b)	58,880	-6
Zn	721	698 ^(b)	644	-11	730	725	651	-11	720	471	221	-69
Cr	309	288	262	-15	313	313	290	-7	309	310	289	-7
As	186	195	192	3	188	194	195	4	186	191	194	4
Se	186	184	180	-3	188	181	191	1	186	186	191	3
Hg	31	5	46	48	31	12	60	95	31	2	43	38

Constituent ^(a)	Simulant 4				Simulant 5				Simulant 6			
	Batched (mg/L)	Initial Analytical (mg/L)	Final Analytical (mg/L)	% Difference (Final vs. Batched)	Batched (mg/L)	Initial Analytical (mg/L)	Final Analytical (mg/L)	% Difference (Final vs. Batched)	Batched (mg/L)	Initial Analytical (mg/L)	Final Analytical (mg/L)	% Difference (Final vs. Batched)
Cl	40,634	41,400	41,400	1.9	25,922	27,100	27,100	4.5	51,161	52,500	52,500	2.6
NO ₂	28,149	27,000	27,000	-4.1	0	ND ^(c)	ND ^(c)	-	0	ND ^(c)	ND ^(c)	-
SO ₄	5,584	5,670	5,670	1.5	42,993	44,700	44,700	4.0	42,426	43,400	43,400	2.3
Constituent ^(a)	Simulant 7				Simulant 8				Avg Simulant			
	Batched (mg/L)	Initial Analytical (mg/L)	Final Analytical (mg/L)	% Difference (Final vs. Batched)	Batched (mg/L)	Initial Analytical (mg/L)	Final Analytical (mg/L)	% Difference (Final vs. Batched)	Batched (mg/L)	Initial Analytical (mg/L)	Final Analytical (mg/L)	% Difference (Initial vs. Batched)
B	1,614	1,560	1,612	0	3,787	3,550	3,533	-7	3,855	3,560	-	-7.7
Na	59,597	57,800	57,040	-4	62,137	59,700	58,880	-5	64,206	58,600	-	-8.7
Zn	718	488	132	-82	722	675	648	-10	721	680	-	-5.7
Cr	308	316	291	-5	309	300	289	-7	309	305	-	-1.4
As	185	186	198	7	186	182	195	5	-	-	-	-
Se	185	192	196	6	186	195	190	2	-	-	-	-
Hg	31	19.3	65	109	31	45	53	71	-	-	-	-
Cl	22,395	23,400	23,400	4.5	25,649	26,200	26,200	2.1	38,992	39,990	-	2.3
NO ₂	37,600	32,900	32,900	-12.5	28,189	26,900	26,900	-4.6	17,584	17,000	-	-3.3
SO ₄	38,141	39,700	39,700	4.1	28,593	29,300	29,300	2.5	23,549	24,000	-	1.9
¹²⁷ I	-	-	-	-	-	-	-	-	26	20.8	-	-20
⁹⁹ Tc	-	-	-	-	-	-	-	-	25	18.3 ± 0.2 ^(d)	-	-27

(a) RCRA metals Cr, As, Se, and Hg added as Na₂CrO₄, As₂O₃, SeO₂, and Hg(NO₃)₂•xH₂O salts. Additional Hg added as Hg(NO₃)₂•xH₂O in 2% HNO₃.

(b) Concentration from replicate sample analyzed 4 days after preparation for analysis (Table 3.5).

(c) ND = not detected

(d) Average ⁹⁹Tc concentration based on the ⁹⁹Tc concentration determined from the aliquot used to make test batches TB27 (18.1 mg/L ⁹⁹Tc) and TB28 (18.5 mg/L ⁹⁹Tc), 1σ standard deviation reported

Table 3.5. Time Between Preparation and Analysis of Simulant Subsamples

Simulant	Prepared	Received	Analytical Sample Prepared	Analytical Sample Analyzed
1	Feb. 6	Feb. 9	Feb. 10	Feb. 10
2	Feb. 7	Feb. 9	Feb. 10	Feb. 10
3 (Replicate)	Jan. 31	Feb. 3 (Feb. 3)	Feb. 6 (Feb. 6)	Feb. 6 (Feb. 10)
4 (Replicate)	Feb. 1	Feb. 3 (Feb. 3)	Feb. 6 (Feb. 6)	Feb. 6 (Feb. 10)
5 (Replicate)	Feb. 1	Feb. 3 (Feb. 3)	Feb. 6 (Feb. 6)	Feb. 6 (Feb. 10)
6 (Replicate)	Feb. 2	Feb. 3 (Feb. 3)	Feb. 6 (Feb. 6)	Feb. 6 (Feb. 10)
7	Feb. 6	Feb. 9	Feb. 10	Feb. 10
8	Feb. 7	Feb. 9	Feb. 10	Feb. 10
Avg	Feb. 8	Feb. 9	Feb. 9	Feb. 9, 10, 23 ^(a)

(a) Feb. 9: ICP-MS metals analysis, Feb. 10: ICP-OES and IC analysis, Feb. 23: ICP-MS for ¹²⁷I analysis.

Replicate samples indicate two sub-samples analyzed from the original simulant aliquot taken for analysis. Replicate sub-samples were analyzed 4 days after the original sub-sample.

Table 3.6. Solution and Solid Phase Analysis on Simulant 1

Chemical	Simulant 1		
	Target ^(a) (ppm)	Batched ^(b) (ppm)	Filtrate + Solids Phase ^(c) (ppm)
Zn	700	732	84 ± 15
Hg	30	33	8.5 ± 1.1

(a) Target: the concentration outlined in TP-SWCS-0019, Rev. 0.1

(b) Batched: the concentration calculated from the chemical mass added during simulant production

(c) Average of duplicate samples, 1σ standard deviation reported

Table 3.7. Acid Digest of Simulant 1 with Hg Spike

Chemical	Simulant 1				
	Target (ppm)	Batched (ppm)	Acid Digest No Spike (ppm)	Acid Digest 21.5 ppm Hg Spike (ppm)	Acid Digest 30 ppm Hg Spike (ppm)
Zn	700	732	722	711	708
Hg	30	33	14.7	30.4 ^(a)	36.8 ^(b)

(a) Target concentration was 30 ppm (21.5 ppm spike + 8.5 ppm (Table 3.6).

(b) Target concentration was 38.5 ppm (30 ppm spike + 8.5 ppm (Table 3.6).

Efforts were made to maintain ECS simulants without precipitates, to avoid precipitates settling during preparation of the grout waste forms and to achieve more homogeneous waste forms. This was especially important since contaminants leach differently depending on whether they are immobilized within the waste form as part of the aqueous phase or as precipitates. Unfortunately, without altering the chemistry of the simulants already prepared, precipitate dissolution via heating was the least disruptive method

available to minimize impacts of precipitates in the simulants. A subsample of Simulant 6, which visually appeared to have the most precipitates present, was heated in a glass beaker covered with a watch glass at $\sim 50^{\circ}\text{C}$ for several hours while stirring. After heating, some precipitates still remained; however, the precipitate had turned from black to white, as shown in Figure 3.1. Since the majority of the precipitate is hypothesized to be Zn compounds, and zinc chromate (ZnCrO_4) is dark in color, this observation suggests that heating the simulant may cause the ZnCrO_4 to react with and/or dissolve into solution. If Zn bound in ZnCrO_4 precipitates does not dissolve, it likely forms ZnO (white) following Cr dissolution. However, it is difficult to conclude whether the white precipitates remaining after heat treatment, proposed to be ZnO, formed as a result of ZnCrO_4 reactions or were already present.



Figure 3.1. Simulant 6 Precipitate after Heating at $\sim 50^{\circ}\text{C}$ for Several Hours

Since the precipitates could not be dissolved by heating, kinetic information was needed to determine how soon a simulant needed to be used before precipitate formation occurred. To do this, a 1 L batch of Simulant 6 was prepared without Hg and observed over time. Simulant 6 was chosen, again, since it visually appeared to be one of the simulants with the most precipitates present. Three hours after preparation, no precipitates were observed; however, the next morning (~ 20 hours after preparation) precipitates had started to form and the amount of precipitate increased with time (Figure 3.2). After 70 hours, 40 ppm of Hg ($\text{Hg}(\text{NO}_3)_2 \cdot x\text{H}_2\text{O}$ in 2% HNO_3) was added to visually determine if the presence of the Hg had an effect on the Zn precipitation, but no effect was observed. Based on this test, it was determined that the cumulative time required to make fresh simulants, allow the simulants to cool to room temperature, and complete grout production would be more than the grout processing facility unit operations could allow and therefore the original simulants would be used.

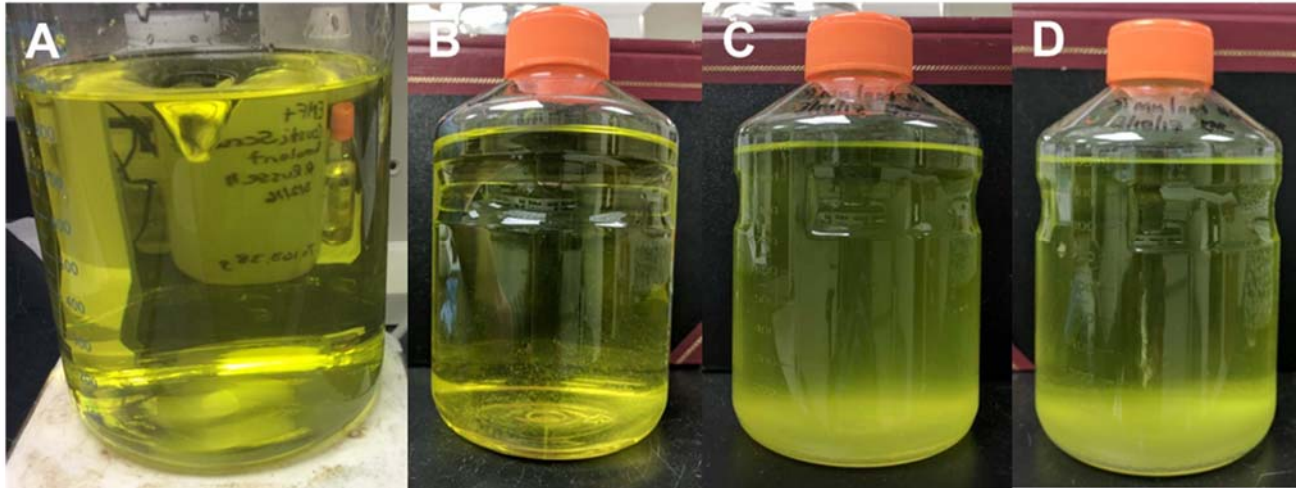


Figure 3.2. Precipitate Formation in a 1 L Batch of Simulant 6 as a Function of Time. Photos taken (A) immediately after simulant preparation was complete and (B) 20 hours, (C) 49 hours, and (D) 70 hours after simulant production. After 70 hours (D), 40 ppm of Hg was spiked into the simulant before observation.

Again, it is important to note that the precipitates observed in the eight ECS simulants were not observed in the Avg simulant used to prepare EQT waste forms.

3.4 Simulant Preparation Conclusions

All ECS simulants contained precipitates, of varying amounts, that could not be completely re-dissolved with heat and mixing. This suggests that the composition matrix of the ECS simulants exceeded the Zn solubility limit, causing Zn to precipitate at room temperature over time. Low simulant Zn concentrations were observed to correlate with low boron simulants, Simulants 2, 3, 6, and 7. These four low-boron simulants were also observed to contain the most precipitates. The EQT Avg simulant, however, did not contain precipitates despite containing ~700 ppm Zn and was within 6% of the target Zn concentration.

Initial analytical results for the eight ECS simulants indicate varying degrees of Hg loss from all but one simulant. The exact cause of Hg loss remains unclear, but could be attributed to 1) Hg adhesion to reaction, containment, and analysis vessels; 2) sampling errors due to the low Hg concentration relative to other constituents; or 3) immediate precipitation of Hg. Based on subsequent testing, using a spike of $\text{Hg}(\text{NO}_3)_2 \cdot x\text{H}_2\text{O}$ in 2% HNO_3 to increase the total Hg concentration in simulant aliquots, it was decided that each simulant aliquot would be spiked with 40 ppm of Hg immediately before grout formulation to help make sure the correct concentration of Hg was present in the simulant during waste form production. An aliquot of the final Hg-spiked simulant was taken and preserved in nitric acid for final metal and compositional analysis.

Efforts to prepare ECS simulants without precipitates, either by heating to dissolve precipitates or by preparing fresh simulant batches for use before the formation of precipitates, were unsuccessful. Future work should evaluate precipitate formation as a function of the variables tested in the test matrix provided by WRPS, both by computational modeling and by additional liquid- and solid-phase analytical methods.

Finally, in the Avg simulant used in EQT formulations, ^{127}I (a surrogate for ^{129}I) and ^{99}Tc were added to the simulant in addition to Zn and Cr. Although the target concentration for both ^{127}I and ^{99}Tc was 25 mg/L, the final concentration in the simulant was 20.8 mg/L ^{127}I and between 18.1 and 18.5 mg/L ^{99}Tc .

(depending on the spiked aliquot of simulant prepared for test batches TB27 and TB28). The 20% to 26% difference in ^{127}I and ^{99}Tc concentrations relative to the target is slightly higher than expected, but did not cause detection limit issues when performing contaminant leach testing as described in later sections of this report.

4.0 Grout Formulation and Sample Preparation

Twenty-four ECS EMF evaporator bottoms waste grout batches were prepared for the EMF evaporator bottoms waste streams formulation and waste form testing activities performed in FY 2017. A designed grout test matrix (Table 4.1) was used to evaluate the effects of key EMF simulant and grout mix parameters on the properties of the grout during and after curing. Each of the 24 unique monolith formulations prepared varies at least one key parameter. Parameters tested include simulant composition (see Section 3.0) and dry ingredient composition. Dry ingredients include OPC, FA, Aquaset II-GH® (Aquaset), and BFS. The OPC, FA, and BFS are the baseline dry ingredients used in the original Cast Stone formulation, while the new grout formulations were prepared with 1:4 ratios of either Aquaset or OPC mixed with BFS. For all 24 formulations, the dry ingredients listed in Table 4.1 were thoroughly mixed and then added to the identified liquid simulant.

The baseline grout dry mix was the original Cast Stone formulation, containing 8 wt% OPC, 45 wt% FA, and 47 wt% BFS, and was used to form monolith test batches 1 through 8. Test batches 9 through 16 contained a 1:4 ratio of Aquaset and BFS (20 wt% Aquaset and 80 wt% BFS) and test batches 17 through 24 contained a 1:4 ratio of OPC and BFS (20 wt% OPC and 80 wt% BFS). To improve slurry flowability, a water-reducing additive (WRA; MasterGlenium 3030 from BASF) was added (as needed), based on a ratio of 0.6 mL of WRA per 100 grams of dry mix (maximum total in any grout batch = 10.5 mL), to monolith formulations immediately after mixing the dry ingredients and selected simulant.

Each of the three dry ingredient formulations was tested against all eight simulant compositions (Table 3.4), which had varying boron, chloride, nitrite, and sulfate concentrations. All of the ECS grout monolith specimens were cured at least 7 days and up to 28 days at room temperature and 80% – 100% relative humidity. One specimen from each test batch was visually monitored over the course of this curing period for the presence of free liquids (see Section 4.0 for details). After 7 days of curing, one monolith specimen from each of the 24 formulations was sent to SwRI, a laboratory certified for performing TCLP analysis under project QA requirements (Section 1.3). Other 28-day cured ECS monolith specimens were archived for future testing and characterization.

In addition to the twenty four ECS test batches, eight EQT test batches were prepared according to the test matrix shown in Table 4.2. In EQT, the original Cast Stone formulation and an HL recipe were tested. To determine the final HL formulation recipe, three “pre-screening” test batches were prepared at varying HL mass contents while maintaining a 4:1 ratio of BFS to OPC: 10 wt% HL (test batch #26.1a), 30 wt% HL (test batch #26.1b), and 50 wt% HL (test batch #26.1c). These three “pre-screening” test batches were evaluated for free liquids and flowability, as described later in this section. The selected formulation, TB 26.1a containing 10 wt% HL, was chosen based on this evaluation because it had the least excess water (free liquids) and maintained flow properties that would facilitate pouring into waste form molds/containers. The 10 wt% HL content was also used in test batches 26.2 and 28.

It is important to note, that due to the increased number of specimens needed to complete physical properties testing for EQT test batches (non-radiological test batches only), duplicate test batches were prepared for both the Cast Stone (test batches 25.1 and 25.2) and HL (26.1a and 26.2) formulations. Furthermore, as with the ECS test batches, a WRA (MasterGlenium 3030 from BASF) was added (as needed), based on a ratio of 0.6 mL of WRA per 100 g of dry mix (maximum total in any grout batch = 10.5 mL), to monolith formulations immediately after blending together the dry ingredients and simulant.

EQT test batches were also cured for at least 7 and up to 28 days at room temperature and 80% to 100% relative humidity. Immediately after mixing, one specimen from each of the final four non-rad test batches (25.1, 25.2, 26.1a, and 26.2) was used to evaluate waste form set time (see Section 5.1). An additional monolith from each of the non-rad test batches (25.1, 25.2, 26.1a, and 26.2) was visually monitored over the course of this curing period for the presence of free liquids (see Section 5.2 for details). After 7 days of curing, one monolith specimen from each of the final six test batches was sent to SwRI for TCLP analysis (see Section 7.0 for details). Other 28-day cured EQT monolith specimens were archived for additional testing and characterization.

Table 4.1. Liquid Secondary Waste Grout Test Matrix for ECS

Test Batch #	Simulant	Water-to-Dry Mix (w/dm) Ratio	Dry Blend Addition	Dry Materials	FA ^(a) (g)	OPC ^(a) (g)	BFS ^(a) (g)	Aquaset II-GH ^(a) (g)	Simulant Mass ^(b) (g)	WRA ^(c) (mL)
1	T1	0.5	8%, 45%, 47%	OPC, FA, BFS	787.50	140.00	822.50	0.00	1,029.4	10.5
2	T2	0.5	8%, 45%, 47%	OPC, FA, BFS	787.50	140.00	822.50	0.00	1,029.4	10.5
3	T3	0.5	8%, 45%, 47%	OPC, FA, BFS	787.50	140.00	822.50	0.00	1,029.4	10.5
4	T4	0.5	8%, 45%, 47%	OPC, FA, BFS	787.50	140.00	822.50	0.00	1,029.4	10.5
5	T5	0.5	8%, 45%, 47%	OPC, FA, BFS	787.50	140.00	822.50	0.00	1,029.4	10.5
6	T6	0.5	8%, 45%, 47%	OPC, FA, BFS	787.50	140.00	822.50	0.00	1,029.4	10.5
7	T7	0.5	8%, 45%, 47%	OPC, FA, BFS	787.50	140.00	822.50	0.00	1,029.4	10.5
8	T8	0.5	8%, 45%, 47%	OPC, FA, BFS	787.50	140.00	822.50	0.00	1,029.4	10.5
9	T1	0.5	20%, 80%	Aquaset ^d , BFS	0.00	0.00	1,400.00	350.00	1,029.4	10.5
10	T2	0.5	20%, 80%	Aquaset ^d , BFS	0.00	0.00	1,400.00	350.00	1,029.4	10.5
11	T3	0.5	20%, 80%	Aquaset ^d , BFS	0.00	0.00	1,400.00	350.00	1,029.4	10.5
12	T4	0.5	20%, 80%	Aquaset ^d , BFS	0.00	0.00	1,400.00	350.00	1,029.4	10.5
13	T5	0.5	20%, 80%	Aquaset ^d , BFS	0.00	0.00	1,400.00	350.00	1,029.4	10.5
14	T6	0.5	20%, 80%	Aquaset ^d , BFS	0.00	0.00	1,400.00	350.00	1,029.4	10.5
15	T7	0.5	20%, 80%	Aquaset ^d , BFS	0.00	0.00	1,400.00	350.00	1,029.4	10.5
16	T8	0.5	20%, 80%	Aquaset ^d , BFS	0.00	0.00	1,400.00	350.00	1,029.4	10.5
17	T1	0.5	20%, 80%	OPC, BFS	0.00	350.00	1,400.00	0.00	1,029.4	10.5
18	T2	0.5	20%, 80%	OPC, BFS	0.00	350.00	1,400.00	0.00	1,029.4	10.5
19	T3	0.5	20%, 80%	OPC, BFS	0.00	350.00	1,400.00	0.00	1,029.4	10.5
20	T4	0.5	20%, 80%	OPC, BFS	0.00	350.00	1,400.00	0.00	1,029.4	10.5
21	T5	0.5	20%, 80%	OPC, BFS	0.00	350.00	1,400.00	0.00	1,029.4	10.5
22	T6	0.5	20%, 80%	OPC, BFS	0.00	350.00	1,400.00	0.00	1,029.4	10.5
23	T7	0.5	20%, 80%	OPC, BFS	0.00	350.00	1,400.00	0.00	1,029.4	10.5
24	T8	0.5	20%, 80%	OPC, BFS	0.00	350.00	1,400.00	0.00	1,029.4	10.5

(a) Dry ingredients were mixed together in a closed plastic bag, and the bag was manipulated until the dry mixture appeared to be homogeneous.

(b) Simulant mass calculated assuming 15 wt% TS, a density of 1.09 g/mL, and a required water mass of 875 g.

(c) WRA: MasterGlenium 3030 (MG 3030) from BASF used as needed, up to 0.6 mL of MG 3030 per 100 g of dry mix, to enhance the cement rheology.

(d) Aquaset II-GH[®] (Fluid Tech, LLC.) is a 1:1 blend of granular sepiolite and OPC with <3% quartz.

Table 4.2. Liquid Secondary Waste Grout Test Matrix for EQT

Test Batch #	Simulant	Water-to-Dry Mix (w/dm) Ratio	Dry Blend Addition	Dry Materials	FA ^(a) (g)	OPC ^(a) (g)	BFS ^(a) (g)	HL ^(a) (g)	Simulant Mass ^(b) (g)	⁹⁹ Tc	WRA ^(c) (mL)
25.1 ^(d)	Avg	0.5	8%, 45%, 47%	OPC, FA, BFS	787.5	140.0	822.5	0.0	1,029.4	-	10.5
25.2 ^(d)	Avg	0.5	8%, 45%, 47%	OPC, FA, BFS	787.5	140.0	822.5	0.0	1,029.4	-	10.5
26.1a ^(d)	Avg	0.5	10%, 18%, 72%	HL, OPC, BFS	0.0	315.0	1,260.0	175.0	1,029.4	-	10.5
26.1b ^(d)	Avg	0.5	30%, 14%, 56%	HL, OPC, BFS	0.0	245.0	980.0	525.0	1,029.4	-	10.5
26.1c ^(d)	Avg	0.5	50%, 10%, 40%	HL, OPC, BFS	0.0	175.0	700.0	875.0	1,029.4	-	10.5
26.2 ^(d)	Avg	0.5	10%, 18%, 72%	HL, OPC, BFS	0.0	315.0	1,260.0	175.0	1,029.4	-	10.5
27 ^(e)	Avg-Rad	0.5	8%, 45%, 47%	OPC, FA, BFS	787.5	140.0	822.5	0.0	1,029.4	⁹⁹ Tc	10.5
28 ^(e)	Avg-Rad	0.5	10%, 18%, 72%	HL, OPC, BFS	0.0	315.0	1,260.0	175.0	1,029.4	⁹⁹ Tc	10.5

(a) Dry ingredients were mixed together in a closed plastic bag, and the bag was manipulated until the dry mixture appeared to be homogeneous.

(b) Simulant mass calculated assuming 15 wt% TS, a density of 1.09 g/mL, and a required water mass of 875 g.

(c) WRA: BASF 3030 may be used to enhance the cement rheology based on 0.6 mL of BASF 3030 per 100 g of dry mix, if needed.

(d) Tests batch #25.1-26.2 prepared as non-⁹⁹Tc-spiked waste form specimens.

(e) Test batch #27 and 28 prepared as ⁹⁹Tc-spiked waste form specimens.

4.1 Preparation of EMF Evaporator Bottoms-Waste Monoliths

Liquid simulant and blended dry ingredients were prepared separately and then combined to prepare the grout specimens. The select dry materials (either [1] OPC, FA, and BFS; [2] Aquaset and BFS; [3] OPC and BFS; or [4] HL, OPC, BFS) were measured, according to the masses specified in advance, into a plastic bag and mixed by manipulating the closed plastic bag until the dry mixture appeared to be homogeneous by visual observation. Aliquots of simulants were also taken from each respective batch at the masses specified in Table 4.1 and Table 4.2. One target w/dm ratio of 0.5 g/g was used for all ECS and EQT monoliths.

4.1.1 Dry Ingredients

The grout monoliths were made using two or three of the five primary dry ingredients, blended together in different ratios. OPC and BFS used in this work were supplied by Lafarge North America, Inc., in Pasco, Washington. According to the OPC mill test report, R-TI-15-04, this is a Type I/II Portland cement produced in Richmond, British Columbia. The BFS, commonly referred to by the trade name NewCem®, meets ASTM C989/C989M-18 requirements for class 100 ground granulated BFS and was processed at Lafarge's Seattle, Washington, plant. The FA used in this work qualifies as both class F and class C FA and was sourced from the Centralia, Washington, power plant. The OPC, BFS, and FA are the same materials used in previous work detailed in Westsik et al. (2013), Serne et al. (2015), and Um et al. (2016). Aquaset II-GH® (Aquaset) is a primary blend of granular sepiolite and OPC and was purchased from Fluid Tech, LLC in Montpelier, Idaho. HL, calcium hydroxide ($\text{Ca}(\text{OH})_2$), was sourced from the Graymont Rivergate facility in Portland, Oregon, and is the same material used in previous work published in Saslow et al. (2017). Each of the dry materials was sent to SwRI to be digested and analyzed for total metals in order to determine the material composition. Individual dry material compositions are reported in Appendix A, Section A.2.

4.1.2 Grout Mixing/Monolith Production

Grout mixing and monolith production followed the procedure outlined in Westsik et al. (2013) and Um et al. (2016).

4.1.2.1 Grout Mixing Summary

Grout mixing and monolith production followed this general outline:

1. place required quantity of simulant into mixing vessel
2. add blended mix of dry ingredients to stirring simulant, 5-minute target duration to complete addition
3. add MG 3030 (if needed) to wetted dry-blend-simulant slurry
4. continue mixing, total of 15 minutes from start of step 2
5. pour well mixed slurry into plastic forms
6. de-air filled plastic forms
7. cure at least 7 days in a humid environment at room temperature.

4.1.2.2 Grout Monolith Production

Grout mixing was performed with a Caframo BDC1850 variable speed overhead stirrer. This style of mixer was used to accommodate a custom 3.5" diameter impeller designed and provided by SRNL. The impeller and mixer head were joined by a 3/8" shaft and the combined mixer apparatus was supported by a Caframo A210 heavy-duty stand and A120 heavy-duty clamp. The mixer shaft was lowered into a 2 L plastic mixing beaker containing the desired aliquot of simulant until the bottom of the impeller was between 0.75" and 1.25" from the bottom of the beaker. The beaker was offset from the mixer shaft so that the impeller was between 0.25" and 0.5" from one sidewall. This offset helped to minimize the creation of a central vortex, and thus air entrainment, during mixing. With the beaker of simulant in place under the mixer, the mixer's stirrer was started at about 200 rpm. Vortex creation and modest air entrainment was acceptable at this point. With the mixer's stirrer turning at about 200 rpm, 4.545 mL of 10,000 ppm Hg spike (in 2% nitric acid) solution was added to the simulant and allowed to mix for ~1 minute (ECS test batches 1 – 24 only). For EQT test batches 27 and 28, 2.360 mL of 10,000 ppm ⁹⁹Tc stock solution (as NH₄TcO₄) was added to each simulant aliquot while stirring the simulant at 200 rpm. Then a 10 mL subsample was taken for additional simulant characterization (Figure 4.1, left) before slowly adding the desired bag of blended dry ingredients to the simulant. To facilitate clean transfer from the bag to the beaker, a 2" diagonal cut was made across one corner of the bag. This corner opening funnels the dry pre-mix into the desired location in the beaker and allows for good control during addition to the beaker. A timer was used to make sure that all dry ingredients were added to the mixing beaker within approximately 5 minutes. As the dry ingredients were added, the mixer rotation speed was increased to maintain obvious surface movement in the slurry with minimal formation of a central vortex and associated air entrainment.

Dry ingredient addition was achieved within ~5 minutes for all test batches except EQT "pre-screening" test batches 26.1b and 26.1c. For TB26.1b, which contained 30 wt% HL, the dry ingredients were added over the course of ~12 minutes due to mixing difficulties caused by poor flowability. The elevated HL content is presumed to be the cause of reduced flowability, since these mixing challenges worsened when preparing TB26.1c, which contained 50 wt% HL. In TB26.1c, ~304 g of blended dry ingredient material could not be mixed into the simulant, even with the mixer set to its maximum speed of 1,400 rpm.

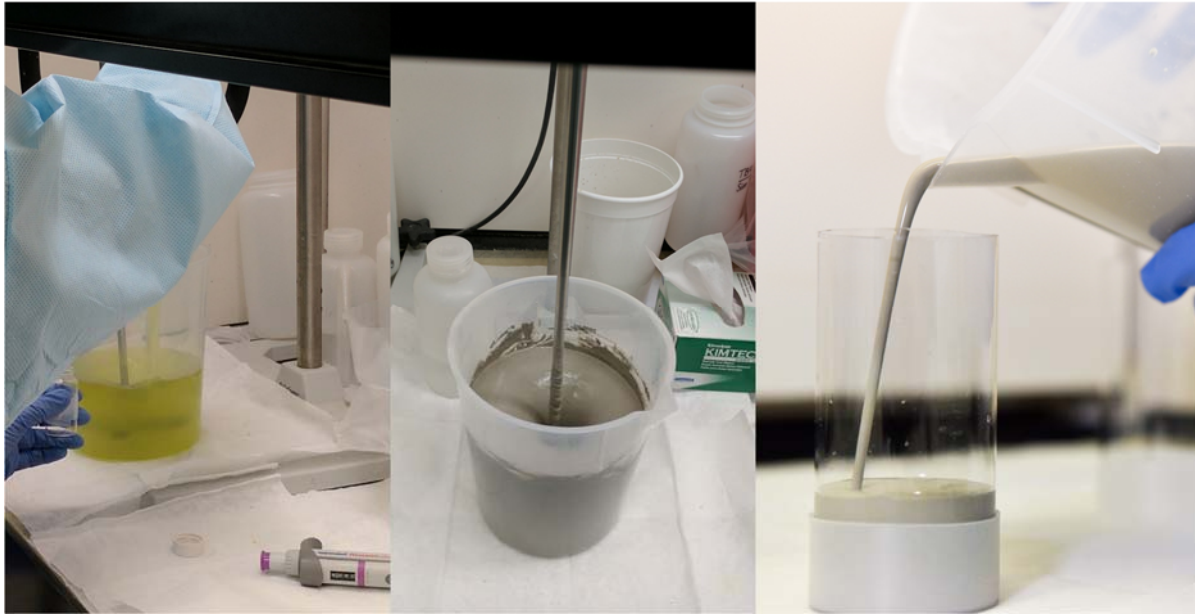


Figure 4.1. Taking Simulant Subsample while Mixing before Dry Ingredient Addition (left), Mixing Grout after Combining Simulant and Dry Ingredients (middle), and Pouring Grout into Plastic Waste Form Mold (right)

As soon as all of the dry ingredients had been added to the mixing beaker, the grout was visually assessed for low flowability. If reduced flowability was determined, MG 3030 was added step-wise to the grout near the vortex. WRA addition was based on operator experience, and awareness that flowability is an important process characteristic when pouring grout waste forms. The MG 3030 significantly reduces viscosity and allows the grout to be “burped” to release entrained air by stopping the mixer for 15 – 30 seconds and tapping the beaker on the benchtop. In the end, only test batches 9, 26.1b, and 26.1c required addition of the WRA, needing 8 to 10.5 mL of WRA to improve grout flowability. Mixing continued until 15 minutes had elapsed from the beginning of dry pre-mix addition (Figure 4.1, middle). Scraping the beaker sides and mixer shaft with a spatula was done as needed. Mixer speed was adjusted to the highest possible level without risking additional air entrainment. This speed varied from batch to batch and was occasionally decreased during mixing as grout slurry shear properties changed over time. For test batches 26.1b and 26.1c, WRA addition helped grout flowability, but mixing over the 15-minute mixing period still proved to be difficult.

At the end of the mixing period, the grout slurry was poured into 2" internal diameter × 4" (or 5") high cylindrical forms (Figure 4.1, right). These forms consist of thin-walled plastic mailing tubes with push-on plastic caps (Icon Plastics in Costa Mesa, California). Each batch of grout was expected to fill approximately six to eight forms. The forms were initially filled about three-quarters full to minimize risk of spillage during mechanical agitation with a vortex mixer to release entrained air in the grout material. Not all grouts slurries appeared to have entrained air, but all specimens were agitated to make sure that minimal entrained air was cured into the monoliths. De-airing required a minute or less per monolith, which helped minimize the effects of grout stratification. De-airing was considered complete when visual inspection detected the cessation of new bubbles rising to the surface of the grout slurry. The forms were then completely filled, gently de-aired, and covered with perforated caps. The caps were left a few millimeters higher than the upper surface of the grout in order to allow a level grout surface to form and to minimize surface imperfections induced by contact with the cap during the slurry setting. At least one additional form, filled one-quarter to one-half full, was also prepared for each grout formulation and used

for residual free liquids observations and density measurements (if needed). All forms were labeled with the year and sample identifier of the following format:

17-EMF-TB#-N

where 17 = last two digits of calendar year
 EMF = EMF evaporator bottoms
 TB# = test batch # from Table 4.1 and Table 4.2
 N = monolith number (starting with 1).

The filled and capped forms were placed into racks, which were then stacked into 5-gallon buckets. Before the racks were installed, the buckets were preloaded with 3/8" to 1" of DIW to maintain a humid environment (relative humidity: ~80% – 100%) inside the sealed bucket at room temperature. Monoliths were allowed to cure at room temperature and with high humidity for a minimum of 7 days inside the sealed buckets. During this period, free-liquid observations were made on at least one monolith from each of the 24 ECS test batches and final 6 EQT test batches (see Section 5.2 for free liquids results). After at least 7 (or 28) days of curing, each cured monolith was removed from its mold and physically examined for cracks, surface voids, irregular shapes, and loose chips. Any loose chips were removed from the monolith and notes on the physical description of each monolith were recorded. The 7-day cured monoliths were used for TCLP testing, while 28-day cured monoliths were archived for future testing. Archived samples were packaged in an open, sealable plastic bag that was then enclosed in a second, sealed plastic bag containing a wet paper towel to maintain relative humidity conditions >80%.

5.0 Waste Form Physical Properties

5.1 Set Time

Set time was measured according to the procedure outlined in ASTM C191-13, *Standard Test Methods for Time of Setting of Hydraulic Cement by Vicat Needle*, to provide an indication of cure progression at a given point in time. This method is also used to determine the time required between pours to prevent excessive hydraulic head on the vault walls and to provide a calculated estimate on material at risk for deflagration (Westsik et al. 2013).

5.1.1 Methods and Materials

Immediately after mixing non-radiological EQT Cast Stone test batches (TB25.1 – TB26.2), one poured specimen from each test batch was used to evaluate waste form set time according to the procedure outlined in ASTM C191-13. Each grout slurry specimen was poured into an ~8 cm diameter × 6 cm tall cup/ring until the cup was full. Any excess material was wiped off the surface so that the grout was level with the top of the sample holder and then the specimen was weighed. Care was taken during this process not to compress the specimen. Once prepared, the specimen was placed under the Vicat needle apparatus (shown in Figure 5.1) to determine the penetration of the 1 mm diameter needle into the grout material and, ultimately, the waste form set time.

Set time measurements were collected at 1-hour intervals during normal working hours. To perform a measurement, the 1 mm needle was lowered until it rested on the surface of the material. The apparatus set screw was then tightened and the indicator at the top of the scale set to zero. The rod holding the needle was then released by loosening the set screw and the needle was allowed to settle for 30 seconds before recording the penetration depth, date, and measurement time. For each penetration measurement, the needle was positioned at least 5 mm away from any previous measurement and at least 10 mm from the edge of the sample ring. Measurements continued at 1-hour intervals until the needle rod no longer left a cylindrical mark on the sample surface. If the grout material was slow to set, the measurement intervals were allowed to increase above 1 hour. Samples were capped with a lid between measurements to maintain humid conditions and prevent water loss via evaporation.



Figure 5.1. Vicat Needle Apparatus Showing Complete Penetration of the 1 mm Diameter Needle Such That the Rod Has Made an Indentation in the Specimen Surface in Previously Tested Areas. The sample shown is not associated with the samples discussed in this report.

5.1.2 Results and Discussion

Sample details and initial and final set time measurements for each EQT specimen analyzed are provided in Table 5.1. Overall, minimal sample mass (~3 wt%) was lost over the course of testing, likely due to water evaporation. For EQT test batches TB25.1 and TB25.2, which used the original Cast Stone formulation to treat the Avg simulant, the total set times were 68.7 and 67.3 hours, respectively. These set times are comparable to the set time reported for similar experimental conditions, 71 hours, by Cozzi and McCabe (2016). Recorded set times for TB26.1a and TB26.2, which used the 10% HL, 18% OPC, and 72% BFS formulation to treat the Avg simulant, were 71.4 and 66.7 hours, respectively, and are similar to those recorded for Cast Stone test batches. However, the range in set time for the HL-based test batches is slightly greater than those made from Cast Stone. Determining whether or not this variability is persistent across multiple test batches would require more than one test specimen from each test batch.

Table 5.1. EQT Set Time Results using ASTM C191-13

Test Batch	Cast Stone (25.1)	Cast Stone (25.2)	HL (26.1a)	HL (26.2)
Sample ID	17-EMF-TB25.1-2	17-EMF-25.2-2	17-EMF-26.1a-2	17-EMF-26.2-7
Initial Specimen Weight (g)	625.4	605.7	618.0	613.7
Initial Specimen Weight Measurement Date (mm/dd/yyyy)	4/4/2017	4/4/2017	4/4/2017	4/4/2017
Final Specimen Weight (g)	611.8	591.3	598.4	599.7
Final Specimen Weight Measurement Date (mm/dd/yyyy)	4/13/2017	4/13/2017	4/13/2017	4/13/2017
Sample Prep Date and Time (mm/dd/yyyy, hr:min)	4/4/17 11:14	4/4/2017 12:40	4/4/2017 8:33	4/4/2017 13:18
Final Vicat Measurement Date and Time (mm/dd/yyyy, hr:min)	4/7/17 07:55	4/7/2017 07:56	4/7/2017 07:54	4/7/2017 7:58
Total Set Time (days)	2.9	2.8	3.0	2.8
Total Set Time (hours)	68.7	67.3	71.4	66.7

5.2 Free Liquids

The sections below describe observations made while monitoring select waste forms for residual free liquids over the 28-day curing period. Per *Hanford Site Solid Waste Acceptance Criteria* (Ramirez 2008), free liquids must not exceed 1% of the total waste volume for a waste form to qualify for on-site disposal.

5.2.1 Methods and Materials

One specimen from all ECS test batches and the final four non-rad EQT test batches (25.1, 25.2, 26.1a, 26.2) were monitored for the presence of free liquids during the 28-day cure period. Observations were made every day for the first 7 days post-production of monolith specimens and at least twice a week until the 28-day cure period was reached or until no free liquids remained. Visual inspection identified free liquids from curing waste form specimens. Visual observations of a few drops of liquid or less on the surface are considered less than 1% of the total waste volume.

5.2.2 Results and Discussion

The presence of free liquids was monitored on one monolith selected from each ECS test batch, TB1 through TB24, and each non-rad EQT test batch, TB25.1, TB25.2, TB26.1a, and TB26.2. On each observation day, a photo was taken to document the presence of free liquids. Photos taken on production day compared to the final observation for each monolith are provided in Appendix A, Section A.1. For all monoliths, yellow free liquid was initially observed on the top surface of the grout monolith. In many instances, the free liquid turned colorless, with some monolith specimens absorbing the free liquid over the course of 3 to 18 days. However, for test batches TB7, TB19, and TB22, free liquids remained throughout the 28- to 30-day observation period. The time required for free liquids to reduce to less than 1% of the total waste volume is illustrated in Figure 5.2 and tabulated in Table 5.2.

Additionally, cured ECS cementitious waste forms containing low boron concentrations (simulants 2, 3, 6, and 7) were observed to be darker in color (green/grey) and in some cases contained white precipitates on the exterior surfaces. This contrasts to the tan color typical for cementitious waste forms produced in previous FY testing activities or with relatively high boron levels in this study (simulants 1, 4, 5, and 8). However, in EQT specimens, both the Cast Stone and HL formulations had one specimen take 8 days to achieve <1% free liquid, whereas its duplicate test batch specimen only took 3 days. In each of these formulations, the specimen with free liquids observed through 8 days after formulation also exhibited a darker green/grey color. This darkening effect was not observed in the duplicate that took 3 days to re-absorb free liquids, suggesting re-absorption time may also contribute to this change in specimen color.

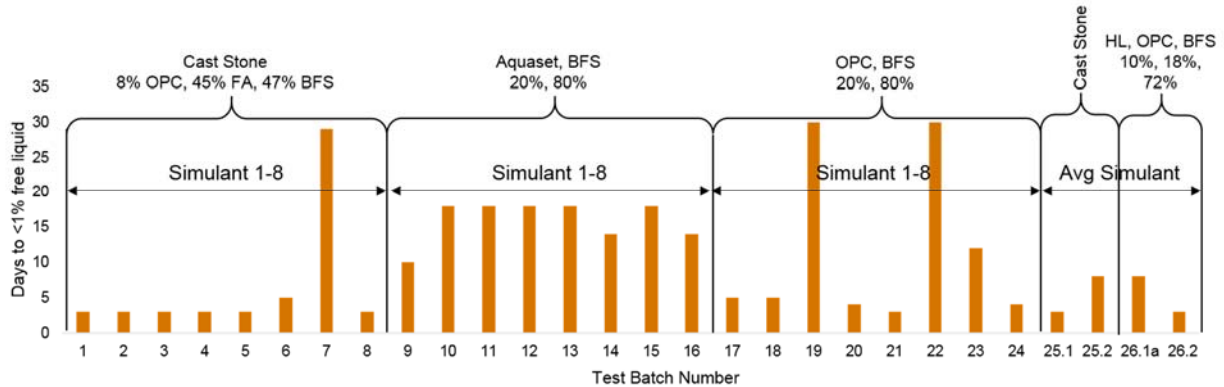


Figure 5.2. Number of Days after Monolith Production for Free Liquids to Decrease to Less Than 1% of the Total Waste Volume for All ECS and Final EQT Non-Rad Test Batches

Table 5.2. Days Required for Free Liquids to Reach Less Than 1% of Total Waste Volume

Simulant	Cast Stone 8% OPC, 45% FA, 47% BFS (days)	Aquaset, BFS 20%, 80% (days)	OPC, BFS 20%, 80% (days)	HL, OPC, BFS 10%, 18%, 72% (days)
1	3	10	5	
2	3	18	5	
3	3	18	30	
4	3	18	4	
5	3	18	3	
6	5	14	30	
7	29	18	12	
8	3	14	4	
Avg	3 – 8	-	-	3 – 8

Based on free-liquids analysis alone, the Cast Stone formulation recipe re-absorbs free liquids within 3 to 5 days for all simulants except ECS Simulant 7 (low Cl and B, high NO₂ and SO₄) and EQT TB25.2 using the Avg simulant. Free liquids were still present at the end of the observation period (29 days) for TB7, which treated Simulant 7 with the Cast Stone formulation, but the Avg simulant was treated within 3 to 8 days using Cast Stone. The Aquaset (20 wt%) and BFS (80 wt%) waste form formulation is recommended for treatment of all ECS simulated wastes, including Simulant 7, based on observations of this study. Free liquid was observed up to 18 days after monolith production using the Aquaset/BFS formulation; however, the presence of free liquids diminished to less than 1% of the total waste volume

for all ECS simulants tested after 18 days. The Aquaset/BFS formulation was not tested on the Avg simulant, but similar results are expected. A formulation of OPC (20 wt%) and BFS (80 wt%) is not recommended for treatment because two of the treated ECS simulants (Simulants 3 and 6) had free liquids remaining even after 30 days. Those simulants successfully treated with the OPC/BFS formulation are treated as well or better with the current Cast Stone formulation, with the exception of Simulant 7. Finally, the HL formulation for treating the Avg simulant was observed to match the Cast Stone free liquids observations, reabsorbing residual free liquids within 3 to 8 days.

The residual free liquid results discussed here are based on observations collected for one specimen from each test batch. Replicate sample observations are needed to confirm these assessments. Once confirmed, the results of this work can be used to select formulations for scale-up tests and to provide baseline guidance for the time required before waste forms may be moved to and be disposed of in the IDF.

5.3 Moisture Content

5.3.1 Methods and Materials

One partially filled 28-day cured monolith from each radiological EQT test batch was placed in an oven set at 105 ± 3 °C for at least 48 ± 1 h to measure the monolith moisture content (MC). To ensure a constant dry mass of the partial monolith, the monolith was removed from the oven after 24 ± 1 h, and allowed to cool to room temperature before a dry weight measurement of the monolith sample was made. Then the partial monolith was returned to the same oven for at least an additional 24 ± 1 h before it was cooled to room temperature and the dry mass was measured again. The two dry mass readings had to be within 1.0 % of one another for the dry mass to be considered constant. If a constant mass was not obtained, the procedure above was repeated for one or more additional 24 h drying cycles until two sequential readings for dry mass met the constant-mass requirements. MC of the each partial monolith was determined by the difference in mass between the monolith sample before and after drying at 105 ± 3 °C using Equation (5.1):

$$MC (\%) = [(M_{\text{wet}} - M_{\text{dry}})/M_{\text{wet}}] \times 100 \quad (5.1)$$

where M_{wet} = initial wet mass of monolith (g); M_{dry} = next-to-last dry mass of monolith after drying (g).

5.3.2 Results and Discussion

The final moisture content and dry solids fraction $\{1 - [MC(\%)/100]\}$ for each monolith are shown in Table 5.3. From this MC analysis it is apparent that the Cast Stone specimen (17-EMF-TB27-8) has an MC ~3% greater than the HL monolith. This difference is likely due to mineral hydration reactions, e.g. ettringite formation, that are capable of trapping water within the mineral structure. In turn this reduces the amount of free water within the cured specimen.

Table 5.3. Moisture Content of the Differently Cured Monoliths

	Specimen ID	
	17-EMF-TB27-8	17-EMF-TB28-8
Moisture Content (%)	27.32	24.24
Dry Fraction	0.73	0.76

5.4 Density

5.4.1 Methods and Materials

One specimen from each non-rad test batch (TB25.1, TB25.2, TB26.1a, and TB26.2) was measured for cured density according to the procedure outlined in ASTM C642-13, *Standard Test Method for Density, Absorption, and Voids in Hardened Concrete*. To summarize this procedure, each monolith specimen was first weighed in a moisture tin, then dried in an oven set to $110^{\circ}\text{C} \pm 10^{\circ}\text{C}$ for at least 24 hours. After 24 hours, the specimen was removed from the oven and allowed to cool briefly before recording the dry specimen mass. The specimen was then returned to the oven and this drying procedure repeated until the difference in successive dry mass values was less than 0.5% of the lesser value. The final sample mass was recorded as the “Mass of Oven-Dried Sample in Air” (Table 5.4). After oven drying, specimens were immersed in approximately $\sim 21^{\circ}\text{C}$ DIW for at least 48 hours and then removed, blotted with a towel to remove excess water, and weighed. Specimen immersion and weighing was repeated for an immersion period of at least 24 hours and deemed complete when the difference in successive mass measurements was less than 0.5% of the lesser value. The final mass of the specimen was recorded as “Mass of Surface-Dry Sample in Air After Immersion.” Finally, each specimen was submerged in boiling DIW for 5 hours before being removed and allowed to cool to room temperature by natural loss of heat for no less than 14 hours. The specimen was surface dried by blotting the surface with an absorbent towel to remove excess liquid and the mass was recorded as “Mass of Surface-Dry Sample in Air After Immersion and Boiling.” These measurements, along with the specimen volume (calculated from average monolith diameter and length), were then used to calculate the specimen density after each drying or immersion step in the procedure and finally the permeable pore space volume for each specimen and overall average for each formulation.

5.4.2 Results and Discussion

Density measurements were performed using one monolith from each non-rad EQT test batch, the results of which are summarized in Table 5.4. The average apparent density for the original Cast Stone formulation was $2.22 \pm 0.03 \text{ Mg/m}^3$ based on the two specimens analyzed with the Cast Stone formulation. For the final HL formulation, the average apparent density, again based on two specimen measurements, was determined to be $2.46 \pm 0.15 \text{ Mg/m}^3$ and is slightly greater than the Cast Stone formulation (within 1σ error). However, using the approach outlined in ASTM C642-13 for calculating the volume of permeable pore space, the difference in permeable pore space between Cast Stone specimens ($42.40\% \pm 0.03\%$) and HL specimens ($43.95\% \pm 2.42\%$) is not statistically significant.

It is important to note that the precipitation and/or dissolution of salts within the pore space during drying, immersion, and boiling may result in lower calculated density values and higher calculated permeable pore space values. Based on mass measurements and volume calculations determined for comparable rad-EQT specimens, the difference between the immersed (wet) density determined using ASTM C642-13 and rad mass/volume calculations is estimated to be approximately 6% and within experimental error.

Table 5.4. Density Measurements for EQT Non-Rad Specimens

Test Batch		Cast Stone (25.1)	Cast Stone (25.2)	HL (26.1a)	HL (26.2)	Variable in ASTM C642-13
Specimen		1	1	8	8	
Initial Specimen Mass	g	106.0518	101.0198	71.5252	79.1061	
Mass of Oven-Dried Sample in Air	g	76.0146	72.6804	53.9896	59.2946	A
Mass of Surface-Dry Sample in Air After Immersion	g	100.9421	96.5875	70.8202	78.7868	B
Mass of Surface-Dry Sample in Air After Immersion and Boiling	g	101.3855	96.5396	70.761	78.728	C
Specimen Volume	cm ³	59.87	56.25	39.70	42.56	
Apparent Mass of Sample in Water After Immersion and Boiling	g	41.5195	40.2879	31.0575	36.1656	D
Bulk Density, Dry	Mg/m ³	1.27	1.29	1.36	1.39	g ₁
Bulk Density after Immersion	Mg/m ³	1.69	1.72	1.78	1.85	
Bulk Density after Immersion and Boiling	Mg/m ³	1.69	1.72	1.78	1.85	
Apparent Density	Mg/m ³	2.20	2.24	2.35	2.56	g ₂
Apparent Density Average for Identical Formulations	Mg/m ³	2.22 ± 0.03		2.46 ± 0.15		
Volume of Permeable Pore Space (voids)	%	42.38	42.42	42.24	45.66	
Volume of Permeable Pore Space Average for Identical Formulations	%	42.40 ± 0.03		43.95 ± 2.42		

5.5 Compressive Strength

5.5.1 Methods and Materials

After curing for at least 28 days, three monolith specimens from each non-rad EQT grout formulation were selected for compressive strength analysis according to ASTM C39/C39M-18 with at least one specimen selected from each of the duplicate non-rad test batches. Selected monoliths were cured in 2" ID x 5" long plastic forms since the normal 4" long forms would not meet the desired specimen length for this analysis. Once cured, the monoliths' flat ends were cut with a saw, while using a miter gauge to keep the sample ends parallel. The final length of the specimen should be no less than 4" and was achieved for all specimens except 17-EMF-TB26.1a-7, which was cut to ~3.9" in length. The reported specimen length and diameter in Table 5.5 is the average of three measurements, where the diameter of the specimen was measured at the bottom, middle, and top of the monolith and the specimen length was measured at three rotational orientations mutually separated by ~120 degrees from an arbitrary starting location using a caliper.

Once each specimen was cut and measured, specimens were loaded into the testing apparatus (MTS model 312.31 servohydraulic frame with a 55 kip actuator and load cell, Figure 5.3). An adapter, adequate to stabilize a 2" ID object, was placed on each end of the monolith specimen and then situated between the two compression platens so that the monolith axis was aligned with the center of thrust. The compression platens were then adjusted so that each was in contact with the adapters, securing the monolith specimen, but without applying a compressive load. The load indicator was set to zero and then a load was applied to the specimen without shock at a stress rate of 0.25 ± 0.05 MPa/s (35 ± 7 psi/s). Sample loading continued until specimen failure, e.g. a well-defined fracture in the monolith specimen. This maximum compressive load was recorded and then used to calculate the compressive strength of the monolith specimen. The results of this analysis are summarized in Table 5.5.

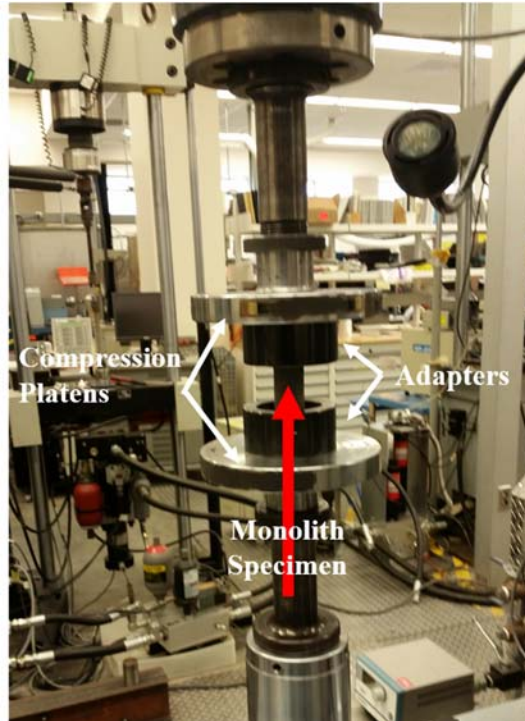


Figure 5.3. MTS Model 312.31 Servohydraulic Frame with a 55 kip Actuator and Load Cell Used for Compressive Strength Measurements.

5.5.2 Results and Discussion

Compressive strength results are summarized in Table 5.5 for the six specimens analyzed. The average compressive strength for each formulation, Cast Stone and HL recipes, was determined from the compressive strength of three specimens from each formulation with at least one specimen sourced from duplicate test batches. Only the non-rad test batches were analyzed by this procedure. All monolith specimens met the minimum compressive strength of 500 psi (Siskind and Cowgill 1992).

Table 5.5. Compressive Strength of Select EQT Non-Rad Specimens

Formulation	Cast Stone			HL		
	TB25.1	TB25.2	TB25.2	TB26.1a	TB26.1a	TB26.2
Test Batch						
Specimen Number	4	4	5	4	7	2
Average Monolith Height (mm)	125.77	123.77	123.60	123.52	99.17	123.95
Average Monolith Diameter (mm)	49.05	48.98	49.41	48.97	49.33	49.22
Specimen Length to Diameter Ratio	2.56	2.53	2.50	2.52	2.01	2.52
Cross-Sectional Area (mm ²)	1,889.33	1,883.95	1,917.69	1,883.18	1,911.23	1,902.71
Cross-Sectional Area (in ²)	2.93	2.92	2.97	2.92	2.96	2.95
Maximum Compressive Load (lbf)	4,990.98	5,029.81	5,427.83	8,151.77	12,546.54	11,943.77
Compressive Strength (psi)	1,704.30	1,722.47	1,826.07	2,792.73	4,235.26	4,049.83
Formulation Average Compressive Strength (psi)	1,751 ± 66			3,693 ± 785		

5.6 Saturated Hydraulic Conductivity

Hydraulic conductivity (K) is a coefficient used to describe the ease with which a fluid can be transmitted through a porous matrix. Typically, the fluid measured is water and the fluid properties such as density, viscosity, and surface tension can influence how a fluid is transmitted. The coefficient K depends on the geometry of porous media, where large connected pores transmit water rapidly and small, poorly connected pores transmit water slowly. Since water saturation can also influence the value for K , it is typical to use the measurement of K under hydraulically saturated conditions (K_{sat}) to allow for comparative values.

5.6.1 Methods and Materials

Two representative samples were selected for analysis of K_{sat} (Table 5.6). The samples had the same average diameters of 4.9 cm and the samples were cut to length using a rock saw, with the Cast Stone sample 17-EMF-25.1-6 being 3.6 cm long and HL sample 17-EMF-26.1a-6 being 3.5 cm long. After being cut, the samples were quickly rinsed of particulates and allowed to saturate in tap water under vacuum to displace air and help saturate the samples. Ordinary tap water was selected for saturating samples and for conducting the K_{sat} test since using DIW can be problematic when conducting a K_{sat} test (ASTM D5084-16a). The saturation bath period was 1 week and testing time was 2 weeks. As such, material leaching (saturation) was not expected to affect the K_{sat} due to this relatively short testing period. Samples were removed from the saturation bath and immediately placed in a flexible wall permeameter (Tri-Flex 2 Permeability Test Cell, ELE International). The sample was placed between two end caps in the permeameter and surrounded by a rubber membrane held in place with O-rings. Once the sample was loaded, the permeameter was filled with water and pressurized with a confining pressure of 150 psi. The influent water pressure was maintained at 130 psi. Each regulated pressure was controlled by calibrated precision controllers (Alicat Scientific Inc.). Initial water breakthrough took more than 1 day and included water filling the dead space in the instrument. Measurements started as soon as the first effluent was observed. Testing was determined complete once conductivity was determined to provide a steady K_{sat} (~5 to 8 measurements).

5.6.2 Results and Discussion

The measured average K_{sat} results for the two samples were similar, with the Cast Stone specimen 17-EMF-TB25.1-6 being $1.3 \times 10^{-10} \text{ cm s}^{-1}$ and the HL formulation sample 17-EMF-TB26.1a-6 being $1.4 \times 10^{-10} \text{ cm s}^{-1}$ (Table 5.6). These K_{sat} results are similar to that which can be measured for water through unweathered granite (Freeze and Cherry 1979) and are an order of magnitude lower than values reported previously for similar waste form materials (Cozzi et al. 2016). However, similar to previously published results by Cozzi et al. (2016), there is a slight temporal variability in measurements, with K_{sat} decreasing over time (Table 5.6). It is probable that there is some reduction in porosity occurring as the material continues to cure, resulting in a reduced K_{sat} . Finally, due to the extremely low K_{sat} values measured here, future K_{sat} measurements on similar high-performing materials might consider the procedure modifications suggested in ASTM D5084-16a for specimens with K_{sat} values lower than $1 \times 10^{-9} \text{ cm/s}$ ($1 \times 10^{-11} \text{ m/s}$), the recommended lower limit of the ASTM D5084-16a procedure.

Table 5.6. Initial and Final Hydraulic Conductivities Measured on Select Samples

Test ID	Dry Blend	Test Time (d)	Hydraulic Conductivity (K_{sat})		
			Initial (cm s^{-1})	Final (cm s^{-1})	Average ^(a) (cm s^{-1})
17-EMF-TB25.1-6	OPC/FA/BFS 8/45/47	15	3.0×10^{-10}	3.6×10^{-11}	1.3×10^{-10}
17-EMF-TB26.1a-6	HL/OPC/BFS 10/18/72	17	2.2×10^{-10}	9.9×10^{-11}	1.4×10^{-10}

(a) Average K_{sat} was determined from five measurements collected on 17-EMF-TB25.1-6 and eight measurements collected on 17-EMF-TB26.1a-6.

6.0 Solid Phase Characterization

6.1 X-ray Diffraction

XRD patterns were collected for ECS (Figure 6.1, Figure 6.2, and Figure 6.3) and EQT (Figure 6.4) monoliths to determine their mineralogical composition after curing for 28 days and after leaching for 63 days (rad EQT monoliths only) (Table 6.1). In all analyzed specimens, the XRD patterns indicate that the majority of the waste form is composed of a calcium silicate hydrate (CSH) amorphous phase (~71 – 85 wt%). The remaining material consisted of mineral phases including portlandite [$\text{Ca}(\text{OH})_2$], ettringite [$\text{Ca}_6\text{Al}_2(\text{SO}_4)_3(\text{OH})_{12}\cdot 26\text{H}_2\text{O}$], calcite [CaCO_3], larnite [Ca_2SiO_4], hydrocalumite [$\text{Ca}_4\text{Al}_2(\text{OH})_{12}(\text{OH})_2\cdot 6\text{H}_2\text{O}$], and quartz [SiO_2]. The presence of rutile/anatase [TiO_2] is due to the internal TiO_2 standard added before XRD analysis and is included for the purpose of determining the relative weight percent of each mineral phase.

For ECS monoliths formulated using the original Cast Stone formulation, the dominating mineral phases were ettringite (1.7 – 6.7 wt%), quartz (1.6 – 2.6 wt%), hydrocalumite (0.6 – 3.0 wt%), larnite (0.9 – 1.8 wt%) and calcite (0.3 – 2.0 wt%), whereas portlandite was not detected. The mineralogical fraction of each of these phases does not vary significantly across specimens produced with the Cast Stone formulation and the eight different ECS simulants, with the exception of ettringite. Ettringite showed a noticeable increase when more sulfate was present (ECS Simulants 5 – 8). Furthermore, the slight decrease in hydrocalumite [$\text{Ca}_4\text{Al}_2(\text{OH})_{12}(\text{OH})_2\cdot 6\text{H}_2\text{O}$] with increasing simulant sulfate concentration suggested that some of the calcium and aluminum resources used in lower sulfate simulants are being redirected to form ettringite over hydrocalumite. This trend is also observed in the Aquaset/BFS formulation, where the formation of ettringite increases from between 0.3 – 5.1 wt% at low sulfate concentrations (ECS Simulants 1 – 4) to between 6.6 – 8.8 wt% at high sulfate concentrations (ECS Simulants 5 – 8). Furthermore, as ettringite formation increased in ECS Simulants 5 – 8, hydrocalumite decreased as seen with the Cast Stone specimens. In the OPC/BFS specimens, a noticeable increase in ettringite for specimens treating ECS Simulants 5 – 8 is not observed. Rather ettringite exhibits a nearly equal compositional fraction in each specimen. This may have implications for long-term Tc immobilization, since ettringite is hypothesized to incorporate ^{99}Tc into its mineral structure, which could increase Tc stability within the waste form (Saslow et al. 2017).

EQT specimens were also analyzed using XRD to determine if there were significant composition differences between the Cast Stone and HL-substituted formulations when treating the Avg simulant (Table 6.1). For each formulation, a rad and non-rad specimen were analyzed. For the non-rad specimens (TB25.1 and TB26.2), material from the interior and exposed outer wall of the waste form was collected to identify mineralogical differences between the more reducing environment found inside the monolith relative to the outer wall where the waste form is exposed to a more oxidizing environment. For the rad specimens, sourced from TB27 and TB28 monoliths, bulk material was collected from an unleached specimen in addition to material sampled from the interior and exposed outer wall of monoliths subjected to 63 days of leaching in DIW (as part of EPA 1315 leach testing, Section 8.0). Similar to the ECS specimens, EQT XRD patterns indicate that the majority of the waste form is an amorphous phase, likely CSH (~73 – 82 wt %). The remaining material again consisted of portlandite [$\text{Ca}(\text{OH})_2$], ettringite [$\text{Ca}_6\text{Al}_2(\text{SO}_4)_3(\text{OH})_{12}\cdot 26\text{H}_2\text{O}$], calcite [CaCO_3], larnite [Ca_2SiO_4], hydrocalumite [$\text{Ca}_4\text{Al}_2(\text{OH})_{12}(\text{OH})_2\cdot 6\text{H}_2\text{O}$], and quartz [SiO_2], and the presence of rutile/anatase [TiO_2] as an internal standard was used to determine the relative weight percent of each mineral phase. Overall, the small quantities of each mineral phase, most less than 5 wt% did not indicate significant trends across formulations and spatial environments. Of note is the increase in ettringite present in the material

collected from the exposed outer wall of unleached and post-leached specimens, which is consistent with previous observations and proposed secondary mineral formation of ettringite as the waste form cures and the outer wall interacts with ions in leachate solutions (Saslow et al. 2017). Furthermore, the presence of portlandite, only found in the HL-based specimens, suggests that there is an excess of calcium added relative to the amount of sulfate requiring sequestration via the formation of ettringite.

Table 6.1. XRD Analysis of ECS and EQT Monoliths

Sample Name	Formulation	Simulant	XRD Analysis (wt%) ^(a)							
			Portlandite	Ettringite	Calcite	Larnite	Hydrocalumite	Quartz	Rutile + Anatase	CSH ^(b)
17-EMF-TB1-3	Cast Stone	1	-	-	0.3%	0.9%	3.0%	1.9%	8.4 + 0.5 %	85.0%
17-EMF-TB2-3		2	-	2.7%	1.3%	1.7%	3.0%	1.8%	8.5 + 0.5 %	80.5%
17-EMF-TB3-3		3	-	4.0%	2.0%	1.5%	2.3%	1.9%	8.3 + 0.4 %	79.6%
17-EMF-TB4-3		4	-	1.7%	1.9%	1.3%	2.7%	2.6%	8.0 + 0.4 %	81.4%
17-EMF-TB5-3		5	-	3.3%	1.4%	1.3%	1.0%	2.3%	8.4 + 0.4 %	81.9%
17-EMF-TB6-3		6	-	5.0%	1.4%	1.8%	1.4%	1.6%	7.9 + 0.4 %	80.5%
17-EMF-TB7-3		7	-	6.7%	1.7%	1.6%	0.6%	1.9%	8.0 + 0.4 %	79.1%
17-EMF-TB8-3		8	-	3.4%	1.8%	1.5%	1.2%	1.9%	8.3 + 0.4 %	81.4%
17-EMF-TB9-3	Aquaset/BFS (20/80)	1	-	0.3%	5.4%	1.4%	3.3%	1.0%	8.4 + 0.4 %	79.8%
17-EMF-TB10-3		2	0.2%	3.4%	2.4%	1.1%	3.1%	0.3%	7.2 + 0.4 %	81.9%
17-EMF-TB11-3		3	0.3%	5.1%	2.0%	1.4%	2.6%	0.3%	7.5 + 0.4 %	80.4%
17-EMF-TB12-3		4	0.3%	4.9%	1.0%	1.0%	1.7%	1.3%	6.9 + 0.4 %	82.5%
17-EMF-TB13-3		5	-	6.9%	0.9%	2.1%	0.5%	0.6%	8.3 + 0.4 %	80.3%
17-EMF-TB14-3		6	-	8.8%	2.9%	3.2%	1.0%	0.7%	7.7 + 0.4 %	75.3%
17-EMF-TB15-3		7	-	8.1%	4.3%	4.4%	0.7%	0.6%	8.5 + 0.4 %	73.0%
17-EMF-TB16-3		8	-	6.6%	3.9%	3.8%	0.6%	0.9%	8.0 + 0.4 %	75.8%
17-EMF-TB17-3	OPC/BFS (20/80)	1	-	4.1%	3.3%	4.4%	2.4%	0.6%	8.4 + 0.5 %	76.3%
17-EMF-TB18-3		2	-	4.6%	3.1%	4.7%	3.9%	0.4%	7.3 + 0.4 %	75.6%
17-EMF-TB19-3		3	-	5.6%	3.1%	5.0%	3.3%	0.5%	8.4 + 0.4 %	73.7%
17-EMF-TB20-3		4	-	3.4%	2.5%	3.7%	2.4%	0.3%	7.5 + 0.4 %	79.8%
17-EMF-TB21-3		5	-	3.7%	3.1%	4.4%	1.9%	-	8.0 + 0.4 %	78.5%
17-EMF-TB22-3		6	-	4.7%	4.6%	6.5%	3.5%	0.1%	8.6 + 0.5 %	71.5%
17-EMF-TB23-3		7	-	5.7%	0.1%	2.8%	2.4%	0.5%	7.6 + 0.4 %	80.5%
17-EMF-TB24-3		8	-	4.8%	0.6%	2.7%	2.7%	0.3%	8.6 + 0.4 %	79.9%
17-EMF-TB25.1-5 Oxidized (outside)	Cast Stone	Avg	-	3.0%	4.0%	1.5%	1.5%	2.9%	7.8 + 0.4 %	78.9%

Sample Name	Formulation	Simulant	XRD Analysis (wt% ^(a))							
			Portlandite	Ettringite	Calcite	Larnite	Hydrocalumite	Quartz	Rutile + Anatase	CSH ^(b)
17-EMF-TB25.1-5 Reduced (Inside)		Avg	-	1.0%	16.7%	-	0.7%	0.5%	7.8 + 0.3 %	73.0%
17-EMF-TB26.2-5 Oxidized (outside)	HL/OPC/BFS (10/18/72)	Avg	4.5%	6.5%	3.8%	4.1%	4.2%	0.2%	9.4 + 0.5 %	66.8%
17-EMF-TB26.2-5 Reduced (Inside)		Avg	2.5%	4.7%	17.4%	-	3.9%	-	8.6 + 0.0 %	62.9%
17-EMF-TB27-3 Bulk, Unleached		Avg, Tc	-	-	2.4%	4.5%	0.4%	0.5%	9.5 + 0.5 %	82.2%
17-EMF-TB27-1 Inside, Leached	Cast Stone	Avg, Tc	-	1.6%	4.5%	9.8%	2.7%	3.2%	9.4 + 0.5 %	68.3%
17-EMF-TB27-1 Outside, Leached		Avg, Tc	-	3.2%	3.3%	1.6%	0.2%	2.2%	9.6 + 0.5 %	79.4%
17-EMF-TB28-3 Bulk, Unleached		Avg, Tc	1.7%	1.8%	4.3%	5.7%	4.3%	0.3%	9.5 + 0.5 %	71.9%
17-EMF-TB28-1 Inside, Leached	HL/OPC/BFS (10/18/72)	Avg, Tc	1.4%	1.2%	4.0%	6.0%	2.2%	-	9.8 + 0.5 %	74.9%
17-EMF-TB28-1 Outside, Leached		Avg, Tc	1.3%	2.2%	5.1%	1.6%	0.5%	0.1%	9.3 + 0.5 %	79.4%

(a) Chemical formulas of minerals: portlandite [Ca(OH)₂], ettringite [Ca₆Al₂(SO₄)₃(OH)₁₂•26H₂O], calcite [CaCO₃], larnite [Ca₂SiO₄], hydrocalumite [Ca₄Al₂(OH)₁₂(OH)₂•6H₂O], quartz [SiO₂], rutile/anatase [TiO₂].

(b) CSH: calcium silicate hydrated amorphous phase
– not detected

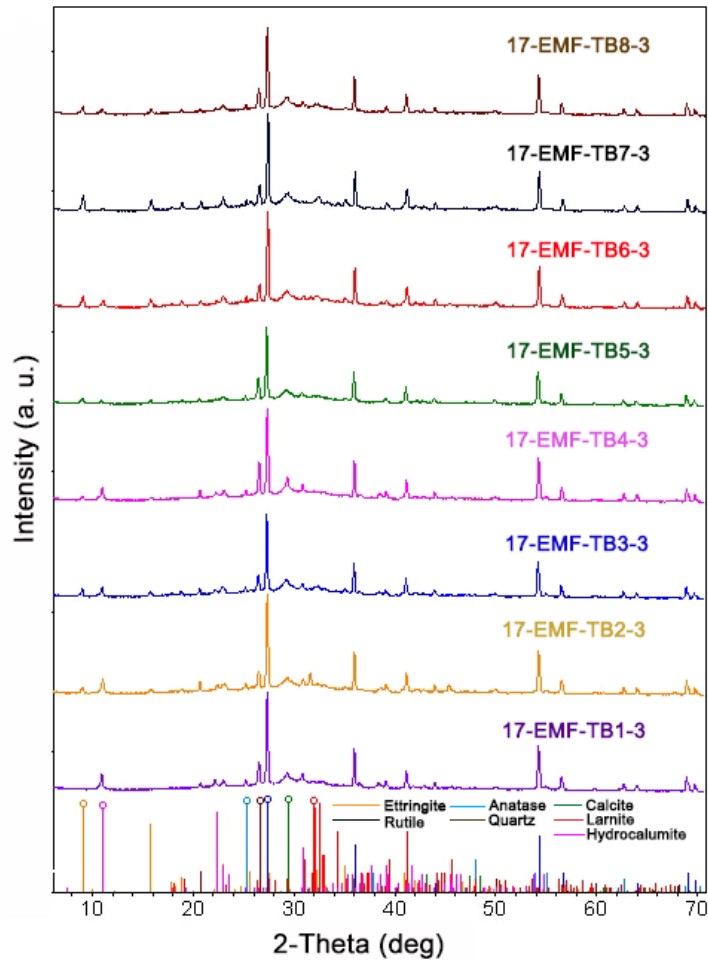


Figure 6.1. XRD Patterns of Monoliths Formulated Using ECS Simulants and the Original Cast Stone Recipe.

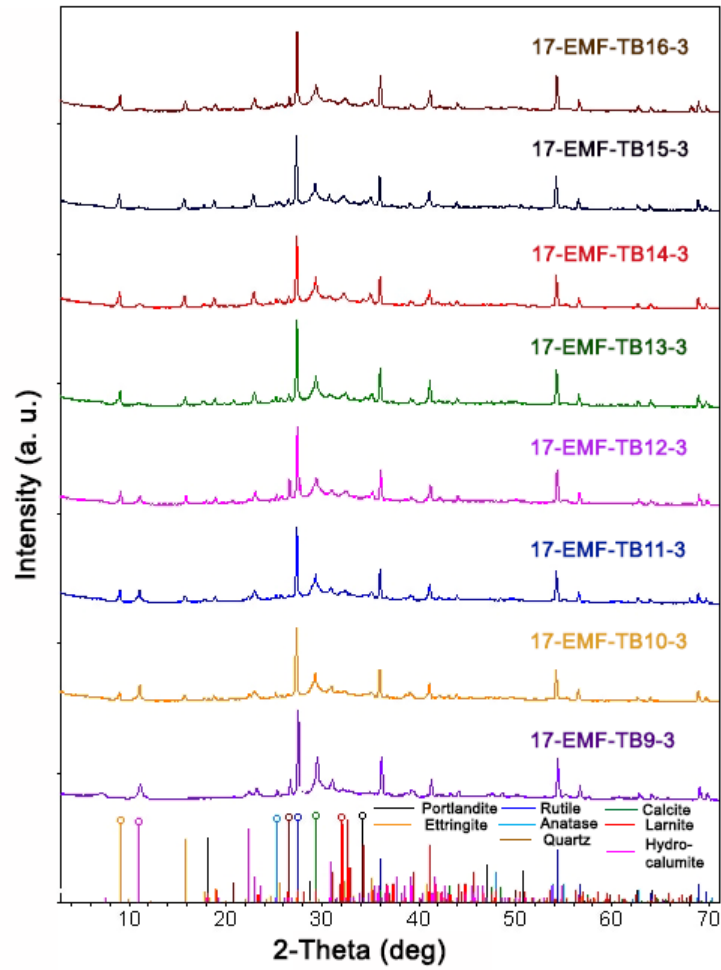


Figure 6.2. XRD Patterns of Monoliths Formulated Using ECS Simulants and a Dry Ingredient Recipe of 20% Aquaset II-GH/80% BFS.

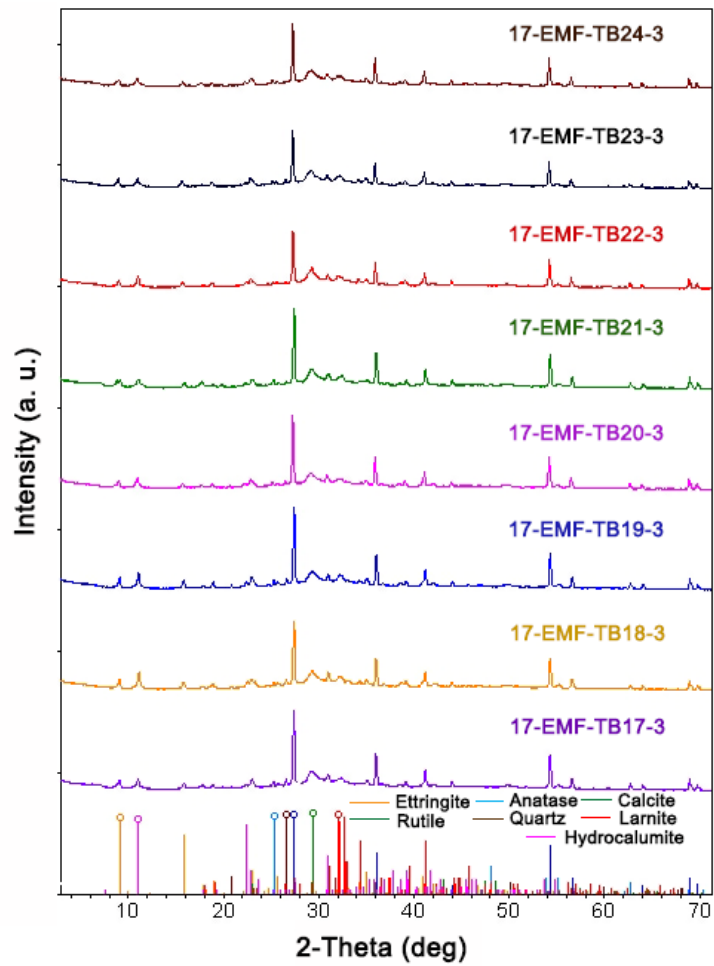


Figure 6.3. XRD Patterns of Monoliths Formulated Using ECS Simulants and a Dry Ingredient Recipe of 20% OPC/80% BFS.

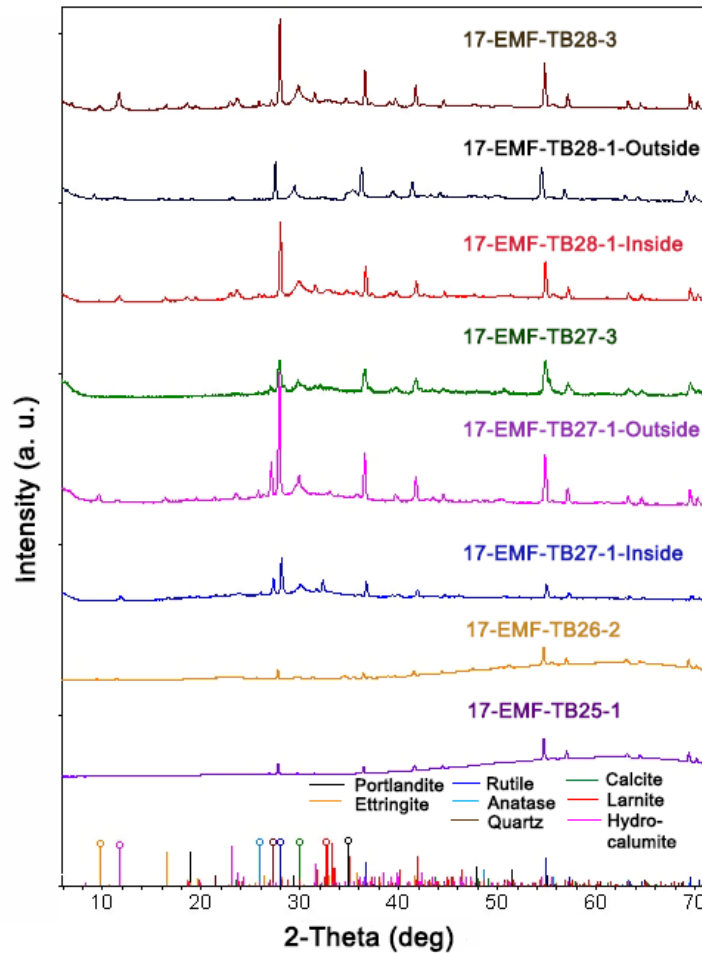


Figure 6.4. EQT XRD Patterns of Monoliths Formulated Using the Avg Simulant and the Cast Stone (TB25.1 and TB27) or HL (TB26.2 and TB28) Formulation Recipe

6.2 Scanning Electron Microscopy (SEM) and Energy Dispersive X-Ray Spectroscopy (EDS)

The morphology and chemical composition of particles found in EQT monoliths were investigated using SEM and EDS, respectively. For the non-rad specimens, monolith material from the exterior and interior of the 28-day cured monolith selected from Cast Stone (TB25.1) and HL (TB26.2) test batches were analyzed. For the rad specimens collected from each Cast Stone (TB27) and HL (TB28) test batch, one sample was prepared with pre-leached material and the second and third material sub-samples were collected from specimens leached in DIW and taken from the exterior wall or interior of the monolith. Based on this analysis, the major difference in the test batch formulations was in particle morphology. In rad specimens collected from TB27 and TB28, ^{99}Tc was not present at levels detectable by EDS; therefore, fractionation among characterized phases was not possible.

6.2.1 SEM/EDS Results for EQT Average Simulant Cast Stone Specimens

For the Cast Stone batches, both rad and non-rad, the morphology reveals the presence of micron size large spherical particles (ranging from 1 – 20 micron size) composed primarily of Ca, Mg, Al, and Si (Figure 6.5). Several SEM micrographs of these spherical particles show that they have a surface coating that is Fe-rich. Furthermore, the spherical particles appear to be highly porous (Figure 6.6), which may suggest solid dissolution during curing/leaching. In addition, several specimen areas were found that have no distinct morphology, but these discrete particles seem to be primarily composed of Fe, likely an Fe oxide or Fe(oxy)hydroxide (Figure 6.7). With respect to minor constituents, in the exterior material characterized from the 63-day leached Cast Stone specimen, platy particles enriched with Ba and S were identified as well as other solid particles without distinct morphological features that contained Cr or Zr (a constituent in found in all dry ingredients used, Table A.1) with elevated levels of Fe measured in the EDS spectra. The presence of comingled Cr and Fe is likely due to the reducing capacity of ferrous iron, which may reduce Cr(VI) to Cr(III) to form Cr(III) oxide or hydroxide phases or amorphous solids with comingled Cr and Fe. Due to the disordered morphology of these regions, it is unlikely that significant mineralogical information could be gathered by the XRD patterns collected from the same material and that these particles would be grouped under the amorphous category of the XRD refinement results. Finally, the major contaminant of interest, ^{99}Tc , was not detected during ^{99}Tc spot EDS analysis of the rad Cast Stone material sourced from both pre-leached and post-leached (interior and exterior) material collected from the monoliths. Despite this observation, ^{99}Tc is still included in the elemental composition maps provided. Considering that only a small fraction of ^{99}Tc was leached from the waste form during EPA Method 1315 testing (Section 8.0), Tc should be present in some of the collected material and the absence of ^{99}Tc in the EDS maps is likely due to the detection limit of the instrument. In the end, although no definitive conclusions can be made for particle-specific ^{99}Tc content, it is possible that ^{99}Tc could be present as a sorbed surface species (either adsorbed or reduced and precipitated) at concentrations that fall below what was detectable using the instrument settings used here.

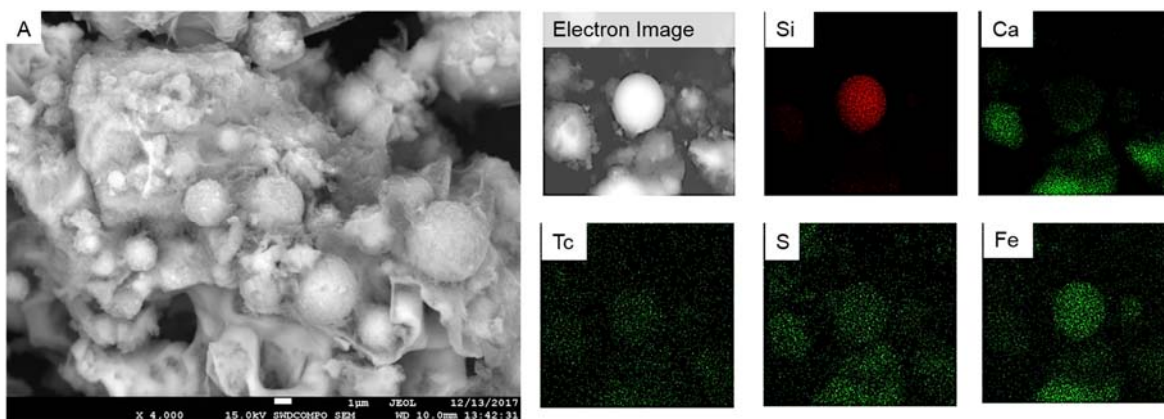


Figure 6.5. SEM and EDS Element Maps for Specimen Material Collected from Cast Stone Monoliths Cured 28 days. (A) SEM image from material collected from the exterior of a cured EQT non-rad Cast Stone monolith (TB25.1). (Electron Image and Maps) SEM image of material collected from a pre-leached Cast Stone rad monolith (TB27) and element maps for Si, Ca, Tc, S, and Fe, corresponding to the particles imaged in (Electron Image).

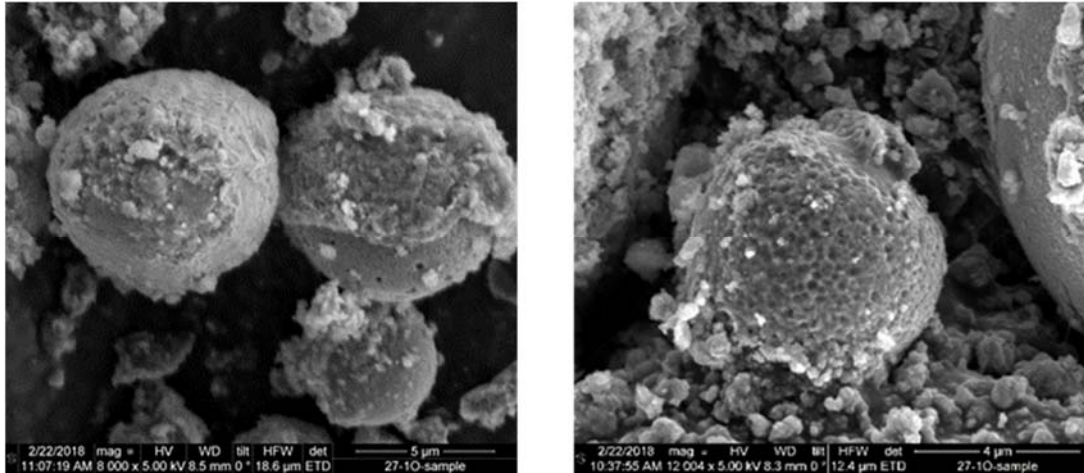


Figure 6.6. The Porous Nature of Spherical Particles Imaged in Cast Stone Based Monoliths Is Illustrated Here with SEM Images Collected for Material Sampled from the Exterior Wall of 63-day Leached Monolith 17-EMF-TB27-1.

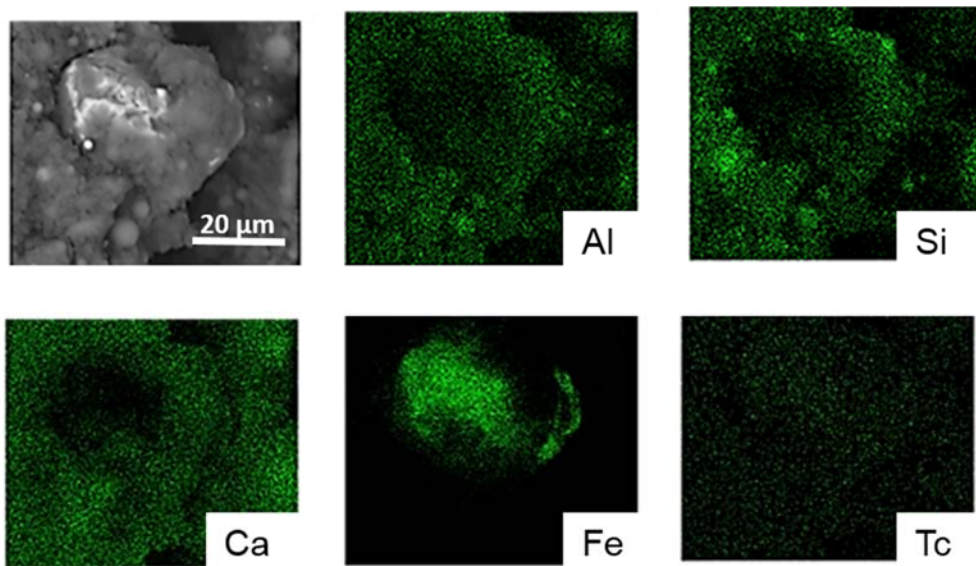


Figure 6.7. SEM Image and Element Mapping of Exterior EQT Cast Stone Material (rad, leached 63 days in DIW) That Shows the Presence of Particles with No Distinct Morphology or Crystalline Order and a Representative Particle Rich in Fe.

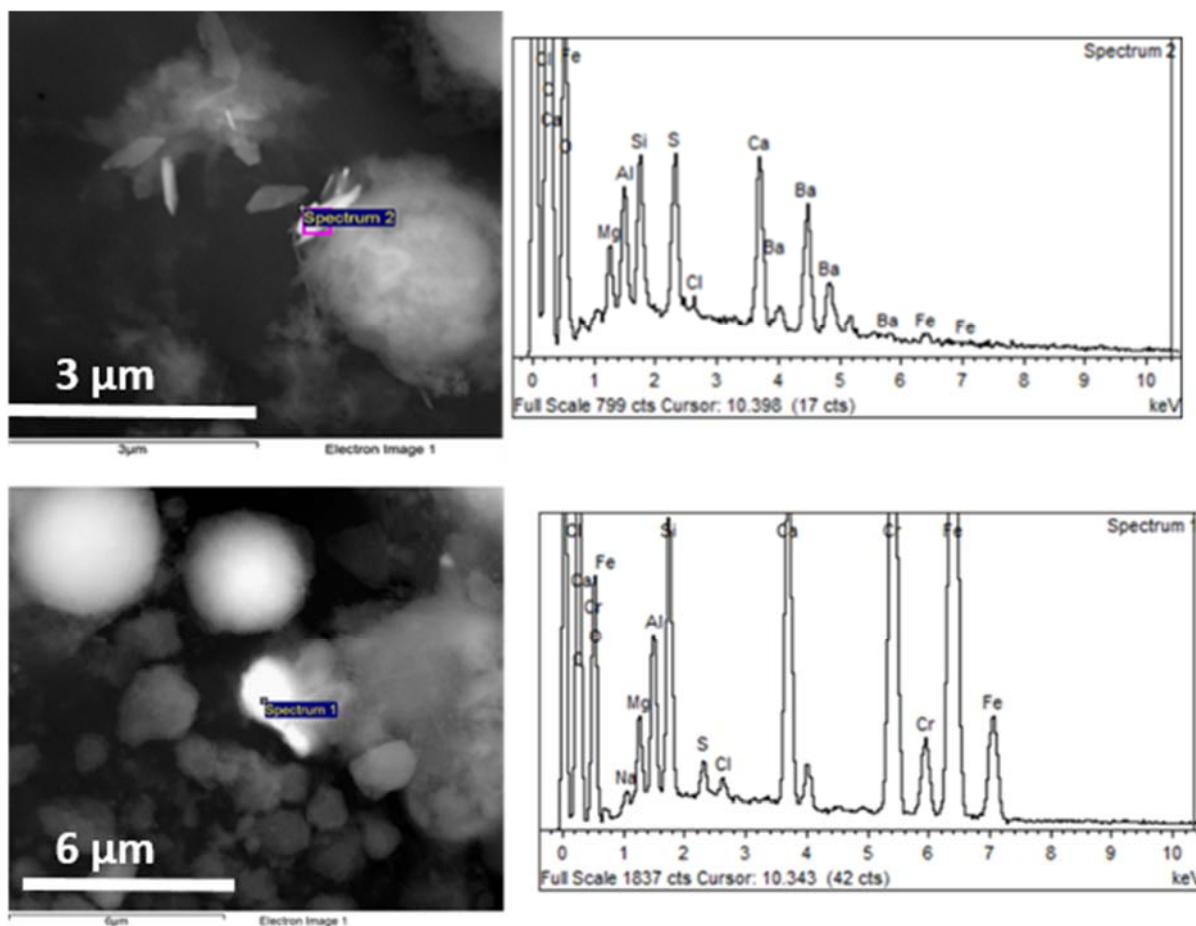


Figure 6.8. SEM Electron Images and EDS Analysis for Minor Phases Identified in the Exterior Material of Cast Stone Monolith TB27-1, Leached for 63 Days in DIW. The Top Two Images Show the Platy Particles Containing Enriched Levels of Ba and S, Relative to Other Samples Analyzed. In the bottom two images, the poorly defined morphology of some particles were enriched in Cr or Zr, with elevated levels of Fe.

6.2.2 SEM/EDS Results for EQT Average Simulant HL Specimens

SEM/EDS characterization of material from HL formulated monoliths reveals very different morphological features compared to the Cast Stone formulated samples described in Section 6.2.1. In all samples (non-rad and rad), there are fewer spherical particles that were commonly imaged in the Cast Stone samples. Instead small particles with either platy or rod-like morphology have formed on the larger micron size grains (Figure 6.9). Interestingly, a few of the large particles imaged appeared unreacted during leaching, as indicated by sharp edges and unaltered surface planes, while the remaining grains have clearly undergone reaction, either dissolution and/or precipitation (Figure 6.10).

Similar to the Cast Stone samples discussed in Section 6.2.1, high Z-contrast images and elemental maps were collected for the HL formulated samples according to the process described in the Cast Stone section. For the most part, concentrated areas of ^{99}Tc were not discernable by EDS analysis, with the exception of one particle imaged in the exterior monolith material collected from the 63-day leached HL-based (TB28-1) monolith. In Figure 6.11, elemental mapping of ^{99}Tc shows a contour that seems to

correlate with a Fe-rich area shown in the corresponding Fe map. This may suggest, but we emphasize that this is not independently confirmed by EDS spot analysis, that ^{99}Tc is present as a surface species during formation of this Fe-rich solid phase. Finally, the formation of both platy particles (shown earlier) and the unique honeycomb pattern shown below, could be indicative of transformation of parent material into a solid phase with clay-like textures.

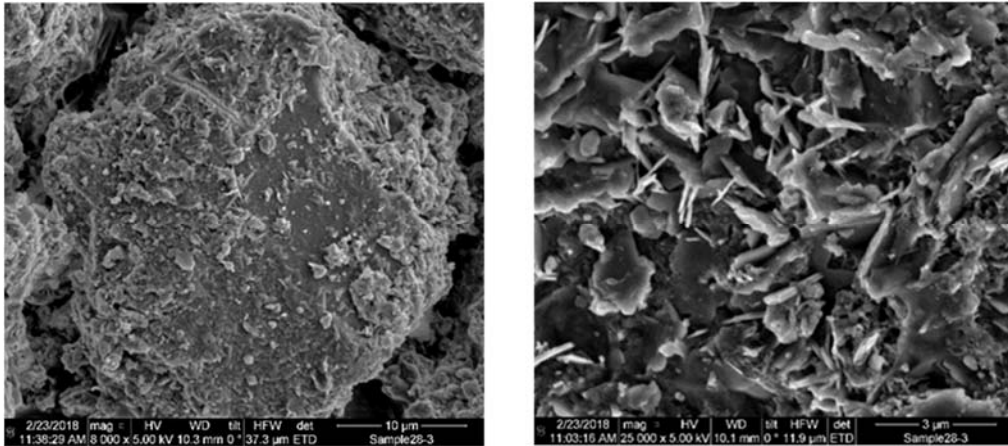


Figure 6.9. Typical SEM Images Collected from HL Specimens. Imaged here is the material collected from the pre-leach, rad TB28-3 specimen.

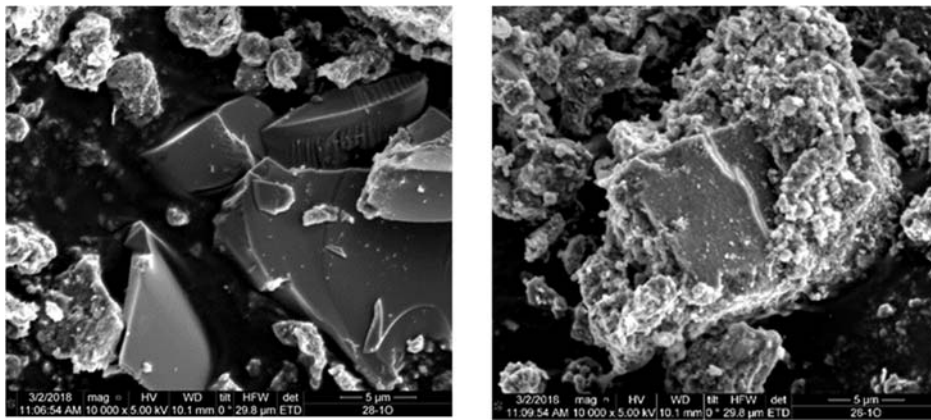


Figure 6.10. Unreacted Large Particles Found in the Exterior Material Collected from HL Based Rad Monolith TB28-1.

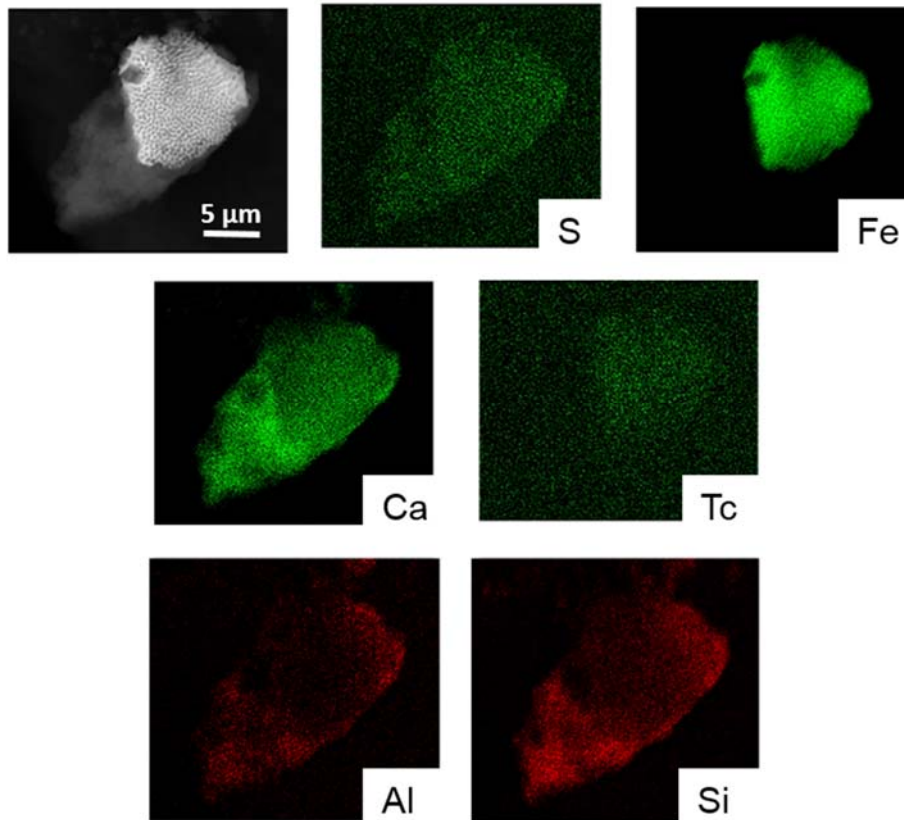


Figure 6.11. SEM Image and EDS Element Mapping for a Particle Found in the Exterior Material Collected from 63-day Leached HL Formulated Monolith (TB28-1).

6.3 Digital Autoradiography

Single particle digital autoradiography was used to image ^{99}Tc distribution within select rad EQT monoliths. Using the iQID, the instrument observes the ^{99}Tc distribution within cross-sectioned pucks from the monoliths. Further information regarding development and use of the technique can be found in Miller et al. (2014, 2015). Briefly, horizontal pucks were sectioned from >2 cm from the top circular face of the monoliths and analyzed using the iQID over a 48-hour interval. The samples analyzed were selected from Cast Stone (TB27) and HL (TB28) monoliths and included both pre- and post-leached specimens (see Section 8.0). Each image contained a reference sample of Tc-loaded Cast Stone to determine the instrument efficiency.

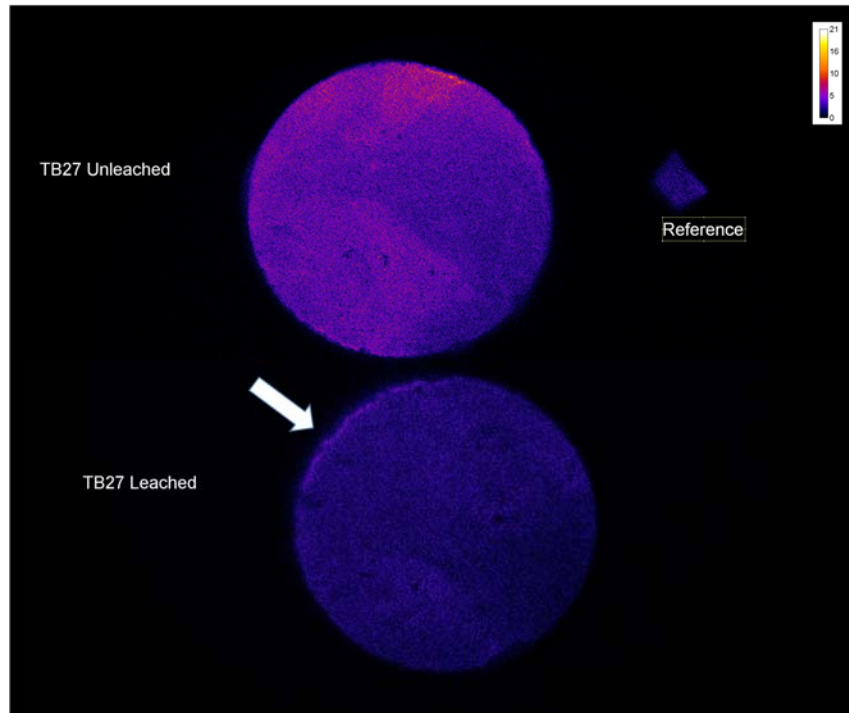


Figure 6.12. iQID Image of TB27 (Cast Stone) Both in Its Cured State (top) and Following 63 d Leaching in DIW (bottom). The white arrow is present to highlight a strong signal from the edge of the leached sample.

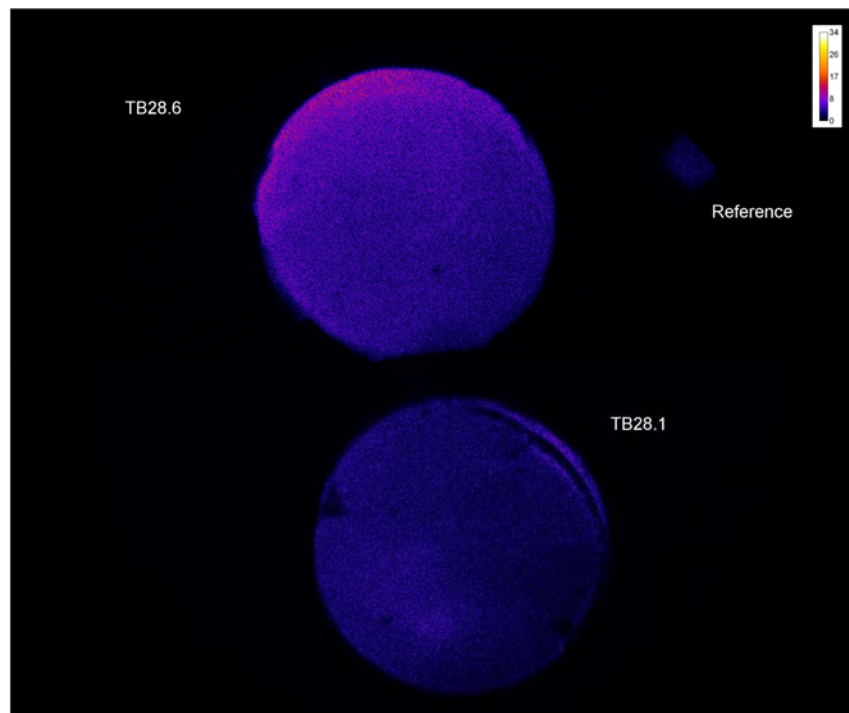


Figure 6.13. iQID Image of TB28 (HL) Both in Its Cured State (top) and Following 63 d Leaching in DIW (bottom).

iQID imaging was used to image the location of Tc within pucks cut from the Cast Stone (TB27) and HL (TB28) monoliths, both pre- and post-leached. Areas that appear brighter in iQID images correlate to regions with higher Tc concentrations. A comparison between the Cast Stone (TB27) samples is shown in Figure 6.12. At the top of the image, a strong Tc signal is observed from throughout the unleached sample (17-EMF-TB27-4). Following 63 d leaching (bottom, specimen 17-EMF-TB27-1) an increased amount of Tc was observed on the outer wall (denoted by the arrow). The brightness of the unleached sample compared with the leached sample is not yet fully understood, but has been seen in previous analysis of Cast Stone samples (Asmussen et. al. 2016). TB28, fabricated using the HL formulation, showed a different trend, Figure 6.13. Higher Tc was observed on the outer edge of the sample for both the unleached (top, specimen 17-EMF-TB28-6) and leached (bottom, specimen 17-EMF-TB28-1) samples. This trend may be due to increased ettringite formation in the HL formulations. With ettringite appearing in higher amounts near the outer surface, as supported by XRD analysis, Tc may become trapped within the ettringite structure. A similar process is also postulated for the post-leached Cast Stone sample in Figure 6.12.

7.0 TCLP Tests

After curing for at least 14 days, select ECS and non-rad EQT waste form specimens were characterized with respect to retention of hazardous constituent using the TCLP test (EPA 1992).

7.1 Methods and Materials

The TCLP test, EPA Method 1311 (EPA 1992), was conducted to demonstrate that the cementitious waste forms developed would meet RCRA LDRs (40 CFR 268, 2015) for hazardous wastes. The EMF evaporator bottoms waste simulants contain Zn and RCRA metals, including Cr and in the ECS simulants As, Hg, and Se. In addition, some of the dry materials may include these and other hazardous materials, e.g., Pb. Waste form specimens from test batches 1 through 26.2 (TB1 – TB26.2) were sent to SwRI for TCLP testing. The results were compared with the Universal Treatment Standards (UTS) in 40 CFR 268, *Land Disposal Restrictions* (40 CFR 268, 2015).

From each test batch, TB1 through TB26.2 (not including pre-screening batches 26.1b and 26.1c), one monolith specimen was selected for TCLP testing at SwRI. The results for the simulant variability samples (ECS) are provided in Table 7.2, Table 7.3, and Table 7.4 according to the dry ingredient recipe used. Results for the average simulant (EQT) monoliths are provided in Table 7.5. Each monolith was removed from its form 7 days after monolith production and packaged in an open, sealable plastic bag that was then enclosed in a second, sealed plastic bag containing a wet paper towel to maintain relative humidity conditions, >80%. Monolith specimens were then shipped overnight to SwRI to make sure that the specimens were ready for TCLP testing 14 days after monolith production. This schedule is summarized in Table 7.1 and matches the timeline used by SRNL for TCLP testing that they performed. In some instances, the monolith specimen was still soft, determined by squeezing the outer plastic wall, on the 7-day opening date. This was noted for TB12, TB13, and TB16. For these specimens, the plastic form was left on the monolith specimen so that the monolith could continue to cure and maintain its shape until the TCLP testing start date. These specimens were packaged and sent to SwRI upright to retain, as much as possible, any free liquids present within the plastic form. The plastic form was removed on the TCLP test start date by SwRI. For monolith 17-EMF-TB13-1, the monolith still had not completely cured by the 14th day and the TCLP test was conducted using the bottom, solidified portion of the monolith.

Table 7.1. Specimen Preparation and TCLP Testing Schedule

Test Batch #	SwRI ID#	Production Date	Monolith Opening Date	Ship Date	TCLP Test Start Date	TCLP Filtration Date
TB1	613739	03/27/2017	04/03/2017	04/05/2017	4/10/2017	4/11/2017
TB2	613748	03/27/2017	04/03/2017	04/05/2017	4/10/2017	4/11/2017
TB3	613749	03/27/2017	04/03/2017	04/05/2017	4/10/2017	4/11/2017
TB4	613750	03/27/2017	04/03/2017	04/05/2017	4/10/2017	4/11/2017
TB5	613751	03/27/2017	04/03/2017	04/05/2017	4/10/2017	4/11/2017
TB6	613752	03/27/2017	04/03/2017	04/05/2017	4/10/2017	4/11/2017
TB7	613753	03/28/2017	04/04/2017	04/05/2017	4/11/2017	4/12/2017
TB8	613754	03/28/2017	04/04/2017	04/05/2017	4/11/2017	4/12/2017
TB9	613755	03/28/2017	04/04/2017	04/05/2017	4/11/2017	4/12/2017
TB10	613738	03/28/2017	04/04/2017	04/05/2017	4/11/2017	4/12/2017
TB11	613740	03/28/2017	04/04/2017	04/05/2017	4/11/2017	4/12/2017
TB12	613741	03/28/2017	04/04/2017 ^(a)	04/05/2017	4/11/2017	4/12/2017
TB13	613742	03/29/2017	04/05/2017 ^(a)	04/05/2017	4/12/2017	4/13/2017
TB14	613743	03/29/2017	04/05/2017	04/05/2017	4/12/2017	4/13/2017
TB15	613744	03/29/2017	04/05/2017	04/05/2017	4/12/2017	4/13/2017
TB16	613745	03/29/2017	04/05/2017 ^(a)	04/05/2017	4/12/2017	4/13/2017
TB17	613746	03/29/2017	04/05/2017	04/05/2017	4/12/2017	4/13/2017
TB18	613747	03/29/2017	04/05/2017	04/05/2017	4/12/2017	4/13/2017
TB19	614014	04/03/2017	04/10/2017	04/11/2017	4/17/2017	4/18/2017
TB20	614015	04/03/2017	04/10/2017	04/11/2017	4/17/2017	4/18/2017
TB21	614016	04/03/2017	04/10/2017	04/11/2017	4/17/2017	4/18/2017
TB22	614017	04/03/2017	04/10/2017	04/11/2017	4/17/2017	4/18/2017
TB23	614018	04/03/2017	04/10/2017	04/11/2017	4/17/2017	4/18/2017
TB24	614019	04/03/2017	04/10/2017	04/11/2017	4/17/2017	4/18/2017
TB25.1	614020	04/04/2017	04/11/2017	04/11/2017	04/18/2017	04/19/2017
TB25.2	614021	04/04/2017	04/11/2017	04/11/2017	04/18/2017	04/19/2017
TB26.1a	614022	04/04/2017	04/11/2017	04/11/2017	04/18/2017	04/19/2017
TB26.2	614023	04/04/2017	04/11/2017	04/11/2017	04/18/2017	04/19/2017

(a) Plastic form was not removed from monolith specimen before shipment due to incomplete curing (monolith was still soft and/or free liquids were present).

7.2 Results and Discussion

The TCLP test results for the Cast Stone formulation used to treat ECS simulants are shown in Table 7.2 along with the UTS (40 CFR 268, 2015) concentrations for hazardous waste constituents required by LDRs. Similarly, Table 7.3 and Table 7.4 show the TCLP concentrations from the Aquaset/BFS and OPC/BFS formulations, respectively. In Table 7.5, TCLP concentrations for Average simulant EQT specimens are also provided. All 28 grout test batches analyzed passed the TCLP when compared to the UTS limit for each contaminant of concern (COC). However, these results are non-conservative for the ECS specimens due to the presence of precipitates in the starting simulants and the fact that COCs immobilized as a solid (precipitate) rather than in the aqueous phase may exhibit different leach behaviors. It is also important to note that these initial TCLP trends are based on the analysis of one specimen from each test batch and replicate specimen analysis by TCLP is recommended for formulations studied in future tests.

It is important to note that all Hg levels were non-detectable or below the detection limit for cold vapor atomic absorption analysis despite being present in the ECS simulants at elevated concentrations (between 38 and 65 ppm, Table 3.4). The retention of Hg at elevated levels is further supported by the concentration of Hg in the monolith specimen after TCLP testing. All specimens analyzed by TCLP were completely digested at SwRI, using a series of acid and fusion digestion methods, to determine the remaining concentration of constituents in the waste form and to better benchmark the starting composition within each grout formulation. Solid digestion results are provided in Appendix A, Section A.2. From these solid digestion results, the Hg remaining in the waste form ranged from 21.8 to 29.9 ppm. This range is approximately what one would expect assuming little Hg was present in the initial dry ingredients (Table A.1), which dilutes the total Hg concentration in the waste form once the dry ingredients (~1,750 g total) and simulant aliquot (~1,029.4 g) are mixed.

Table 7.2. TCLP Results for Simulants Treated with Cast Stone Formulation Recipe

Simulant	1	2	3	4	5	6	7	8	UTS Limit (mg/L) ^(a)	Pass/Fail 40 CFR 268
Sample ID	17-EMF- TB1-04	17-EMF- TB2-02	17-EMF- TB3-02	17-EMF- TB4-02	17-EMF- TB5-02	17-EMF- TB6-02	17-EMF- TB7-02	17-EMF- TB8-02		
RCRA Metals, (mg/L)										
As	0.0254	0.0416	0.0428	0.0397	0.0487	0.0421	0.0511	0.0504	5.0	Pass
Ba	0.238	0.295	0.271	0.266	0.164	0.181	0.204	0.190	21	Pass
Cd	<0.00500	<0.00500	<0.00500	<0.00500	<0.00500	<0.00500	<0.00500	<0.00500	0.11	Pass
Cr	0.0533	<0.00500	0.0196	0.0265	0.0166	<0.00500	0.00834	0.0427	0.60	Pass
Pb	<0.00500	<0.00500	<0.00500	0.0342	<0.00500	<0.00500	<0.00500	<0.00500	0.75	Pass
Hg	<0.00100	<0.00100	<0.00100	<0.00100	<0.00100	<0.00100	<0.00100	<0.00100	0.025	Pass
Se	0.357	0.275	0.577	0.603	0.347	0.256	0.472	0.591	5.7	Pass
Ag	<0.00500	<0.00500	<0.00500	<0.00500	<0.00500	<0.00500	<0.00500	<0.00500	0.14	Pass
Underlying Hazardous Constituents, (mg/L)										
Sb	0.0106	0.0116	0.0111	0.0114	0.0119	0.0103	0.0105	0.0111	1.15	Pass
Be	<0.00500	<0.00500	<0.00500	<0.00500	<0.00500	<0.00500	<0.00500	<0.00500	1.22	Pass
Ni	<0.00500	<0.00500	<0.00500	<0.00500	<0.00500	<0.00500	0.00643	<0.00500	11	Pass
Tl	<0.00500	<0.00500	<0.00500	<0.00500	<0.00500	<0.00500	<0.00500	<0.00500	0.20	Pass
Other Metals, (mg/L)										
Zn	<0.00500	<0.00500	<0.00500	0.00977	<0.00500	<0.00500	0.0277	<0.00500	4.3	Pass
(a) As reported in 40 CFR 268, 2015										

Table 7.3. TCLP Results for Simulants Treated with Aquaset/BFS Formulation Recipe

Simulant	1	2	3	4	5	6	7	8	UTS Limit (ppm) ^(a)	Pass/Fail 40 CFR 268
Sample ID	17-EMF- TB9-02	17-EMF- TB10-02	17-EMF- TB11-02	17-EMF- TB12-02	17-EMF- TB13-01	17-EMF- TB14-01	17-EMF- TB15-01	17-EMF- TB16-01		
RCRA Metals, (mg/L)										
As	0.0369	0.0503	0.0573	0.1030	0.0916	0.0693	0.0749	0.0748	5.0	Pass
Ba	0.284	0.329	0.335	0.274	0.208	0.218	0.215	0.243	21	Pass
Cd	<0.00500	<0.00500	<0.00500	<0.00500	<0.00500	<0.00500	<0.00500	<0.00500	0.11	Pass
Cr	0.00634	<0.00500	<0.00500	<0.00500	0.00989	<0.00500	<0.00500	0.005	0.60	Pass
Pb	<0.00500	<0.00500	<0.00500	<0.00500	<0.00500	<0.00500	<0.00500	<0.00500	0.75	Pass
Hg	<0.00100	<0.00100	<0.00100	<0.00100	<0.00100	<0.00100	<0.00100	<0.00100	0.025	Pass
Se	0.525	0.224	0.387	0.513	0.358	0.252	0.363	0.364	5.7	Pass
Ag	<0.00500	<0.00500	<0.00500	<0.00500	<0.00500	<0.00500	<0.00500	<0.00500	0.14	Pass
Underlying Hazardous Constituents, (mg/L)										
Sb	<0.00500	<0.00500	<0.00500	0.00501	<0.00500	<0.00500	0.00507	<0.00500	1.15	Pass
Be	<0.00500	<0.00500	<0.00500	<0.00500	<0.00500	<0.00500	<0.00500	<0.00500	1.22	Pass
Ni	<0.00500	<0.00500	<0.00500	<0.00500	<0.00500	<0.00500	<0.00500	<0.00500	11	Pass
Tl	<0.00500	<0.00500	<0.00500	<0.00500	<0.00500	<0.00500	<0.00500	<0.00500	0.20	Pass
Other Metals, (mg/L)										
Zn	<0.00500	<0.00500	<0.00500	<0.00500	<0.00500	<0.00500	0.0107	<0.00500	4.3	Pass

(a) As reported in 40 CFR 268, 2015

Table 7.4. TCLP Results for Simulants Treated with OPC/BFS Formulation Recipe

Simulant	1	2	3	4	5	6	7	8	UTS Limit (ppm) ^(a)	Pass/Fail 40 CFR 268
Sample ID	17-EMF- TB17-01	17-EMF- TB18-01	17-EMF- TB19-01	17-EMF- TB20-01	17-EMF- TB21-01	17-EMF- TB22-01	17-EMF- TB23-01	17-EMF- TB24-01		
RCRA Metals, (mg/L)										
As	0.0311	0.0525	0.0250	0.0196	0.0164	0.0202	0.0227	0.0194	5.0	Pass
Ba	0.309	0.315	0.297	0.304	0.269	0.265	0.272	0.306	21	Pass
Cd	<0.00500	<0.00500	<0.00500	<0.00500	<0.00500	<0.00500	<0.00500	<0.00500	0.11	Pass
Cr	0.0105	0.00507	0.00824	0.0182	0.0202	0.00591	0.00991	0.0189	0.60	Pass
Pb	<0.00500	<0.00500	<0.00500	<0.00500	<0.00500	<0.00500	<0.00500	<0.00500	0.75	Pass
Hg	<0.00100	<0.00100	<0.00100	<0.00100	<0.00100	<0.00100	<0.00100	<0.00100	0.025	Pass
Se	0.388	0.245	0.253	0.283	0.309	0.203	0.269	0.316	5.7	Pass
Ag	<0.00500	<0.00500	<0.00500	<0.00500	<0.00500	<0.00500	<0.00500	<0.00500	0.14	Pass
Underlying Hazardous Constituents, (mg/L)										
Sb	0.0108	0.0131	0.0067	0.00607	0.00566	0.00808	0.00681	0.00662	1.15	Pass
Be	<0.00500	<0.00500	<0.00500	<0.00500	<0.00500	<0.00500	<0.00500	<0.00500	1.22	Pass
Ni	<0.00500	<0.00500	<0.00500	<0.00500	<0.00500	<0.00500	<0.00500	<0.00500	11	Pass
Tl	<0.00500	<0.00500	<0.00500	<0.00500	<0.00500	<0.00500	<0.00500	<0.00500	0.20	Pass
Other Metals, (mg/L)										
Zn	<0.00500	<0.00500	<0.00500	<0.00500	<0.00500	<0.00500	<0.00500	<0.00500	4.3	Pass

(a) As reported in 40 CFR 268, 2015

Table 7.5. TCLP Results for EQT Specimens Treating the Avg Simulant with Cast Stone and HL Formulation Recipes

Simulant	Avg	Avg	Avg	Avg	UTS Limit (ppm) ^(a)	Pass/Fail 40 CFR 268
Formulation	Cast Stone	Cast Stone	HL, OPC, BFS	HL, OPC, BFS		
Sample ID	17-EMF-TB25.1-03	17-EMF-TB25.2-03	17-EMF-TB26.1a-03	17-EMF-TB26.2-03		
RCRA Metals, (mg/L)						
As	<0.0100	<0.0100	<0.0100	<0.0100	5.0	Pass
Ba	0.204	0.199	0.397	0.414	21	Pass
Cd	<0.00500	<0.00500	<0.00500	<0.00500	0.11	Pass
Cr	0.0163	0.0107	<0.00500	0.0128	0.60	Pass
Pb	<0.00500	<0.00500	<0.00500	<0.00500	0.75	Pass
Hg	<0.00100	<0.00100	<0.00100	<0.00100	0.025	Pass
Se	0.0496	0.0399	<0.0200	<0.0200	5.7	Pass
Ag	<0.00500	<0.00500	<0.00500	<0.00500	0.14	Pass
Underlying Hazardous Constituents, (mg/L)						
Sb	0.0113	0.0106	0.00532	<0.00500	1.15	Pass
Be	<0.00500	<0.00500	<0.00500	<0.00500	1.22	Pass
Ni	0.00507	<0.00500	<0.00500	<0.00500	11	Pass
Tl	<0.00500	<0.00500	<0.00500	<0.00500	0.20	Pass
Other Metals, (mg/L)						
Zn	0.0823	<0.00500	<0.00500	<0.00500	4.3	Pass

(a) As reported in 40 CFR 268, 2015

8.0 EPA Method 1315 Leach Testing

The EPA Method 1315 leach test measures the effective (or observed) diffusivity of species of interest using a semi-dynamic leaching procedure. The effective diffusion coefficient accounts for all physical and chemical retention factors influencing mass transfer of the COC and is calculated according to Fick's second law of diffusion. Leach testing was performed on Average Simulant EQT cylindrical monoliths for a minimum of 63 days leaching in DIW in accordance with the instructions and approach described in EPA Method 1315 (EPA 2013). Effective diffusivities were calculated for key constituents including technetium, iodide, and sodium.

8.1 Methods and Materials

The EPA Method 1315 test is a semi-dynamic leach test that consists of submerging a monolith in leachant at a fixed ratio of liquid volume to solid geometric surface area. Monoliths from Average Simulant test batches Cast Stone (TB27) and HL (TB28) were placed into the centers of leaching vessels containing sufficient leachant (DIW) to maintain a solution-to-solid geometric surface area ratio of $9 \pm 1 \text{ mL/cm}^2$. Monolith stands and holders were used to maximize the contact area of the monolith with the leaching solution. The surface area of each monolith and the DIW target volumes were calculated before starting the EPA Method 1315 leach test based on physical measurements determined for each specimen. Specifically, the diameter of each specimen was measured at the bottom, middle, and top and the specimen length was measured at three rotational orientations mutually separated by ~ 120 degrees from an arbitrary starting location using a caliper. These measurements were averaged to determine the average specimen diameter and length for calculating total surface area.

Appropriate containers (2 L plastic buckets) with lids were used to fully immerse each monolith in the leaching solution. Duplicate monoliths from each test batch were leached in DIW, labeled 1 and 2. Leachate sampling was done at fixed intervals, with cumulative leach times of 0.08, 1, 2, 7, 14, 28, 42, 49, and 63 days. At each sampling interval, the monolith was removed from the leaching solution, the monolith mass was recorded after draining as much surface water as possible, and it was placed in a new 2 L bucket containing fresh DIW leachant. The contacted leachate pH, E_h , EC, ammonia concentration and alkalinity were measured at each time interval and recorded on the data sheet. The remaining leachate was subsampled into several aliquots (each ~ 20 mL) for subsequent analysis. Analysis focused on leached components for which effective or observed diffusivities are needed (e.g., ^{99}Tc , ^{127}I , and Na^+) and overall chemical composition. Analytical methods used include ICP-OES for cation concentrations, ICP-MS for ^{99}Tc and ^{127}I concentrations, and IC for anion concentrations.

Initial concentrations, $C(0)$, of the constituents of interest in the pre-leached monoliths, specifically ^{99}Tc , ^{127}I , and Na^+ , are given in Table 8.1. Initial ^{99}Tc , ^{127}I , and Na^+ concentrations in the cured monoliths were calculated from the constituent's initial concentration in the ^{99}Tc -spiked Avg simulant (Table 3.4) and the mass of dry ingredients and liquid simulant used. This approach is based on the assumption that there is no leachable ^{99}Tc and relatively negligible ^{127}I , or Na^+ sources in the dry ingredients.

Table 8.1. Initial Concentrations, $C(0)$, of ^{99}Tc , ^{127}I , and Na^+ used in Diffusivity Calculations

Test Batch #	^{99}Tc (mg/kg-dry)	^{127}I (mg/kg-dry)	Na^+ (mg/kg-dry)
27	8.21	9.44	26,600
28	8.05	9.05	25,500

The observed or effective diffusivities for ^{99}Tc , ^{127}I , and Na^+ were calculated using the analytical solution for Fick's second law and Equation 8.1 for simple radial diffusion from a cylinder into an infinite bath as detailed by EPA Method 1315 (EPA 2013). The effective or observed diffusion coefficient, D_{eff} or D_{obs} , accounts for all physical and chemical retention factors influencing mass transfer of the COC. In this report, the term "effective diffusion coefficient" is used and is equivalent to the term "observed diffusion coefficient" used in EPA Method 1315, the symbol D used in ANSI/ANS-16.1 (ANSI/ANS-16.1-2003), and the symbol D_e used in the ASTM C1308-08 (2017) method. In some literature, this parameter, the D_{eff} value in Equation 8.1, is called the apparent diffusion coefficient, D_a (see, for example, Grathwohl 1998). All of these names are equivalent and are "quantified" in standard leach tests.

$$D_{eff} = 10000 * D_{obs(i)} = \pi \left[\frac{M_{ti}}{2\rho C_o (\sqrt{t_i} - \sqrt{t_{i-1}})} \right]^2 \quad (8.1)$$

where

- D_{eff} = effective diffusion coefficient (cm^2/s)
- $D_{obs(i)}$ = observed effective diffusivity of a specific constituent for leaching interval i (m^2/s)
- M_{ti} = mass of specific constituent released during leaching interval i (mg/m^2)
- t_i = cumulative contact time after leaching interval i (s)
- t_{i-1} = cumulative contact time after the previous leaching interval, $i - 1$ (s)
- C_o = initial concentration of constituent in the dry grout ($\text{mg}/\text{kg-dry}$)
- ρ = grout dry bulk density ($\text{kg-dry}/\text{m}^3$), determined as oven dried mass divided by the calculated volume of the monolith.

The leachability index (LI), a unitless parameter derived from the interval effective diffusion coefficient values (D_i , here using D_{eff}), is calculated using Equation 8.2, in which β is a defined constant ($1.0 \text{ cm}^2/\text{s}$) from ANSI/ANS-16.1 (ANSI/ANS-16.1-2003). A low diffusivity results in a larger LI.

$$LI_i = \frac{1}{n} \sum_1^n \left[\log \left(\frac{\beta}{D_i} \right) \right]_n \quad (8.2)$$

8.2 Results and Discussion

Monoliths used in EPA Method 1315 leach testing were photographed before leaching and after the 63-day leach period had elapsed to record observations of cracking and monolith degradation. For all specimens subjected to leach testing, visible cracking or degradation was not observed (Figure 8.1). The calculated effective diffusivity coefficients (D_{eff}) and LI values for ^{99}Tc , ^{127}I , and Na^+ through 63 cumulative leaching days are provided in Table 8.2. Calculated D_{eff} values for ^{99}Tc , ^{127}I , and Na^+ are also shown graphically in Figure 8.2. Duplicate monoliths cured for 28 days are differentiated by the test number followed by either 1 or 2 for DIW-leached monoliths e.g., TB27-1 and TB27-2. For non-detect (ND) ^{127}I concentrations in the leachates, the estimated quantitation limit (EQL) value of ICP-MS for ^{127}I ($<0.126 \mu\text{g}/\text{L}$) was used to calculate ^{127}I less than D_{eff} and greater than LI values, respectively. Control leachate samples, from buckets containing only DIW, were also collected at each sampling interval to determine the background concentrations of ^{99}Tc , ^{127}I , and Na^+ . Background concentrations for all four constituents were non-detect for all sampling intervals; therefore, a background subtraction was not required to determine the actual leached concentration. No ND, zero, or negative leachate concentration

values were encountered for ^{99}Tc and Na^+ during the cumulative 63-day leaching test. For ^{127}I , ND concentrations were measured only for TB28 monolith leachates and only for the first sampling at 0.08 days.

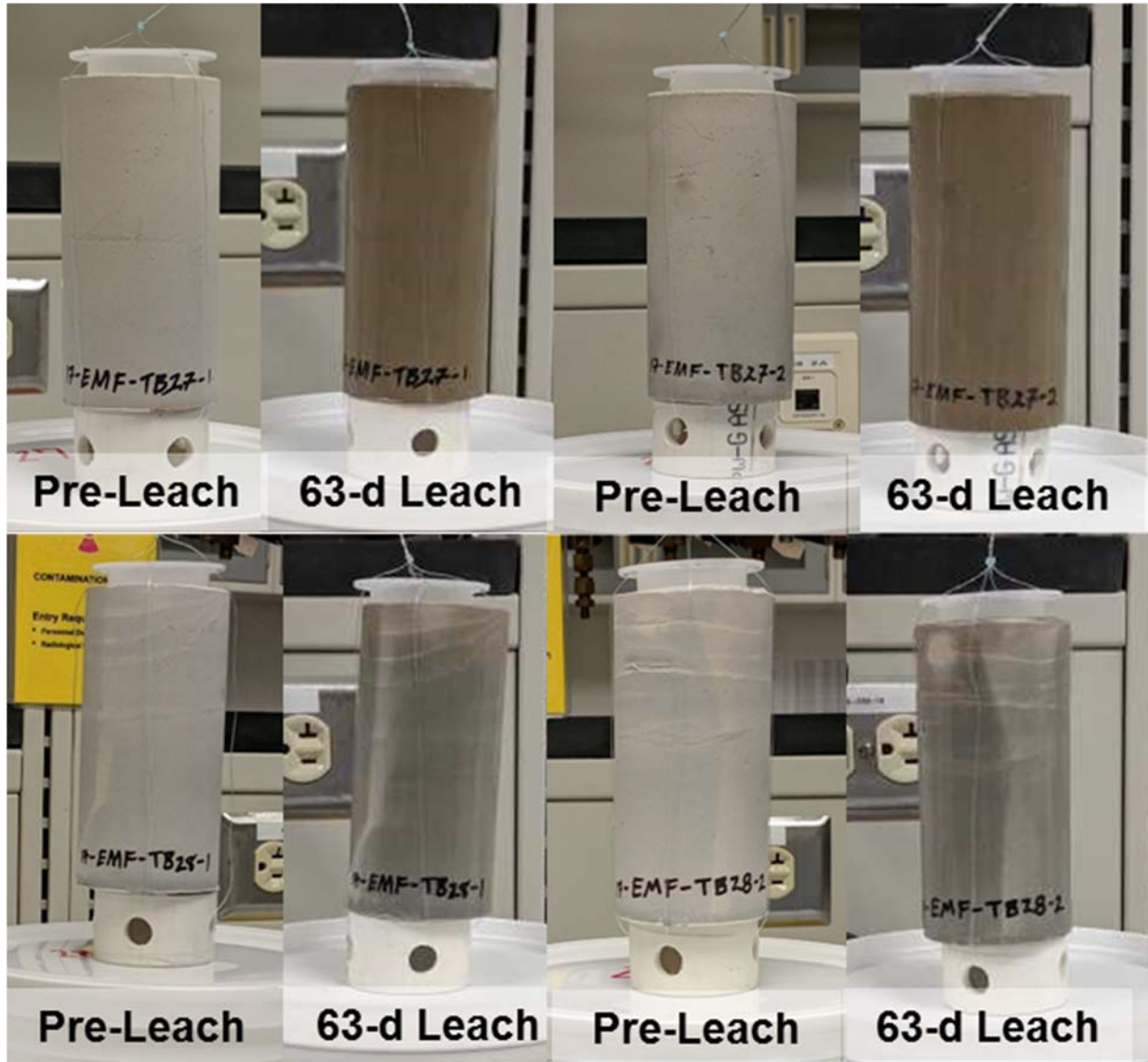


Figure 8.1. EQT Specimens Used in EPA Method 1315 Leach Testing Before Leaching (Pre-Leach) and after the 63-day Leach Period Had Elapsed (63-d Leach). Specimens included 17-EMF-TB27-1, 17-EMF-TB27-2, 17-EMF-TB28-1, and 17-EMF-TB28-2. Each 63-day leached specimen is darker in color because it is still damp from the leaching solution.

Table 8.2. Diffusivity and LI Values of ⁹⁹Tc, ¹²⁷I, and Na⁺ in DIW Leaching Solution

Cumulative Leach Time (day)	TB27-1 for ⁹⁹ Tc		TB27-2 for ⁹⁹ Tc		TB27-1 for ¹²⁷ I		TB27-2 for ¹²⁷ I		TB27-1 for Na ⁺		TB27-2 for Na ⁺	
	<i>D_{eff}</i> (cm ² /s)	LI [-]										
0.08	7.15E-11	10.1	1.61E-10	9.8	5.42E-10	9.3	1.54E-09	8.8	1.39E-09	8.9	3.87E-09	8.4
1.0	4.64E-10	9.3	4.58E-10	9.3	2.59E-09	8.6	2.81E-09	8.6	4.90E-09	8.3	5.09E-09	8.3
2.0	4.66E-10	9.3	2.76E-10	9.6	2.17E-09	8.7	1.55E-09	8.8	3.78E-09	8.4	2.67E-09	8.6
7.0	4.18E-10	9.4	3.02E-10	9.5	2.13E-09	8.7	2.07E-09	8.7	3.47E-09	8.5	3.43E-09	8.5
14.0	1.86E-10	9.7	1.18E-10	9.9	1.38E-09	8.9	1.26E-09	8.9	2.78E-09	8.6	2.91E-09	8.5
28.0	7.96E-11	10.1	6.66E-11	10.2	8.88E-10	9.1	8.51E-10	9.1	2.24E-09	8.6	2.03E-09	8.7
42.0	4.36E-11	10.4	4.57E-11	10.3	5.11E-10	9.3	5.04E-10	9.3	1.54E-09	8.8	1.83E-09	8.7
49.0	4.26E-11	10.4	4.91E-11	10.3	4.08E-10	9.4	4.52E-10	9.3	1.47E-09	8.8	1.67E-09	8.8
63.0	4.60E-11	10.3	5.78E-11	10.2	4.01E-10	9.4	3.88E-10	9.4	1.27E-09	8.9	1.48E-09	8.8
Cumulative Leach Time (day)	TB28-1 for ⁹⁹ Tc		TB28-2 for ⁹⁹ Tc		TB28-1 for ¹²⁷ I		TB28-2 for ¹²⁷ I		TB28-1 for Na ⁺		TB28-2 for Na ⁺	
	<i>D_{eff}</i> (cm ² /s)	LI [-]										
0.08	2.94E-11	10.5	1.54E-11	10.8	8.78E-13	12.1	8.93E-13	12.0	8.43E-10	9.1	6.14E-10	9.2
1.0	1.50E-10	9.8	1.69E-10	9.8	3.36E-11	10.5	3.74E-11	10.4	3.09E-09	8.5	3.20E-09	8.5
2.0	3.76E-10	9.4	2.41E-10	9.6	1.13E-10	9.9	6.82E-11	10.2	5.77E-09	8.2	4.29E-09	8.4
7.0	3.15E-10	9.5	2.68E-10	9.6	4.09E-11	10.4	3.68E-11	10.4	5.33E-09	8.3	4.71E-09	8.3
14.0	1.37E-10	9.9	1.30E-10	9.9	3.98E-11	10.4	3.92E-11	10.4	4.48E-09	8.3	4.27E-09	8.4
28.0	2.21E-11	10.7	2.49E-11	10.6	4.36E-11	10.4	2.95E-11	10.5	6.50E-09	8.2	3.84E-09	8.4
42.0	4.08E-12	11.4	6.44E-12	11.2	3.25E-11	10.5	3.02E-11	10.5	3.88E-09	8.4	2.59E-09	8.6
49.0	6.42E-12	11.2	7.24E-12	11.1	6.17E-11	10.2	5.82E-11	10.2	3.65E-09	8.4	2.33E-09	8.6
63.0	6.42E-12	11.2	8.01E-12	11.1	4.53E-11	10.3	3.77E-11	10.4	2.92E-09	8.5	1.89E-09	8.7

Values in red use EQL values to determine *D_{eff}* and LI.

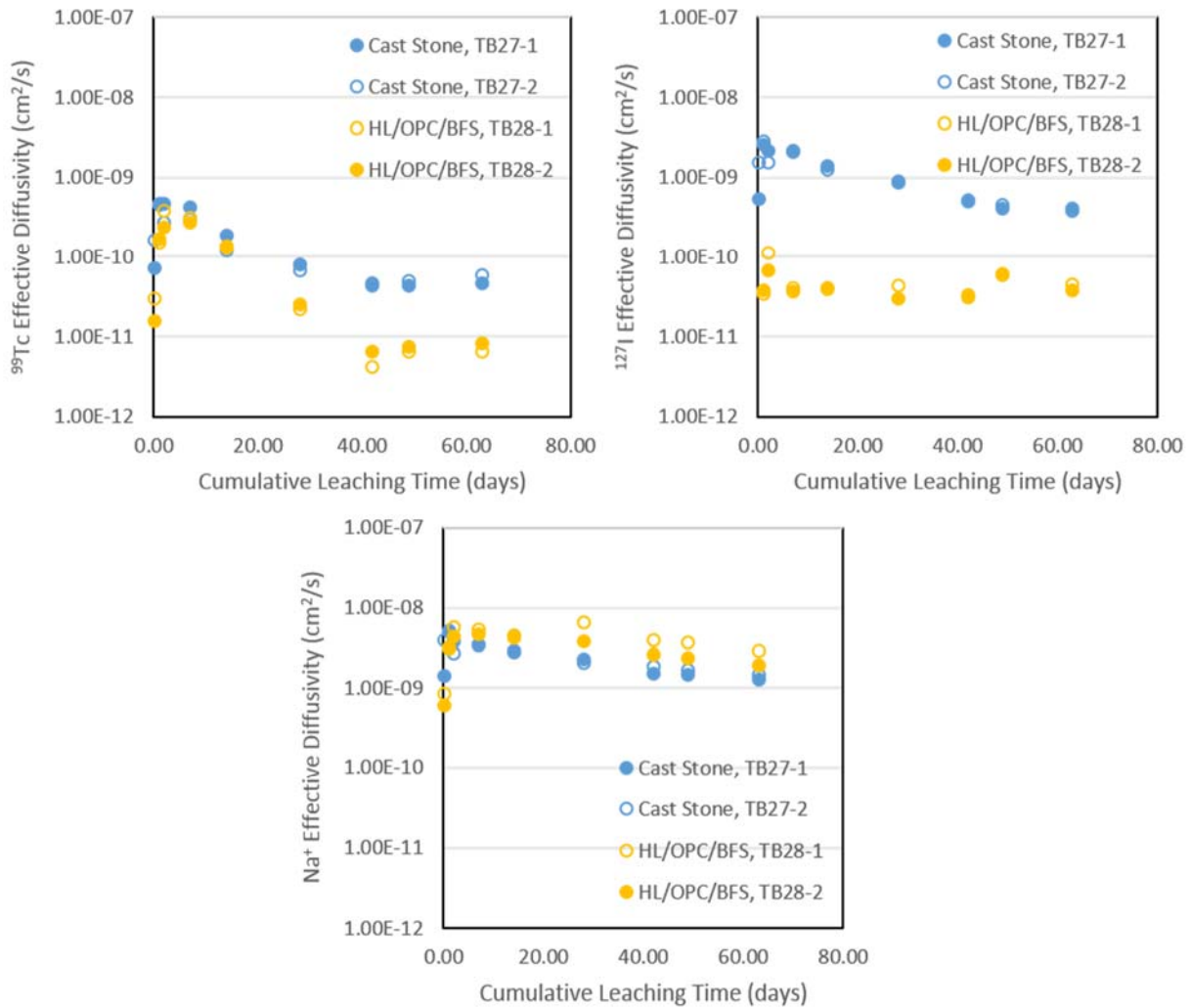


Figure 8.2. Effective Diffusivity Values of ^{99}Tc (top, left), ^{127}I (top, right), and Na^+ (bottom) from Avg Simulant (EQT) Radiological Specimens Leached for a Cumulative 63 days in DIW. Monoliths were tested using the original Cast Stone recipe (TB27-1 and TB27-2) and a HL recipe (TB28-1 and TB28-2).

A time-invariant average D_{eff} value was calculated for the three constituents of concern by averaging the D_{eff} values determined for leach samples between 28 and 63 days. Average D_{eff} values are provided in Table 8.3, in addition to the fraction of total constituent mass released after the 63-day cumulative leach period relative to the initial mass of constituent in the monolith before leaching. Because the fraction of total released mass of ^{99}Tc during early leach periods, 0.08 to 14 days, is less than 20% of the total initial mass of ^{99}Tc , the time-invariant ^{99}Tc D_{eff} value was determined from the later leach periods, between 28 and 63 days. This approach is supported by the less significant effect of early leaching on full-sized cementitious waste forms to be disposed of in the IDF. In addition, average ^{99}Tc D_{eff} values with their uncertainty ranges can cover the minor artifacts that might result from the early stages of leaching (e.g., surface wash off), if there are any. For consistency, this approach to calculating average D_{eff} values is used for all three constituents.

In general, early ^{99}Tc D_{eff} values, up to the cumulative 14 days, were slightly greater and at times nearly two orders of magnitude higher than D_{eff} values measured during later leach periods because of the initial removal of surface-bound ^{99}Tc . However, the difference in ^{99}Tc D_{eff} between early (0.08 – 14 days) and late (28 – 63 days) leaching periods was less pronounced with the Cast Stone formulation, with averaged early to late ^{99}Tc D_{eff} values decreasing by slightly less than an order of magnitude. For the HL-formulation, the average ^{99}Tc D_{eff} for early and late leaching periods differed by greater than an order of magnitude. Averaged ^{99}Tc D_{eff} values for individual monoliths after 28-day curing and from the cumulative 28-day to 63-day leaching in DIW ranged from 9.76×10^{-12} to 5.48×10^{-11} cm^2/s (Table 8.3). Furthermore, all average ^{99}Tc D_{eff} values for individual monoliths showed lower D_{eff} values than other highly mobile non-reactive constituents (e.g. Na^+).

If the total fraction of ^{99}Tc mass released from the monoliths is less than 20% over the course of EPA Method 1315 leach testing, then the D_{eff} values determined are valid and meet the semi-infinite source term assumption and effective diffusion coefficient calculations defined by Equation 8.1 and per discussion in ANSI/ANS-16.1 (ANSI/ANS-16.1-2003). Thus, D_{eff} corrections for inventory depletion are not necessary. For all monoliths (see Table 8.3) leached in DIW, the average total fraction of ^{99}Tc mass leached from monoliths did not exceed 20% of the initial ^{99}Tc mass over the 63-day cumulative leaching period. However, specimens formulated from the Cast Stone recipe (TB27) leached more ^{99}Tc than the HL-based monoliths. For ^{127}I , the amount of iodine released remained below 20% of the initial ^{127}I mass and the calculated D_{eff} values show a greater improvement in ^{127}I diffusivity from HL-based specimens versus Cast Stone specimens relative to the reduction in ^{99}Tc diffusivity when comparing HL-based and Cast Stone formulations. The average total fraction of Na^+ , similar to ^{99}Tc and ^{127}I , leached less than 20% of the original Na^+ mass in each specimen at the end of the 63-day leach period. However, the fraction of Na^+ leached from the HL-based specimens was relatively greater than the Cast Stone-based specimens.

Some release of ^{99}Tc and ^{127}I did not follow a pure diffusion trend, also found in previous work (Um et al. 2016; Saslow et al. 2017), showing a low slope beyond the acceptable limit for the EPA 1315 Method (a slope of 0.5 ± 0.15). Deviation from a diffusion-driven release mechanism is shown for each contaminant in Figure A.29 through Figure A.31 in Appendix A, Section A.4. Therefore, the calculated diffusivity values in Table 8.2 and Table 8.3 should be used with care. In addition, the cumulative releases of ^{99}Tc , ^{127}I , and Na^+ as a function leaching time are also reported for qualitative understanding of release in Table A.6 and Table A.7.

Table 8.3. Calculated Dry Bulk Density of Each Monolith and Averaged D_{eff} Values of ^{99}Tc , I^- , and Na^+ from the Cumulative 28-Day to 63-Day Leaching in DIW with Average Fraction of Released Mass in Duplicates of Individual Monolith Batches

Formulation	Test Batch	Dry Bulk Density (g/cm^3)	DIW Leaching Solution					
			^{99}Tc D_{eff} [cm^2/s]	F ^(a)	I^- D_{eff} [cm^2/s]	F	Na^+ D_{eff} [cm^2/s]	F
Cast Stone	TB27-1	1.33	5.29×10^{-11}	0.033	5.52×10^{-10}	0.088	1.63×10^{-9}	0.131
Cast Stone	TB27-2	1.34	5.48×10^{-11}	0.030	5.49×10^{-10}	0.088	1.75×10^{-9}	0.135
HL	TB28-1	1.40	9.76×10^{-12}	0.022	4.58×10^{-11}	0.017	4.24×10^{-9}	0.175
HL	TB28-2	1.38	1.17×10^{-11}	0.021	3.89×10^{-11}	0.016	2.66×10^{-9}	0.151

(a) F indicates fraction of total mass released for each constituent in DIW leaching solution compared to initial mass of constituent in each monolith after 63 days leaching.

8.2.1 ⁹⁹Tc Leachability in DIW

The results for the cumulative 63-day leaching for ⁹⁹Tc in DIW are shown in Figure 8.2 (top, left). The release of ⁹⁹Tc from both the Cast Stone and HL-based monoliths is not considered to follow a pure diffusion trend due to the decrease in release rate during the later leach periods (≥ 28 days). As such, the release of ⁹⁹Tc is likely influenced by additional chemical reactions as reported in previous reports (Um et al. 2016; Saslow et al. 2017). Chemical reactions could be (1) ⁹⁹Tc incorporation into ettringite in either the pre-leached cured grout or incorporation into newly formed ettringite from transformation of portlandite during the active leaching stage, (2) ion exchange between ⁹⁹Tc and sulfate in ettringite, (3) ⁹⁹Tc removal by continuous and slow hydration reactions, or (4) continuous, slow ⁹⁹Tc reduction (or incorporation into a mineral phase) by slow dissolution of BFS. Based on the XRD results discussed in Section 6.1, if the chemical process driving ⁹⁹Tc release from the monoliths involves reactions (1) and/or (2), which depend on the formation and ⁹⁹Tc incorporation into ettringite, the HL-based waste forms will perform slightly better than the Cast Stone-based waste forms when treating a waste stream similar to the Avg simulant used here. The average ⁹⁹Tc D_{eff} values support this mechanism of chemical leaching via ettringite mineral formation.

8.2.2 ¹²⁷I Leachability in DIW

The results for the cumulative 63-day leaching for ¹²⁷I in DIW are shown in Figure 8.2 (top, right). As expected, there is an immediate increase in ¹²⁷I D_{eff} during early leaching periods; however, this trend is more pronounced in the monoliths formulated using the Cast Stone recipe compared to the HL-based monoliths. The HL-based specimens (TB28-1 and TB28-2) show a slight increase in D_{eff} through 2 days of leaching, and then D_{eff} remains relatively constant through the 63-day leach period. Furthermore, specimens with the HL formulation demonstrate at least an approximate order of magnitude improvement (decrease) in ¹²⁷I D_{eff} values relative to Cast Stone formulated monoliths throughout the 63-day leach period. This trend is also evident by the total fraction of ¹²⁷I released, where Cast Stone formulated specimens released nearly 9% of the initial ¹²⁷I mass in the cementitious waste form and the HL monoliths leached less than 2% of the initial ¹²⁷I mass.

8.2.3 Leachability of Na⁺ in DIW

The results for the cumulative 63-day leaching for Na⁺ in DIW are shown in Figure 8.2 (bottom). Average Na⁺ D_{eff} values for the cumulative 63-day leaching are an order of magnitude higher than average D_{eff} values for ⁹⁹Tc and for ¹²⁷I released from HL-based monoliths. For leached Cast Stone monoliths, the Na⁺ release is less than a magnitude greater than ¹²⁷I release throughout the cumulative 63-day leaching period. In all monoliths, the fraction of total Na⁺ mass released is less than 20% (Table 8.3), despite substantial Na content in the dry ingredients (Table A.1), up to 27,800 mg/kg as seen in FA.

8.2.4 Other Measurements in DIW

Additional cations and anions measured in EPA 1315 Method leaching tests can be found in Appendix A, Table A.6 and Table A.7. Other measurements, including pH, EC, ammonia and alkalinity, were made for each leachate and individual monolith at each leaching interval. The measured pH in the DIW leachates showed a range between 10.6 and 12.0. The measured ECs in DIW leaching solutions were initially low, 0.1 to ~1.0 mS/cm over the first 7 days of leaching, but increased typically above 1.0 mS/cm during the later leaching periods. Overall the EC values measured for Cast Stone monoliths were lower than HL-based monoliths. Alkalinity (measured as CaCO₃) values were already as high as 24.6-35.2 mg/L at the 2-hour interval in DIW leaching solutions, and increased until a cumulative leaching time up to 28 days

before decreasing again. The increase is due to the release of hydroxyl and carbonate ions, and the late decrease in alkalinity is attributed to precipitation of carbonate minerals (e.g., calcite). In all leachate solutions, ammonia concentrations were all measured as non-detectable levels. Additional pH values and other measurements are found in Appendix A, Table A.8.

9.0 ⁹⁹Tc Desorption Testing

This section presents time-dependent ⁹⁹Tc desorption K_d measurements performed after an initial 30-day sorption phase. Preliminary ⁹⁹Tc sorption tests were conducted using Average Simulant (EQT) non-⁹⁹Tc-spiked monolith crushed material from both Cast Stone (TB25.1) and HL (TB26.2) formulations. After the initial 30-day sorption phase, the ⁹⁹Tc-laden material was used to perform ⁹⁹Tc desorption K_d tests. Sorption testing was performed under reducing conditions to maximize ⁹⁹Tc sorption, whereas desorption tests were performed under oxidizing conditions. The procedure used to perform these tests was adapted from ASTM C1733-17a, *Standard Test Method for Distribution Coefficients of Inorganic Species by the Batch Method*.

9.1 Methods and Materials

For all ⁹⁹Tc sorption and desorption tests, non-⁹⁹Tc-spiked monolith material from Cast Stone specimen 17-EMF-TB25.1-5 and HL specimen 17-EMF-TB26.2-5 were used. Monoliths from TB25.1 were prepared with the original Cast Stone recipe (8% OPC, 45% FA, and 47% BFS) and monoliths from TB26.2 were prepared with 10% HL, 18% OPC, and 72% BFS at a w/dm ratio of 0.5 using the Avg simulant.

9.1.1.1 Material Preparation

After 28 days of curing, one monolith from each test batch (Cast Stone TB25.1 and HL TB26.3) was removed from its form and transferred to an anoxic chamber filled with a mixture of N₂ (98%) and H₂ (2%) gases and with a palladium catalyst to maintain an O₂-free environment (<20 ppm O₂). Once in the chamber, the oxidized region on the monolith's exterior was removed using a file and the most internal solid portion of each monolith was exposed by cracking the specimen. Interior pieces of monolith material were then reduced to a size fraction of 0.425 – 2 mm using a hydraulic press and/or mortar and pestle. The crushed material was then size fractionated by dry sieving. Effort was made to avoid near-surface material, which may have oxidized during the curing or crushing process. A portion of this ground material was used to determine the MC of the size-reduced powders using the procedure described in Section 5.3. Three ~5 g sub-samples from each size-reduced monolith were analyzed for MC and averaged to determine the final MC percent. For 17-EMF-TB25.1-5, the MC was determined to be 27.49% ± 0.05% and for 17-EMF-TB26.2-5 the average MC was determined to be 23.62% ± 0.08%. These values are similar to those determined for the radiological monoliths from TB27 and TB28, respectively, as reported in Section 5.3. Size-reduced material was stored in a sealed container in the anoxic chamber until needed.

9.1.1.2 ⁹⁹Tc Sorption Phase Using non-⁹⁹Tc-Spiked Cementitious Material

Separate Ca(OH)₂-saturated solutions pre-equilibrated with either 0.425 – 2 mm size-reduced TB25.1-5 or TB26.2-5 monolith material were used for all ⁹⁹Tc sorption and desorption experiments. The pre-equilibration step was used to prevent large changes in pH and aqueous chemistry composition during the sorption phase in hopes of minimizing other processes, such as ⁹⁹Tc precipitation, that could affect the desorption behavior and change the pH of the Ca(OH)₂-saturated solution (Almond et al. 2012; Kaplan 2010). The Ca(OH)₂-saturated solution simulates young/moderately aged cement pore solution and was prepared by adding approximately 20 g of reagent grade Ca(OH)₂(s) to 2 L of DIW that had been purged with N₂ (98%) and H₂ (2%) gases. After stirring for at least 2 days, the Ca(OH)₂-saturated solution was filtered using a 0.45 μm filter into a separate container and transferred into the anoxic chamber. To the

filtered Ca(OH)₂-saturated solution, 0.425 – 2 mm size-reduced monolith material from TB25.1-5 or TB26.2-5 was added at a 1 g/40 mL ratio inside the anoxic chamber. Over the course of at least 9 days, the solid material was allowed to react in solution, shaken periodically to promote mixing. After 9 days of reaction, the pH and E_h of the solution were measured. If the E_h was below ~ -400 mV (SHE corrected), the target E_h value for reducing conditions based on previous tests (Saslow et al. 2017; Um et al. 2016), no more reaction time was required; however, if above ~ -400 mV, the reaction was allowed to continue. Ultimately, the target E_h (-400 mV SHE corrected) was not achieved, even after equilibrating under anoxic conditions for a total of 19 days, and is likely a result of the waste form chemistry. The Cast Stone (TB25.1) equilibrated Ca(OH)₂-saturated solution achieved an E_h value of -94 mV (SHE) and the HL (TB26.2) equilibrated Ca(OH)₂-saturated solution had an E_h value of -192 mV (SHE) (Table 9.1). After 14 days of equilibrating, ~ 0.5 L of equilibrated Ca(OH)₂-saturated solution was transferred to a separate container for each monolith material and spiked with ~ 0.5 mL of 1 ppm ⁹⁹Tc using NH₄TcO₄ stock solution to achieve a final concentration of ~ 1 ppb ⁹⁹Tc.

All ⁹⁹Tc sorption batch experiments were performed inside the anoxic chamber. Sorption tests were performed at two solution:solid ratios: 10 mL/g and 25 mL/g. For samples with a desired solution:solid ratio of 10, about 21 mL of the ⁹⁹Tc (1.0 ppb)-spiked Ca(OH)₂ solution was added to a 50 mL centrifuge tube containing ~ 3 g of the matching 0.425 – 2 mm size-reduced monolith powder. For samples with a desired solution:solid ratio of 25, about 18 – 19 mL of the ⁹⁹Tc (1.0 ppb)-spiked Ca(OH)₂ solution was added to a 50 mL centrifuge tube containing ~ 1 g of the matching 0.425 – 2 mm size-reduced monolith powder. In total, twelve 50 mL centrifuge tubes were prepared for each monolith (24 total) for the sorption phase testing that is followed by the desorption phase, which requires triplicate samples for two different reaction times (30 and 44 days). Triplicate control samples, containing 21 mL of the ⁹⁹Tc (1.0 ppb)-spiked Ca(OH)₂ solution in 50 mL centrifuge tubes without solids, were also prepared for each monolith (TB25.1-5 and TB26.2-5). The total sorption reaction time was 30 days, which was previously determined to be enough time for ⁹⁹Tc in this size fraction to reach steady state (Um et al. 2016). Over the course of the sorption phase, the centrifuge tubes were shaken within the anoxic chamber by hand for ~ 15 seconds once a day between days 0 and 7 and twice a week between days 7 and 29.

After reacting for 30 days, a ~ 15 mL aliquot of supernatant was filtered using a 0.45 μ m syringe filter. A 2 mL subsample of filtered supernatant was then transferred to a 20 mL plastic vial and spiked with 0.02 mL of ultrapure nitric acid before it was submitted for ⁹⁹Tc analysis by ICP-MS. These acidified samples were stored in the refrigerator (outside the chamber) until ICP-MS analysis. Inside the anoxic chamber, a second filtered aliquot was used to measure the E_h and pH. The measured E_h values, using a Hanna E_h probe, were SHE corrected by adding $+208$ mV to the recorded value. The remainder of the filtered subsample was archived inside the anoxic chamber.

The ⁹⁹Tc sorption coefficient, K_d , was calculated according to Equation (9.1),

$$K_d = \frac{(C_i - C_t)V}{C_t m_{solid}} \quad (9.1)$$

where C_i is the initial aqueous total ⁹⁹Tc concentration (μ g/mL) in the supernatant determined from the control samples, C_t is the final aqueous equilibrated ⁹⁹Tc concentration (μ g/mL), V is the solution volume in the final equilibrated suspension (mL), and m_{solid} is the dry solid mass of the sample (g). The dry solid mass was corrected by the determined MC for this size fraction (Section 9.1.1.1).

9.1.1.3 Desorption ⁹⁹Tc K_d Measurements using ⁹⁹Tc-Sorbed Cementitious Material

The same crushed monolith material used to measure sorption K_d values was used for ⁹⁹Tc desorption tests. Two different desorption reaction times (30 and 44 days) were used under oxidizing conditions in

air; tubes were on the bench top and no longer in the anoxic chamber. An equilibrated $\text{Ca}(\text{OH})_2$ -saturated solution was prepared according to the procedure described in Section 9.1.1.2, but under oxidizing conditions (outside the anoxic chamber) in air with a target E_h value greater than +250 mV (SHE corrected). After removing as much solution as possible from the centrifuge tubes used for the 30-day ^{99}Tc sorption phase of testing, the weight of the wet slurry remaining in each 50 mL centrifuge tube was recorded before the ^{99}Tc desorption process was started. Desorption testing was started by adding about 18 to 21 mL of the respective equilibrated $\text{Ca}(\text{OH})_2$ -saturated solution (prepared under oxidizing conditions) into the centrifuge tube containing the ^{99}Tc -laden crushed monolith material. The total solution volume depended on the solution:solid ratio as described in Section 9.1.1.2. The desorption vials were also shaken by hand for ~15 seconds daily for the first week, after which they were shaken one to two times per week. In addition, once a week the samples were sparged with air for 1 hour and then weighed. Mass lost due to evaporation or entrainment in escaping air bubbles during the air sparging was replenished with fresh equilibrated $\text{Ca}(\text{OH})_2$ -saturated solution to maintain a constant sample weight for a constant solution:solid ratio. Two desorption reaction times (30 and 44 days) were tested, with triplicate samples prepared for each reaction time. After the target desorption reaction period was reached, the desorption tubes were centrifuged and the supernatant was removed from each tube using a pipette and then filtered using a 0.45 μm syringe filter. A 2 mL filtered subsample was spiked with 0.02 mL of ultrapure nitric acid and stored in a refrigerator before ^{99}Tc concentration analysis by ICP-MS. The remaining filtered aliquot was divided between two separate containers: one for pH and E_h analysis and one as an archive. For E_h analysis, a YSI E_h probe was used, requiring +211 mV be added to the recorded E_h value for SHE correction, according to the YSI probe manual.

The desorption ^{99}Tc K_d was calculated using Equation (9.2),

$$K_d = \frac{C_s}{C_t} = \frac{\left(\frac{m_r}{V} - C_t\right)V}{m_{\text{solid}}C_t} \quad (9.2)$$

where C_s is the final ^{99}Tc concentration ($\mu\text{g/g}$) on the solid after the desorption test. C_s is determined by taking the difference between the initially sorbed ^{99}Tc mass on the solids after the sorption phase of the test and the final ^{99}Tc mass in the desorption solution at steady state. C_t is the final aqueous ^{99}Tc concentration for the desorption test ($\mu\text{g/mL}$), and m_r is the remaining ^{99}Tc mass (μg) in the sorption tube before starting the desorption experiment. m_r was calculated by multiplying the desorption aqueous total ^{99}Tc concentration by the remaining solution (mL) in the sorption phase, based on the weight of slurry before starting desorption, and subtracting this value from the total ^{99}Tc mass on the solid at the start of the desorption experiment. To determine the total ^{99}Tc mass on the solid at the start of the desorption experiment, the average total ^{99}Tc concentration determined from the sorption control samples was multiplied by the starting sorption supernatant volume, and any ^{99}Tc mass removed through supernatant removal at the start of the desorption tests was subtracted. Finally, V is the total solution volume in the final equilibrated desorption suspension (including the residual volume of sorption liquid plus the ~21 mL of fresh desorption solution added) (mL) and m_{solid} is the dry solid mass (g) of the crushed cementitious material. We assume no cementitious mass is lost during all the tube manipulations (centrifuging, and removing supernatant solutions for filtering).

9.2 Results and Discussion

9.2.1 ^{99}Tc Sorption on Non- ^{99}Tc -Spiked Monolith Crushed Material

All ^{99}Tc sorption tests were conducted inside an anoxic chamber to maintain reducing conditions. The pH and E_h values of the initial ^{99}Tc (1.0 ppb)-spiked $\text{Ca}(\text{OH})_2$ solution equilibrated with size-reduced Cast Stone (TB25.1-5) monolith material were determined to be 12.36 and -94 mV (SHE corrected),

respectively. For the initial ^{99}Tc (1.0 ppb)-spiked $\text{Ca}(\text{OH})_2$ solution equilibrated with size reduced HL (TB26.2-5) monolith material, the measured pH and E_h values were 12.27 and -192 mV (SHE corrected), respectively. The approximate 100 mV difference between the Cast Stone equilibrated solution and the HL equilibrated solution is likely a result of the reducing capacity provided by the BFS, which has a greater impact in the HL formulation where the BFS content (72%) is almost double the BFS content (47%) in the Cast Stone recipe.

At the end of the sorption test, pH and E_h measurements were collected for each supernatant and the E_h measurements were SHE corrected by adding +208 mV to the measured value. These pH and SHE-corrected E_h values are tabulated in Table 9.1. For all Cast Stone (TB25.1-5) based samples containing crushed monolith, the measured pH values for supernatants were between 11.90 and 12.60 and E_h (SHE corrected) values fell in the range of 50 to 90 mV. Control samples, with no solid powders added, were similar, with pH ~12.10 and E_h values between 56 and 63 mV. When compared to the initial conditions recorded for the Cast Stone (TB25.1-5) equilibrated ^{99}Tc (1.0 ppb)-spiked $\text{Ca}(\text{OH})_2$ solution, these values indicate that significant chemical changes occurred during sorption testing, affecting the reducing conditions of the system. Evidence for chemical changes in the sorption experiments using HL (TB26.2-5) material can also be gathered from the final pH and E_h values measured. For all HL (TB26.2-5) based samples containing crushed monolith, the measured pH values for supernatants were between 12.30 and 12.70 and E_h (SHE corrected) values fell in the range of -51 to 26 mV. Control samples, with no solid powders added, were similar, with pH ~12.30 and E_h values between 1 and 14 mV. Based on these changes and published Pourbaix diagrams for ^{99}Tc speciation under these pH and E_h conditions (Darab and Smith 1996), ^{99}Tc likely persisted in these systems as oxidized Tc(VII) in the form of pertechnetate (TcO_4^-) rather than reduced Tc(IV) species.

Table 9.1. pH and E_h Results from ^{99}Tc Sorption and Desorption Tests^(a)

^{99}Tc Sorption Tests			^{99}Tc Desorption Tests		
Sample ID	pH	E_h , SHE (mV)	Sample ID	pH	E_h , SHE (mV)
Cast Stone (TB25.1)					
TB25.1 ^{99}Tc (1.0 ppb)-spiked $\text{Ca}(\text{OH})_2$	12.36	-94	TB25.1 $\text{Ca}(\text{OH})_2$ solution, no ^{99}Tc	12.25	175.3
KS-TB25.1-S1-D30-SS10	12.50	56	KD-TB25.1-S1-D30-SS10	12.00	177.3
KS-TB25.1-S2-D30-SS10	12.60	60	KD-TB25.1-S2-D30-SS10	12.10	174.1
KS-TB25.1-S3-D30-SS10	12.60	57	KD-TB25.1-S3-D30-SS10	12.10	174.9
KS-TB25.1-S1-D30-SS25	12.20	61	KD-TB25.1-S1-D30-SS25	11.50	217.0
KS-TB25.1-S2-D30-SS25	12.20	73	KD-TB25.1-S2-D30-SS25	11.50	211.9
KS-TB25.1-S3-D30-SS25	12.00	66	KD-TB25.1-S3-D30-SS25	11.40	207.9
KS-TB25.1-S1-D44-SS10	12.00	56	KD-TB25.1-S1-D44-SS10	12.00	168.7
KS-TB25.1-S2-D44-SS10	12.00	51	KD-TB25.1-S2-D44-SS10	12.00	160.2
KS-TB25.1-S3-D44-SS10	12.00	50	KD-TB25.1-S3-D44-SS10	12.10	158.6
KS-TB25.1-S1-D44-SS25	11.90	51	KD-TB25.1-S1-D44-SS25	11.50	188.8
KS-TB25.1-S2-D44-SS25	11.90	90	KD-TB25.1-S2-D44-SS25	11.30	200.4
KS-TB25.1-S3-D44-SS25	12.00	70	KD-TB25.1-S3-D44-SS25	11.20	205.0
KS-TB25.1-C1	12.10	63			
KS-TB25.1-C2	12.10	58			
KS-TB25.1-C3	12.20	56			
HL (TB26.2)					
TB26.2 ^{99}Tc (1.0 ppb)-spiked $\text{Ca}(\text{OH})_2$	12.27	-192	TB26.2 $\text{Ca}(\text{OH})_2$ solution, no ^{99}Tc	12.28	166.8
KS-TB26.2-S1-D30-SS10	12.30	7	KD-TB26.2-S1-D30-SS10	12.40	151.3
KS-TB26.2-S2-D30-SS10	12.50	1	KD-TB26.2-S2-D30-SS10	12.40	138.3

⁹⁹ Tc Sorption Tests			⁹⁹ Tc Desorption Tests		
Sample ID	pH	E_h , SHE (mV)	Sample ID	pH	E_h , SHE (mV)
KS-TB26.2-S3-D30-SS10	12.40	0	KD-TB26.2-S3-D30-SS10	12.50	139.6
KS-TB26.2-S1-D30-SS25	12.30	5	KD-TB26.2-S1-D30-SS25	12.00	176.7
KS-TB26.2-S2-D30-SS25	12.30	-2	KD-TB26.2-S2-D30-SS25	12.10	173.4
KS-TB26.2-S3-D30-SS25	12.70	26	KD-TB26.2-S3-D30-SS25	12.20	172.1
KS-TB26.2-S1-D44-SS10	12.60	-5	KD-TB26.2-S1-D44-SS10	12.40	152.7
KS-TB26.2-S2-D44-SS10	12.60	-14	KD-TB26.2-S2-D44-SS10	12.30	153.7
KS-TB26.2-S3-D44-SS10	12.60	-20	KD-TB26.2-S3-D44-SS10	12.40	155.4
KS-TB26.2-S1-D44-SS25	12.50	-18	KD-TB26.2-S1-D44-SS25	12.10	191.4
KS-TB26.2-S2-D44-SS25	12.50	-16	KD-TB26.2-S2-D44-SS25	12.20	185.6
KS-TB26.2-S3-D44-SS25	12.50	-51	KD-TB26.2-S3-D44-SS25	12.20	181.5
KS-TB26.2-C1	12.30	14			
KS-TB26.2-C2	12.30	3			
KS-TB26.2-C3	12.30	1			

- a. Label format for ⁹⁹Tc sorption samples: KS-TB#-S# (for different samples)-D# (for different desorption reaction times) -SS# (for different solution:solid ratios). Label format for ⁹⁹Tc desorption test: KD--TB#-S# (for different samples) -D# (for different desorption reaction times) -SS# (for different solution:solid ratios). "C" indicates the control sample for ⁹⁹Tc K_d sorption tests. Actual reaction times are 30 and 44 days; actual solution:solid ratios include 10 and 25 mL/g. NA = not applicable; no sorbing solids in control tubes.

The ⁹⁹Tc concentrations measured in the supernatant collected from sorption samples after 30 days of testing are presented in Figure 9.1. The initial concentration of ⁹⁹Tc present in the ⁹⁹Tc-spiked Ca(OH)₂ solution equilibrated with size-reduced monolith material from either 17-EMF-TB25.1-5 or 17-EMF-TB26.2-5 is 1.10 ppb and 1.06 ppb, respectively, for Cast Stone (TB25.1) and HL (TB26.2). However, when comparing the initial stock concentrations to the final ⁹⁹Tc concentration in each of the control samples (no solid added) for both the Cast Stone and HL systems, the measured ⁹⁹Tc concentration is ~40% below the initial stock concentration for all control samples. This drop in ⁹⁹Tc concentration combined with the increase in measured E_h values suggests that significant chemical processes occurred within the system. However, without solid material present in the control samples, the possibility of ⁹⁹Tc sorption to the solid material cannot explain this observation. Considering, however, that the only differences between the starting stock solutions and the control samples analyzed after 30 days is the containment containers and that the control samples were filtered using a 0.45 μm filter, this would suggest that some of the ⁹⁹Tc may adhere to the sample vials or persist as adsorbates on suspended colloids that are removed during the filtration process. Yet, the presence of black precipitates, indicative of TcO₂(s), was not observed during this testing and is not expected given the measured E_h conditions, which would suggest Tc is present as pertechnetate (TcO₄⁻).

The complexity of these systems is also apparent when comparing the measured ⁹⁹Tc concentrations in the sorption samples (solid included) to the stock and control samples, especially for TB25.1 sorption samples. For those samples using Cast Stone monolith material (TB25.1), the ⁹⁹Tc concentration in all but two samples is greater than the ⁹⁹Tc concentration measured in the control samples. This suggests that with the solid material present, ⁹⁹Tc is not sorbing to the solid material and partitions into solution where the effects observed in the control samples (adhesion to the sample vial or interactions with suspended colloids) is less pronounced if not non-existent. This would be expected for TcO₄⁻ where anion repulsion would prevent adsorption to negatively charged solid material under these pH and E_h conditions. For the HL/BFS/OPC monolith material (TB26.2), this trend was not observed and the ⁹⁹Tc concentration decreased in all sorption samples with solid present. Despite the increase in E_h conditions throughout the

30-day sorption period, the elevated BFS content in the HL-based material may provide localized reduction sites for Tc(VII) reduction to Tc(IV) and Tc(IV) adsorption to the solid material.

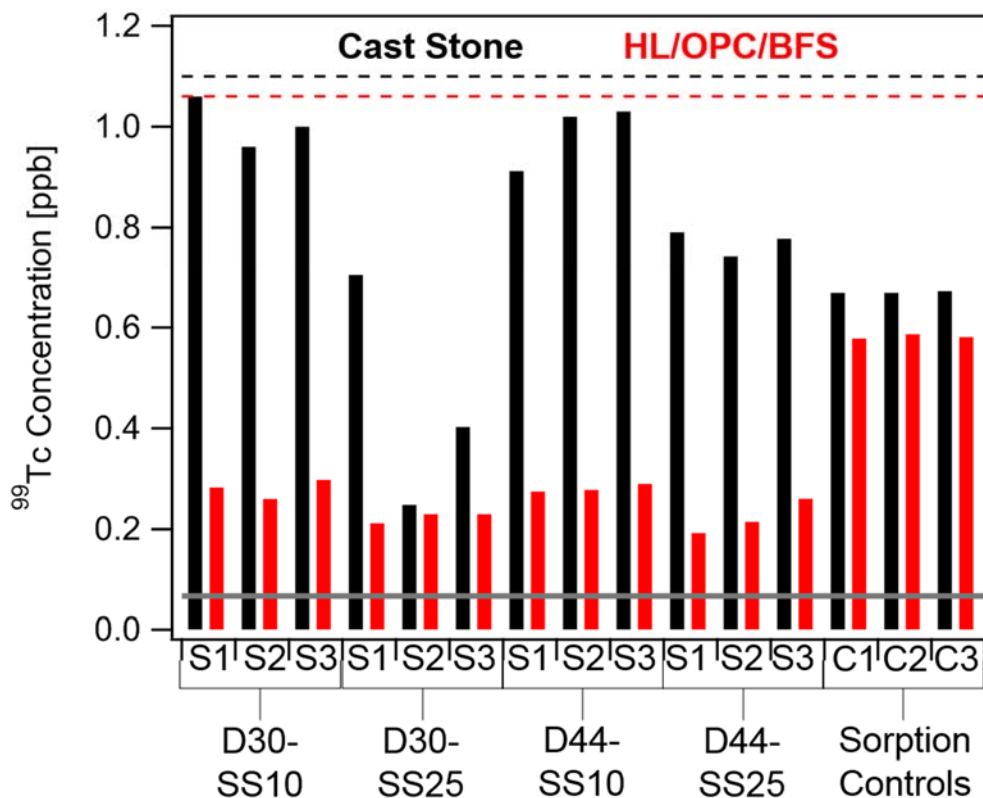


Figure 9.1. ^{99}Tc Concentrations in the Supernatants after 30-Day Sorption Testing for Cast Stone (TB25.1, black) and HL (TB26.2, red). The black and red dashed lines indicate the initial ^{99}Tc concentration [ppb] measured in the starting ^{99}Tc -spiked $\text{Ca}(\text{OH})_2$ solution equilibrated with size-reduced monolith material from either 17-EMF-TB25.1-5 (black) or 17-EMF-TB26.2-5 (red). The black and red bars indicate the measured ^{99}Tc concentration in the supernatant after the 30-day sorption period for all controls (C1-C3) and samples (S1-S3) reacted at a solution:solid ratio of 10 (SS10) or 25 (SS25) and with a target desorption time of 30 days (D30) or 44 days (D44). The grey line represents the EQL for ^{99}Tc analysis by ICP-MS, 0.066 $\mu\text{g}/\text{L}$.

The calculated ^{99}Tc sorption K_d values for individual samples are provided in Table 9.2. For each sample, the K_d value was calculated using the initial ^{99}Tc concentration measured in the stock solution and the average ^{99}Tc concentration determined from the three replicate control samples. In this way, the actual K_d values can be better constrained, despite the chemical processes that have occurred in each of these systems. However, further investigation into the cause for observations in the control samples is necessary to better understand trends in sorption K_d values. For Cast Stone (TB25.1) sorption samples, the average ^{99}Tc sorption K_d value is greater (but not within error) for both calculations for samples with a solution:solid ratio of 25 mL/g ($K_d \approx 27 \pm 29$ mL/g (stock), 7 ± 18 mL/g (control average)) compared to samples prepared at 10 mL/g ($K_d \approx 0.6 \pm 0.6$ mL/g (stock), -3.5 ± 0.3 mL/g (control average)). Here, 1σ standard deviation of the average is reported. For HL (TB26.2) sorption samples, the sorption K_d values are greater and less variable relative to Cast Stone (TB25.1) samples. However, the increase in K_d values with increasing solution:solid ratio is also observed, where samples with a solution:solid ratio of 25 mL/g

have K_d values equal to 92 ± 12 mL/g (stock)/ 39 ± 6 mL/g (control average) and at 10 mL/g the K_d values decrease to 25 ± 2 mL/g (stock)/ 9.6 ± 0.9 mL/g (control average).

Table 9.2. K_d Results from ^{99}Tc Sorption and Desorption Tests

^{99}Tc Sorption Tests			^{99}Tc Desorption Tests				
Sample ID	K_d , Stock ^(a) (mL/g)	K_d , Control ^(b) (mL/g)	Sample ID	K_d , Stock ^(a) (mL/g)	Average K_d , Stock ^(a) (mL/g)	K_d , Control ^(b) (mL/g)	Average K_d , Control ^(b) (mL/g)
Cast Stone (TB25.1)							
KS-TB25.1-S1-D30-SS10	-0.02	-3.85	KD-TB25.1-S1-D30-SS10	5.86		-27.16	
KS-TB25.1-S2-D30-SS10	1.02	-3.28	KD-TB25.1-S2-D30-SS10	15.34	12 ± 5	-25.60	-29 ± 4
KS-TB25.1-S3-D30-SS10	0.59	-3.59	KD-TB25.1-S3-D30-SS10	15.06		-33.81	
KS-TB25.1-S1-D30-SS25	13.17	-1.54	KD-TB25.1-S1-D30-SS25	77.48		-20.26	
KS-TB25.1-S2-D30-SS25	81.68	40.26	KD-TB25.1-S2-D30-SS25	75.33	77 ± 2	25.23	8 ± 24
KS-TB25.1-S3-D30-SS25	39.28	14.81	KD-TB25.1-S3-D30-SS25	78.28		17.80	
KS-TB25.1-S1-D44-SS10	1.62	-2.95	KD-TB25.1-S1-D44-SS10	10.80		-19.42	
KS-TB25.1-S2-D44-SS10	0.38	-3.69	KD-TB25.1-S2-D44-SS10	4.59	8 ± 3	-26.84	-24 ± 4
KS-TB25.1-S3-D44-SS10	0.27	-3.73	KD-TB25.1-S3-D44-SS10	7.91		-25.61	
KS-TB25.1-S1-D44-SS25	9.38	-4.20	KD-TB25.1-S1-D44-SS25	69.44		-48.78	
KS-TB25.1-S2-D44-SS25	11.15	-2.74	KD-TB25.1-S2-D44-SS25	23.99	45 ± 23	-24.69	-37 ± 12
KS-TB25.1-S3-D44-SS25	9.73	-3.77	KD-TB25.1-S3-D44-SS25	41.35		-36.42	
KS-TB25.1-SS10 Average	0.6 ± 0.6	-3.5 ± 0.3					
KS-TB25.1-SS25 Average	27 ± 29	7 ± 18					
HL (TB26.2)							
KS-TB26.2-S1-D30-SS10	24.69	9.31	KD-TB26.2-S1-D30-SS10	101.73 ^(c)		35.79	
KS-TB26.2-S2-D30-SS10	27.95	11.06	KD-TB26.2-S2-D30-SS10	105.57 ^(c)	103 ± 2	39.06	37 ± 2
KS-TB26.2-S3-D30-SS10	23.11	8.42	KD-TB26.2-S3-D30-SS10	101.25 ^(c)		34.90	
KS-TB26.2-S1-D30-SS25	95.67	41.57	KD-TB26.2-S1-D30-SS25	287.10 ^(c)		113.32	
KS-TB26.2-S2-D30-SS25	87.95	37.12	KD-TB26.2-S2-D30-SS25	286.77 ^(c)	285 ± 2	109.65	111 ± 2
KS-TB26.2-S3-D30-SS25	86.97	36.71	KD-TB26.2-S3-D30-SS25	284.11 ^(c)		108.95	
KS-TB26.2-S1-D44-SS10	25.84	9.92	KD-TB26.2-S1-D44-SS10	97.67		34.76	
KS-TB26.2-S2-D44-SS10	25.44	9.70	KD-TB26.2-S2-D44-SS10	97.82	99 ± 2	35.05	34.9 ± 0.2
KS-TB26.2-S3-D44-SS10	23.92	8.88	KD-TB26.2-S3-D44-SS10	100.90 ^(c)		34.82	
KS-TB26.2-S1-D44-SS25	109.68	49.04	KD-TB26.2-S1-D44-SS25	300.36 ^(c)		123.03	
KS-TB26.2-S2-D44-SS25	95.86	41.46	KD-TB26.2-S2-D44-SS25	292.51 ^(c)	289 ± 13	115.29	112 ± 12

⁹⁹ Tc Sorption Tests			⁹⁹ Tc Desorption Tests				
Sample ID	K_d , Stock ^(a) (mL/g)	K_d , Control ^(b) (mL/g)	Sample ID	K_d , Stock ^(a) (mL/g)	Average K_d , Stock ^(a) (mL/g)	K_d , Control ^(b) (mL/g)	Average K_d , Control ^(b) (mL/g)
KS-TB26.2-S3-D44-SS25	74.45	29.73	KD-TB26.2-S3-D44-SS25	275.53 ^(c)		98.66	
KS-TB26.2-SS10 Average	25 ± 2	9.6 ± 0.9					
KS-TB26.2-SS25 Average	92 ± 12	39 ± 6					

(a) The ⁹⁹Tc concentration in the initial stock solution was used to calculate the K_d value.

(b) The average ⁹⁹Tc concentration calculated from the three control samples was used to calculate the K_d value.

(c) ⁹⁹Tc K_d value calculated using EQL value of 0.066 µg/L.

9.2.2 ⁹⁹Tc Desorption K_d s using ⁹⁹Tc Sorbed Monolith Powders

The wet slurry remaining from the ⁹⁹Tc sorption phase of testing was used for ⁹⁹Tc desorption testing by refilling the sorption sample vials with 18 to 21 mL (depending on the desired solution:solid ratio) of Cast Stone (TB25.1) or HL (TB26.2) equilibrated, saturated Ca(OH)₂ solution under oxidizing conditions for two reaction times (30 and 44 days). Before starting the desorption phase of testing, the pH and E_h of the oxidized and equilibrated, saturated Ca(OH)₂ solution were measured and determined to be 12.25 and +175.3 mV (SHE corrected), respectively, for Cast Stone (TB25.1) samples and 12.28 and +166.8 mV, respectively, for HL (TB26.2) samples. At the end of each desorption reaction period, the pH and SHE-corrected E_h of each respective filtered supernatant solution were determined (Table 9.1). The final pH values measured following desorption testing for Cast Stone (TB25.1) monolith material ranged from 11.20 to 12.10 and SHE-corrected E_h values ranged from 158.6 to 217.0 mV. For HL (TB26.2) desorption samples, the final pH values ranged from 12.00 to 12.50 and the SHE-corrected E_h values ranged from 138.3 to 191.4 mV. Based on these E_h results, it is evident that oxidizing conditions ($E_h > 100$ mV, SHE corrected) and consistent pH conditions were maintained in all samples throughout desorption testing.

For all Cast Stone (TB25.1) desorption samples and two HL desorption (TB26.2) samples, ⁹⁹Tc concentrations were measured above the EQL level for ⁹⁹Tc and are shown in Figure 9.2. These values were used to calculate individual sample ⁹⁹Tc desorption K_d values and average K_d values for each desorption testing period, which are reported in Table 9.2 for two scenarios: (1) using the starting ⁹⁹Tc concentration based on the measured ⁹⁹Tc concentration in the stock solution used in the sorption experiments, or (2) the average ⁹⁹Tc concentration determined from the control sorption experiments. For those samples with ⁹⁹Tc concentrations at or below the EQL concentration for ⁹⁹Tc (0.066 µg/L), the EQL value was used to calculate desorption K_d values.

Overall, the average ⁹⁹Tc desorption K_d value does not change (within error) for samples with the same composition but different solution:solid ratios from 30 to 44 days of desorption, with the exception of Cast Stone (TB25.1) with a solution:solid ratio of 25 mL/g where the average K_d decreased from 30 to 44 days. These results imply that for most conditions tested, the samples reached equilibrium within the 30-day testing period. However, there was a significant increase in K_d values across both formulations when increasing the solution:solid ratio from 10 to 25 mL/g. To summarize, the average K_d values for Cast Stone (TB25.1) samples after 30 days and with a solution:solid ratio of 10 mL/g were 12 ± 5 mL/g (stock) / -29 ± 4 mL/g (control average) and did not change within experimental error after 44 days where K_d values were 8 ± 3 mL/g (stock) / -24 ± 4 mL/g (control average). But when the solution:solid ratio was increased to 25 mL/g, the K_d values increased for Cast Stone samples to 77 ± 2 mL/g (stock) / 8 ± 24 mL/g (control average) at 30 days desorption and 45 ± 23 mL/g (stock) / -37 ± 12 mL/g (control average) after 44 days desorption. Here the control average K_d value at 44 days and a solution:solid ratio of 25 mL/g is an outlier to this trend. In the HL (TB26.2) samples, the difference between solution:solid ratios is less pronounced, but the K_d values are greater in magnitude. After 30 days, average K_d values for HL desorption samples with a solution:solid ratio of 10 mL/g were 103 ± 2 mL/g (stock) / 37 ± 2 mL/g (control average) and did not change within experimental error after 44 days where K_d values were 99 ± 2 mL/g (stock) / 111 ± 2 mL/g (control average). But when the solution:solid ratio was increased to 25 mL/g, the K_d values increased to 285 ± 2 mL/g (stock) / 111 ± 2 mL/g (control average) at 30 days desorption and 289 ± 13 mL/g (stock) / 112 ± 12 mL/g (control average) after 44 days desorption. Based on these ⁹⁹Tc desorption K_d values and trends, the HL-based material outperforms the Cast Stone material and is best when present at solution:solid ratios of 25 mL/g.

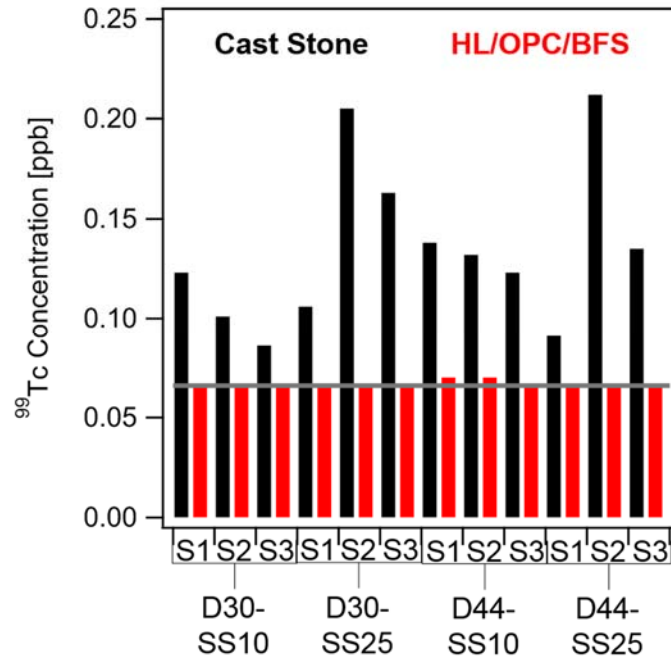


Figure 9.2. ⁹⁹Tc Concentrations (μg/L) Measured in the Filtered Supernatants Collected after Desorption Testing Periods for Cast Stone (TB25.1, black) and HL (TB26.2, red) Samples. Sample names containing D30 and D44 correspond with desorption testing periods of 30 and 44 days, respectively. SS10 and SS25 correspond with solution:solid ratios of 10 mL/g and 25 mL/g, respectively. Triplicate samples are labelled S1, S2, or S3. The grey line indicates the EQL concentration for ⁹⁹Tc (0.066 μg/L). For those samples with ⁹⁹Tc concentrations below the EQL, the EQL value was used to calculate ⁹⁹Tc desorption K_d values in Table 9.2.

10.0 Summary and Recommendations

This section summarizes the key conclusions from each activity performed during FY 2017 and FY 2018 for EMF evaporator bottoms screening tests (ECS) and qualification testing (EQT) of formulated cementitious waste forms. The results obtained help fill existing data gaps, support final selection of a potential cementitious waste form for the future EMF evaporator bottoms waste stream, and improve the technical defensibility of long-term waste form performance estimates. Recommendations for further testing needed, to provide additional information for waste form development and to support future IDF PA maintenance, are also addressed.

Specific formulation and waste form qualification testing efforts described in this report include

1. production of eight EMF evaporator bottoms waste simulant solutions containing a range of major salt species (boron, chloride, nitrite, and sulfate) and one average EMF evaporator bottoms-waste simulant,
2. formulation and characterization of cementitious waste forms for treatment of the eight ECS and/or average EQT simulants using five final dry ingredient recipes: the original Cast Stone recipe (8% OPC, 45% FA, and 47% BFS); 20% Aquaset II-GH®/80% BFS; 20% OPC/80% BFS; and 10% HL/18% OPC/72% BFS.
3. observations of residual free liquid from ECS and EQT cementitious waste forms over the 28-day cure period to assess the storage time necessary before disposal according to Hanford Site solid waste acceptance criteria (Ramirez 2008),
4. physical properties measurements for EQT non-radiological formulations that can be used to infer the properties of ⁹⁹Tc-laden cementitious waste forms generated with the same dry ingredient formulation,
5. detailed solid characterization of EQT monoliths, both radiologic and non-radiologic specimens,
6. TCLP testing to demonstrate that waste form(s) will meet RCRA LDRs for hazardous wastes when compared to the UTS in 40 CFR 268 (2015),
7. determination of effective diffusivity (D_{eff}) values for ⁹⁹Tc, ¹²⁷I, and Na⁺ in DIW using EPA Method 1315 to assess the long-term immobilization potential of Cast Stone and HL formulation cementitious waste forms, and
8. quantification of ⁹⁹Tc desorption K_d (distribution coefficient) values from the Cast Stone and HL cementitious material with the average simulant under oxidizing conditions to support maintenance of the Hanford IDF PA predictions for ⁹⁹Tc transport.

10.1 Conclusions

The eight ECS simulants used in this report were developed according to a test matrix to allow a small set of simulants to be prepared with varying boron, chloride, nitrite, and sulfate concentrations. All ECS simulants were spiked with Zn (~700 ppm) and RCRA metals, As (~180 ppm), Se (~180 ppm), Cr (~300 ppm), and Hg (>30 ppm). All ECS simulants contained precipitates, of varying amounts, that could not be completely re-dissolved with heat and vigorous mixing. This suggests that the composition matrix of the ECS simulants exceeded the Zn solubility limit, causing Zn to precipitate at room temperature over time. Zn precipitation was most evident in simulants with low boron levels, with analytical values significantly lower than the concentration expected by mass-balance calculations. Furthermore, maintaining the target

Hg concentrations proved especially difficult, with none of the simulants meeting the target concentration (30 ppm) within $\pm 10\%$. The exact cause for the Hg variation remains unclear, but it could be attributed to Hg adhesion to reaction, containment, and analysis vessels, or sampling errors due to the low Hg concentration relative to other constituents and/or immediate precipitation of some insoluble Hg compound. Consequently, 40 ppm Hg was added to each simulant aliquot, as $\text{Hg}(\text{NO}_3)_2 \cdot x\text{H}_2\text{O}$ in 2% HNO_3 , in addition to the Hg already present in order to increase the total Hg concentration and make sure the correct level of Hg was present during waste form preparation. Analytical results from an aliquot of the final Hg-spiked simulant showed that for each simulant aliquot, the target concentration (30 ppm) was met and often exceeded. For the Avg simulant used in the EQT formulations, which had a target concentration equal to the average of the eight ECS simulants, precipitation was not observed. The Avg simulant was spiked with Zn (~700 ppm), Cr (~300 ppm), ^{127}I (~25 ppm, surrogate for ^{129}I), and ^{99}Tc (~25 ppm). The actual concentration of the Avg simulant was within 9% of the target values for all constituents except, ^{99}Tc and ^{127}I , which were ~ 27% and 20% their batched values, respectively. Despite these lower than expected concentrations for ^{99}Tc and ^{127}I , detection limit issues when performing contaminant leach testing was not a problem and the concentrations remain above those concentrations expected for the EMF evaporator bottoms waste stream.

Grout formulation for immobilization of each of the eight ECS simulants was tested with three dry ingredient recipes: the original Cast Stone recipe (8% OPC, 45% FA, and 47% BFS), 20% Aquaset II-GH®/80% BFS, and 20% OPC/80% BFS. A total of 24 ECS test batches were produced and used to make eight monolith specimens from each simulant-dry blend formulation. The Avg simulant used for EQT tests was immobilized using two grout formulations: the original Cast Stone recipe and a 10% HL/18% OPC/72% BFS recipe. This HL recipe was down-selected from three HL recipes containing 10%, 30%, or 50% HL and a 4:1 ratio of BFS:OPC for the remaining dry ingredient mass. For the HL contents greater than 10%, the flowability of the grout was significantly reduced; and at 50% HL, only a fraction of the dry ingredients required could be mixed into the aliquot of the Avg simulant. For EQT formulations, non-radiological and ^{99}Tc -containing test batches were produced. For all formulations, a w/dm ratio of 0.5 was used and a WRA (MasterGlenium 3030 from BASF Corp.) was added when necessary to reduce viscosity and improve flowability of the mix. Monolith specimens from ECS and non-radiological specimens from EQT intended for TCLP analysis were cured for 7 days before being packaged at >80% relative humidity for transport to SwRI for analysis. The remaining cementitious waste forms were cured for at least 28 days before they were opened and archived for use in additional tests in the last quarter of FY 2017 or in FY 2018.

Residual free liquids were monitored for one monolith specimen from each grout test batch for at least 28 days or until no free liquids (<1% of the total waste volume) were observed. ECS test batches using the original Cast Stone formulation recipe re-absorbed residual free liquids to below 1 vol% within 3 to 5 days for all simulants except Simulant 7 (low Cl and B, high NO_2 and SO_4). Only the Aquaset/BFS formulation re-absorbed residual free liquids from all eight treated ECS simulants, but required up to 18 days to achieve <1 vol% residual free liquid. Simulant immobilization by the OPC/BFS formulation reabsorbed liquids within a broad range of 3 to 30 days. For EQT treatment of the Avg simulant, Cast Stone and HL formulations performed equally when reabsorbing free liquids. Residual free liquid observations are based on observations collected for one specimen from each test batch and replicate sample observations in future tests are recommended to confirm these assessments. Once confirmed, these results should be considered when selecting formulations for scale-up tests and to provide baseline guidance for the time required before waste forms may be transported to and disposed of in the IDF.

Physical properties measured for the Cast Stone and HL-based formulations used to immobilize the Avg EQT simulant included set time, moisture content, density, compressive strength, and saturated hydraulic conductivity. Both the Cast Stone and HL formulations performed similarly across most tests, with the exception of compressive strength (Table 10.1). When evaluating compressive strength, the HL monoliths

outperformed the Cast Stone monoliths by over double, with an average compressive strength of 3693 ± 785 psi compared to 1751 ± 66 psi, respectively.

Table 10.1. Summary of Physical Properties for EQT Formulations

Physical Property Test	Cast Stone	HL
Set Time	67.3 – 68.7 hours	66.7 – 71.4 hours
Residual Free Liquids	3 – 8 days	3 – 8 days
Moisture Content (MC)	27.32 %	24.24 %
Apparent Density	2.22 ± 0.03 Mg/m ³	2.46 ± 0.15 Mg/m ³
Volume of Permeable Pore Space	42.40 ± 0.03 %	43.95 ± 2.42 %
Compressive Strength	$1,751 \pm 66$ psi	$3,693 \pm 785$ psi
Saturated Hydraulic Conductivity (K_{sat})	1.3×10^{-10} cm/s	1.4×10^{-10} cm/s

Solid phase characterization of ECS and EQT specimens by XRD showed that the majority of the waste form is composed of an amorphous, likely CSH, phase (~71 – 85 wt %). The remaining material consisted of mineral phases including portlandite [$\text{Ca}(\text{OH})_2$], ettringite [$\text{Ca}_6\text{Al}_2(\text{SO}_4)_3(\text{OH})_{12} \cdot 26\text{H}_2\text{O}$], calcite [CaCO_3], larnite [Ca_2SiO_4], hydrocalumite [$\text{Ca}_4\text{Al}_2(\text{OH})_{12}(\text{OH})_2 \cdot 6\text{H}_2\text{O}$], and quartz [SiO_2]. In ECS monoliths made from high sulfate simulants, there was a noticeable increase in ettringite formation for Cast Stone and Aquaset/BFS formulations. For OPC/BFS specimens, ettringite formation stayed relatively constant. These mineralogical observations may have implications for long-term Tc immobilization, since ettringite is hypothesized to incorporate Tc into its mineral structure, which could increase Tc stability within the waste form. For the EQT monoliths, the small quantities of each crystalline mineral phase, most less than 5 wt%, did not indicate significant trends across formulations and spatial environments. However, there is an increase in ettringite present in the material collected from the outer wall of non-leached and post-leached specimens and is consistent with previous observations (Saslow et al. 2017). Furthermore, the presence of portlandite, only found in the HL-based specimens, suggests that there is an excess of calcium added relative to the amount of sulfate requiring sequestration via the formation of ettringite.

Further solid phase characterization of EQT specimens included SEM/EDS to assess particle morphology and digital autoradiography (iQID) to identify regions or hot spots of concentrated ⁹⁹Tc within radiological monoliths used in EPA Method 1315 leach testing. From SEM/EDS results, it is immediately apparent that the morphology of Cast Stone-based monoliths used to treat the Avg simulant is very different from the HL monoliths imaged. In the Cast Stone samples, spherical particles are present throughout these samples that are often porous and sometimes coated in a poorly crystalline Fe phase. These particles are high in Al, Ca, Mg, and Si. Also present are platy particles that are enriched in Ba and S and contain Cr or Zr. In contrast, the HL-based specimens, fewer spherical particles are present and instead small particles with either platy or rod-like morphology have formed. Furthermore, some of the large particles imaged in these HL-based samples appeared unreacted during leaching. Overall, ⁹⁹Tc was not detected in concentrated areas for most analyzed samples, except for one particle in the exterior material collected from TB28 (HL/OPC/BS) after 63 days of leaching. In this particle, the ⁹⁹Tc was found to be concentrated in a particle with high Fe content. For digital autoradiography (iQID) measurements, both pre- and post-leached specimens were analyzed from rad EQT test batches (TB27 and TB28). In Cast Stone formulated monoliths, a strong Tc signal is observed throughout the unleached sample, whereas after the 63-day leach period an increased amount of ⁹⁹Tc was observed on the outer wall. However, in HL formulated monoliths, higher Tc was observed on the outer edge of both the unleached and leached samples. This trend may be due to increased ettringite formation in the HL formulations. With ettringite appearing in higher amounts near the outer surface, as supported by XRD analysis, Tc may

become trapped within the ettringite structure. A similar process is also postulated for the post-leached Cast Stone sample.

Monoliths were analyzed by TCLP 14 days after production to match the TCLP analysis timeline used by SRNL (Cozzi and McCabe 2016). The TCLP test results, when compared to the UTS limits used to meet LDRs (40 CFR 268, 2015) for hazardous wastes, show that all ECS and EQT test batches passed LDRs for As, Se, Cr, and Hg, thus qualifying the waste forms for off-site disposal and potentially on-site disposal at the IDF. A final observation worth noting is that all Hg levels were non-detectable in the leachate despite being present in the simulants used to make the cementitious waste forms at elevated concentrations (≥ 38 ppm in each).

EPA Method 1315 leach testing was performed on radioactive EQT monoliths from Cast Stone and HL test batches. All monoliths remained intact during the 63-day leach period, showing no signs of cracking. For ^{99}Tc , D_{eff} values for monoliths leached in DIW increased during early leach periods, up to 14 days, but gradually decreased through the cumulative 63-day leach period. ^{99}Tc D_{eff} values after 28-day leaching for Cast Stone monoliths are $\sim 5 \times 10^{-11}$ cm^2/s and $\sim 1 \times 10^{-11}$ for HL-based monoliths, indicating the HL-based formulation outperforms Cast Stone with regard to ^{99}Tc retention. For ^{127}I , the amount of iodine released remained below 20% of the initial ^{127}I mass and the calculated D_{eff} values show a greater improvement in ^{127}I diffusivity from HL-based specimens ($\sim 4 \times 10^{-11}$ to 5×10^{-11} cm^2/s) versus Cast Stone specimens ($\sim 5 \times 10^{-10}$ cm^2/s) relative to the reduction in ^{99}Tc diffusivity when comparing HL-based and Cast Stone formulations. It should be noted that throughout the 63-day leach period, some periods of ^{99}Tc and ^{127}I release did not follow a pure diffusion trend, suggesting additional chemical reactions may influence contaminant leaching from the waste form. This observation was especially prevalent in the HL formulated specimens. As such, the calculated and reported diffusivity values should be used with care since the EPA Method 1315 assumes diffusion-controlled contaminant release.

All ^{99}Tc sorption tests were conducted on EQT non-rad monoliths inside an anoxic chamber to attempt to maintain reducing conditions and used size-reduced (0.425 – 2 mm) Cast Stone and HL monolith material to initially sorb ~ 1.1 ppb of soluble ^{99}Tc for 30 days at solution solid ratios of 25 mL/g and 10 mL/g. At the end of the sorption period, Cast Stone formulated monoliths showed variable ^{99}Tc sorption values, with those samples prepared at 10 mL/g sorbing less than $\sim 10\%$ of ^{99}Tc from the 1.1 ppb initial stock solution. The 25 mL/g Cast Stone sorption samples sorbed more ^{99}Tc , but showed more variability across the samples. The HL-based samples successfully removed $\sim 80\%$ of ^{99}Tc in solution across all samples. It is critical to note that the sorption K_d values reported should be used with care due to the unexpected decrease in ^{99}Tc concentration measured in the control samples, where no solid was present, suggesting that additional chemical reactions (not facilitated by the solid phase) are occurring that influence the ^{99}Tc sorption. For the desorption tests, the ^{99}Tc -sorbed material was used to perform ^{99}Tc desorption testing under oxidizing conditions for two reaction times (30 and 44 days). Overall, the average ^{99}Tc desorption K_d value does not change (within error) for samples with the same composition but different solution:solid ratios from 30 to 44 days of desorption, with the exception of Cast Stone (TB25.1) with a solution:solid ratio of 25 mL/g. These results imply that for most conditions tested, the samples reached equilibrium within the 30-day testing period. However, there was a significant increase in K_d values across both formulations when increasing the solution:solid ratio from 10 to 25 mL/g. To summarize (using the ^{99}Tc concentration in the starting stock solution as reference), the average K_d values for Cast Stone (TB25.1) samples after 30 days and 44 days with a solution:solid ratio of 10 mL/g were 12 ± 5 mL/g and 8 ± 3 mL/g, respectively. At 25 mL/g, the Cast Stone-based K_d values increased to 77 ± 2 mL/g at 30 days desorption and 45 ± 23 mL/g after 44 days desorption. In the HL (TB26.2) samples, the difference between solution:solid ratios is less pronounced, although the K_d values are greater in magnitude. HL average K_d values with a solution:solid ratio of 10 mL/g were 103 ± 2 mL/g (30 days desorption) and 99 ± 2 mL/g (44 days desorption). At 25 mL/g, the K_d values increased to 285 ± 2 mL/g

at 30 days desorption and 289 ± 13 mL/g after 44 days desorption. Based on these ^{99}Tc desorption K_d values and trends, the HL-based material outperforms the Cast Stone material.

10.2 Recommendations

The results described herein help fill existing data gaps and should support final selection of a cementitious waste form for incorporating EMF evaporator bottoms waste streams. Recommendations for additional studies to provide more technical defensibility for long-term waste form performance are listed below:

1. Precipitate formation as a function of the variables tested in the test matrix provided by WRPS, both by computational modeling and by additional liquid- and solid-phase analytical methods, should be performed to better understand the chemical and physical properties of the EMF evaporator bottoms-waste stream and how these properties might influence waste form selection for immobilization.
2. The dry-blend formulation should be optimized to improve contaminant and radionuclide (^{99}Tc and ^{129}I) retention. Based on recent advancements controlling natural long-term mineral growth and using material additions (e.g., getters) that stabilize specific COCs within the waste form, effective diffusivity values as low as 10^{-15} cm²/s (reported for ^{99}Tc) are achievable by cementitious waste forms (Saslow et al. 2017; Um et al. 2016; Asmussen et al. 2016). This leaves room for at least three orders of magnitude improvement based on the D_{eff} values reported herein. Variables to consider include increasing the w/dm ratio, which will increase waste loading; alternative dry blend formulations (e.g., magnesium phosphate- and wollastonite-based cement currently under investigation by the French Alternative Energies and Atomic Energy Commission, CEA France, for stabilizing radionuclides (Cau Dit Coumes et al. 2014; Lambertin et al. 2017); targeted long-term mineral growth (e.g., ettringite); and the incorporation of getters for retention of ^{99}Tc and redox sensitive contaminants such as Cr. EPA Method 1315 leach testing should also be performed in simulated vadose zone pore water, which is more representative of the waste form leach environment when disposed of at the IDF, rather than just DIW. Under vadose zone leach conditions, ^{99}Tc D_{eff} values have been shown to decrease by orders of magnitude relative to DIW conditions recommended by the EPA Method 1315 procedure (Asmussen et al. 2016).
3. Qualification testing for monoliths cured for a range of cure times (e.g., 7 days, 28 days, 60 days) should be performed to improve waste form production and rate of waste form disposal at their final off-site or on-site disposal facility (e.g., avoid long hold times due to conservative cure times and reabsorption periods for residual free liquids). Testing scope should include methods to determine the effective (observed) diffusivity of COCs (e.g., ^{99}Tc and ^{129}I) and desorption coefficients (K_d) for the same key COCs to assess whether cure time affects these values. Results from these recommended studies would help support future maintenance of the IDF PA and guide waste form selection to support the implementation of alternative waste pathways for waste streams to be generated at the EMF during DFLAW operations.
4. Due to the low ^{99}Tc sorption capacity of the Cast Stone-based monoliths prepared with the Avg simulant and apparent dependence on solution:solid ratio, further investigation into sorption and desorption partition coefficients (K_d) values is needed to better inform PA models. Studies that consider ^{99}Tc sorption/desorption on formulated cementitious waste forms for periods other than 30 or 44 days is recommended to identify whether these processes are rate dependent. Furthermore, assessing the rate of waste form material oxidation over the K_d testing period would provide essential

data for informing the PA model, where assumptions are typically made for how long waste forms remain in a reduced state and thus influence predictions made for long-term waste form performance.

11.0 References

40 CFR 268. 2015. "Land Disposal Restrictions." *Code of Federal Regulations*, U.S. Environmental Protection Agency, Washington, DC. Accessed June 1, 2017, at <https://www.gpo.gov/fdsys/pkg/CFR-2012-title40-vol28/xml/CFR-2012-title40-vol28-part268.xml>.

Abramowitz H, M Brandys, R Cecil, N D'Angelo, KS Matlack, IS Muller, IL Pegg, RA Callow, and I Joseph. 2012. *Technetium Retention in WTP LAW Glass with Recycle Flow-Sheet DM10 Melter Testing*. VSL-12R2640-1, Vitreous State Laboratory, Washington, D.C. Accessed June 1, 2017, at <https://digital.library.unt.edu/ark:/67531/metadc842091/m1/>.

Adamson, DJ, CA Nash, AM Howe, DH Jones, and DJ McCabe. 2017. *Preparation and Evaporation of Hanford Waste Treatment Plant Direct Feed Low Activity Waste Effluent Management Facility Simulant*. SRNL-STI-2017-00465, Savannah River National Laboratory, Aiken, SC.

Almond PM, DI Kaplan, and EP Shine. 2012. *Variability of K_d Values in Cementitious Materials and Sediments*. SRNL-STI-2011-00672, Savannah River National Laboratory, Aiken, SC. Accessed March 21, 2017, at <https://www.nrc.gov/docs/ML1218/ML12185A072.pdf>.

ANSI/ANS-16.1-2003; R2008; R2017: *Measurement of the Leachability of Solidified Low-Level Radioactive Wastes by a Short-Term Test Procedure*. American Nuclear Society, La Grange Park, IL.

ASME – American Society of Mechanical Engineers. 2000. *Quality Assurance Requirements for Nuclear Facility Applications*. ASME NQA-1-2000, New York, NY.

Asmussen RM, CI Pearce, AR Lawter, RE Clayton, J Stephenson, B Miller, M Bowden, E Buck, N Washon, BD Williams, J Neeway, and NP Qafoku. 2016. *Getter Incorporation into Cast Stone and Solid State Characterizations*. PNNL-25577, Pacific Northwest National Laboratory, Richland, WA. Accessed April 11, 2018, at https://www.pnnl.gov/main/publications/external/technical_reports/PNNL-25577REV0.pdf.

ASTM C1308-08(2017), *Standard Test Method for Accelerated Leach Test for Diffusive Releases from Solidified Waste and a Computer Program to Model Diffusive, Fractional Leaching from Cylindrical Waste Forms*. ASTM International, West Conshohocken, PA, www.astm.org.

ASTM C1733-17a, *Standard Test Method for Distribution Coefficients of Inorganic Species by the Batch Method*. ASTM International, West Conshohocken, PA.

ASTM C191-13, *Standard Test Method for Time of Setting of Hydraulic Cement by Vicat Needle*. ASTM International, West Conshohocken, PA.

ASTM C39/C39M-18(2018), *Standard Test Method for Compressive Strength of Cylindrical Concrete Specimens*, ASTM International, West Conshohocken, PA, www.astm.org.

ASTM C642-13, *Standard Test Method for Density, Absorption, and Voids in Hardened Concrete*. ASTM International, West Conshohocken, PA.

ASTM C989/C989M-188, *Standard Specification for Slag Cement for Use in Concrete and Mortars*. ASTM International, West Conshohocken, PA.

ASTM D1426-15, *Standard Test Methods for Ammonia Nitrogen in Water*. ASTM International, West Conshohocken, PA.

ASTM D5084-16a. 2018. *Standard Test Methods for Measurement of Hydraulic Conductivity of Saturated Porous Materials Using a Flexible Wall Permeameter*. West Conshohocken, PA.

Cau Dit Coumes, C, D Lambertin, H Lahalle, P Antonucci, C Cannes, and S Delpéch. 2014. “Selection of a mineral binder with potentialities for the stabilization/solidification of aluminum metal.” *J. Nucl. Mater.* 453:31-40.

Cozzi AD and DJ McCabe. 2016. *Phase 1 Testing Results of Immobilization of WTP Effluent Management Facility Evaporator Bottoms Core Simulant*. SRNL-STI-2016-00675, Savannah River National Laboratory, Aiken, SC. Accessed May 26, 2017, at <http://sti.srs.gov/fulltext/SRNL-STI-2016-00675.pdf>.

Cozzi AD, KL Dixon, KA Hill, WD King, and RL Nichols. 2016. *Liquid Secondary Waste: Waste Form Formulation and Qualification*. SRNL-STI-2015-00685. Savannah River National Laboratory, Aiken, SC. Accessed May 26, 2017, at <https://sti.srs.gov/fulltext/SRNL-STI-2015-00685.pdf>.

Darab JG and PA Smith. 1996. “Chemistry of Technetium and Rhenium Species during Low-Level Radioactive Waste Vitrification.” *Chemistry of Materials* 8:1004.

EPA – U.S. Environmental Protection Agency. 1992. Method 1311, Revision 0 – Toxicity Characteristic Leaching Procedure. In *Test Methods for Evaluating Solid Waste: Physical/Chemical Methods*. EPA SW 846, U.S. Environmental Protection Agency, Washington, D.C. Accessed May 26, 2017, at <https://www.epa.gov/sites/production/files/2015-12/documents/1311.pdf>.

EPA – U.S. Environmental Protection Agency. 2013. *Method 1315, Revision 0 – Mass Transfer Rates of Constituents in Monolithic or Compacted Granular Materials Using a Semi-Dynamic Tank Leaching Procedure*. U.S. Environmental Protection Agency, Washington, D.C. Accessed March 21, 2017, at <https://www.epa.gov/sites/production/files/2015-12/documents/1315.pdf>.

Freeze RH and JA Cherry. 1979. *Groundwater*. Prentice-Hall, Inc.: Englewood Cliffs, NJ.

Grathwohl P. 1998. *Diffusion in Natural Porous Media: Contaminant Transport, Sorption/Desorption and Dissolution Kinetics*. Kluwer Academic Publishers, Berlin, Germany. ISBN 0-7923-8102-5.

Kaplan DI. 2010. *Geochemical Data Package for Performance Assessment Calculations Related to the Savannah River Site*. SRNL-STI-2009-00473, Savannah River National Laboratory, Aiken, SC. Accessed March 21, 2017, at <https://www.nrc.gov/docs/ML1133/ML113320386.pdf>.

Lambertin D, C Lemoine, C Cau-dit-Coumes, F Frizon, and C Decanis. 2017. “Selection of Binders for a Reactive Metal (Tungsten) Encapsulation.” Paper 17211 in *Proceedings of Waste Management Symposium 2017*, Phoenix, Arizona, March 2017.

Manahan SE. 1994. *Environmental Chemistry*, Sixth Edition. Lewis Publishers.

McCabe DJ, CA Nash, and DJ Adamson. 2016. *Formulation and preparation of Hanford Waste Treatment Plant Direct Feed Low Activity Waste Effluent Management Facility Core Simulant*. SRNL-STI-2016-00313, Savannah River National Laboratory, Aiken, SC. Accessed May 26, 2017, at <http://sti.srs.gov/fulltext/SRNL-STI-2016-00313.pdf>.

Miller BW, SH Frost, SL Frayo, AL Kenoyer, E Santos, JC Jones, DJ Green, DK Hamlin, DS Wilbur, and DR Fisher. 2015. "Quantitative single-particle digital autoradiography with α -particle emitters for targeted radionuclide therapy using the iQID camera." *Medical Physics* 42(2015):4094-4105.

Miller BW, SJ Gregory, ES Fuller, HH Barrett, HB Barber, and LR Furenlid. 2014. "The iQID camera: An ionizing-radiation quantum imaging detector." *Nuclear Instruments and Methods in Physics Research Section A: Accelerators, Spectrometers, Detectors and Associated Equipment* 767(2014):146-152.

Nordstrom DK and FD Wilde. 2005. *Reduction Oxidation Potential (Electrode Method), version 1.2*. U.S. Geological Survey Techniques of Water-Resources Investigations, Book 9, Chap. A6. Sec. 6.5, September 2005. Accessed March 31st, 2018, at <http://pubs.water.usgs.gov/twri9A6/>.

Qian G, DD Sun, and JH Tay. 2003. "Immobilization of mercury and zinc in an alkali-activated slag matrix." *J. Hazard. Mater.* 101(1):65-77.

Ramirez AJ. 2008. *Hanford Site Solid Waste Acceptance Criteria*. HNF-EP-0063, Rev. 14, Fluor Federal Services, Inc., Richland, WA. Accessed May 31, 2017, at http://www.hanford.gov/files.cfm/WAC_HNF-EP-0063_%20CurrentRv.pdf.

RCRA – Resource Conservation and Recovery Act. 1976. Public Law 94-580, as amended, 42 USC 6901 et seq. and 42 USC 6927(c) et seq. Accessed May 31, 2017, at <https://www.epw.senate.gov/rcra.pdf>.

Reigel MM, AD Cozzi, and DJ McCabe. 2017. *Phase 2 Testing Results of Immobilization of WTP Effluent Management Facility Evaporator Bottoms Simulant*. SRNL-STI-2017-00498, Rev. 0, Savannah River National Laboratory, Aiken, SC.

Saslow SA, W Um, RL Russell, G Wang, RM Asmussen, and R Sahajpal. 2017. *Updated Liquid Secondary Waste Grout Formulation and Preliminary Waste Form Qualification*. PNNL-26443, Pacific Northwest National Laboratory, Richland, WA. Accessed April 5, 2018, at https://www.pnnl.gov/main/publications/external/technical_reports/PNNL-26443.pdf.

Serne RJ, JH Westsik, Jr., BD Williams, HB Jung, and G Wang. 2015. *Extended Leach Testing of Simulated LAW Cast Stone Monoliths*. PNNL-24297, Rev. 1, Pacific Northwest National Laboratory, Richland, WA. Accessed March 21, 2017, at http://www.pnnl.gov/main/publications/external/technical_reports/PNNL-24297.pdf.

Siskind B and MG Cowgill. 1992. *Technical Justifications for the Tests and Criteria in the Waste Form Technical Position Appendix on Cement Stabilization*. BNL-NUREG-47121, Brookhaven National Laboratory, Upton, NY.

Um W, BD Williams, MMV Snyder, and G Wang. 2016. *Liquid Secondary Waste Grout Formulation and Waste Form Qualification*. PNNL-25129, Pacific Northwest National Laboratory, Richland, WA. Accessed March 21, 2017, at http://www.pnnl.gov/main/publications/external/technical_reports/PNNL-25129.pdf.

USGS – U.S. Geological Survey. 2004. "Alkalinity and Acid Neutralizing Capacity." In: *National Field Manual for the Collection of Water-Quality Data*, Second Edition. SA Rounds and FD Wilde, Editors. Accessed April 26, 2018, at <https://water.usgs.gov/owq/FieldManual/Chapter6/section6.6/html/section6.6.htm>.

Westsik, JH, Jr., GF Piepel, MJ Lindberg, PG Heasler, TM Mercier, RL Russell, AD Cozzi, WE Daniel RE Eibling, EK Hansen, MM Reigel, and DJ Swanberg. 2013. *Supplemental Immobilization of Hanford Low-Activity Waste: Cast Stone Screening Tests*. PNNL-22747, Pacific Northwest National Laboratory, Richland, WA; SRNL-STI-2013-00465, Savannah River National Laboratory, Aiken, SC. Accessed March 21, 2017, at http://www.pnnl.gov/main/publications/external/technical_reports/PNNL-22747.pdf.

Appendix A
Additional Data

Appendix A

Additional Data

A.1 Free Liquids Photos

For each Effluent Management Facility Composition Screening and Extended Qualification Test monolith monitored for free liquids, a photo was taken for every day an observation was made. The photos taken on the day of production and on the final observation day are provided in this section as Figure A.1–Figure A.28.

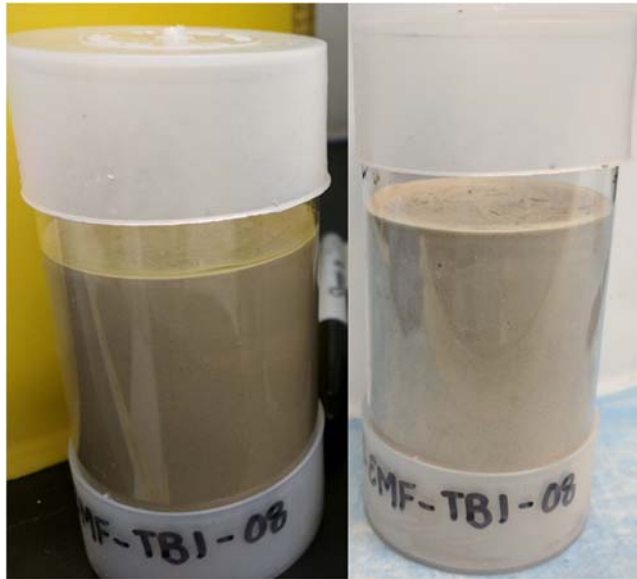


Figure A.1. Free liquid photos for TB1 (Simulant 1, Cast Stone) on the day of production (left) and three days after production, when no free liquids were observed (right).



Figure A.2. Free liquid photos for TB2 (Simulant 2, Cast Stone) on the day of production (left) and three days after production, when no free liquids were observed (right).



Figure A.3. Free liquid photos for TB3 (Simulant 3, Cast Stone) on the day of production (left) and three days after production, when no free liquids were observed (right).

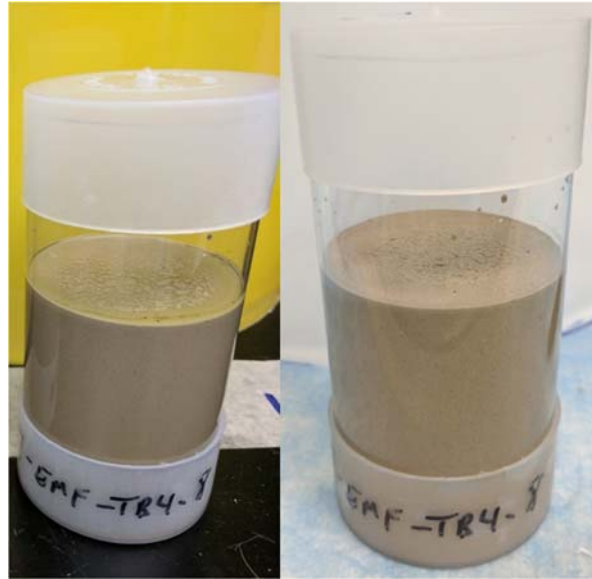


Figure A.4. Free liquid photos for TB4 (Simulant 4, Cast Stone) on the day of production (left) and three days after production, when no free liquids were observed (right).



Figure A.5. Free liquid photos for TB5 (Simulant 5, Cast Stone) on the day of production (left) and three days after production, when no free liquids were observed (right).



Figure A.6. Free liquid photos for TB6 (Simulant 6, Cast Stone) on the day of production (left) and five days after production, when no free liquids were observed (right).

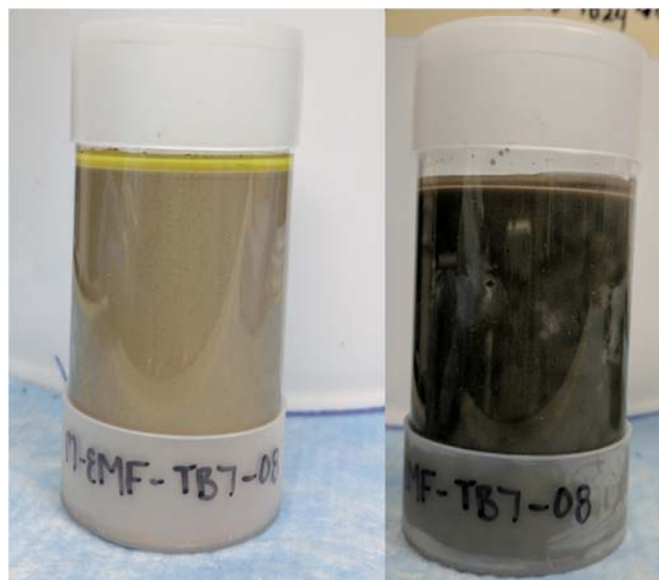


Figure A.7. Free liquid photos for TB7 (Simulant 7, Cast Stone) on the day of production (left) and on the final observation day, 29 days after production, with free liquids still present (right).

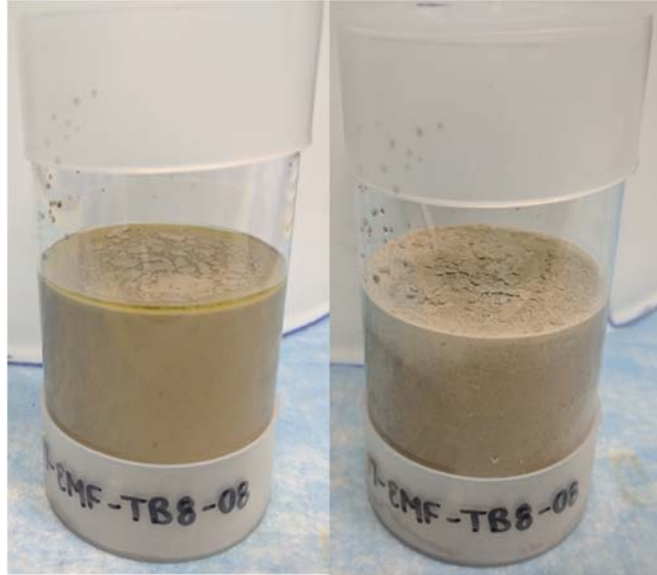


Figure A.8. Free liquid photos for TB8 (Simulant 8, Cast Stone) on the day of production (left) and three days after production, when no free liquids were observed (right).

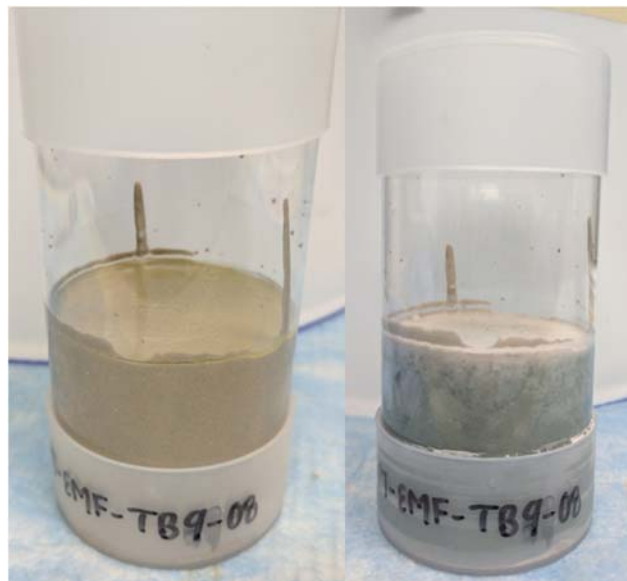


Figure A.9. Free liquid photos for TB9 (Simulant 1, Aquaset/blast furnace slag [BFS]) on the day of production (left) and 10 days after production, when no free liquids were observed (right).

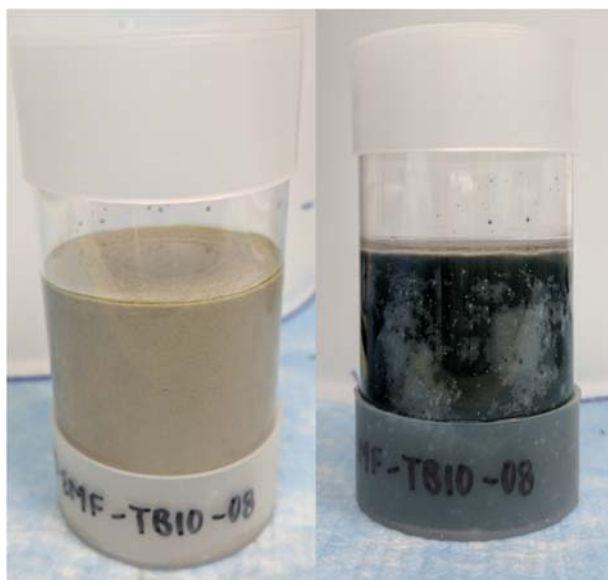


Figure A.10. Free liquid photos for TB10 (Simulant 2, Aquaset/BFS) on the day of production (left) and 18 days after production, when <1 vol% free liquids were observed (right).



Figure A.11. Free liquid photos for TB11 (Simulant 3, Aquaset/BFS) on the day of production (left) and 18 days after production, when <1 vol% free liquids were observed (right).



Figure A.12. Free liquid photos for TB12 (Simulant 4, Aquaset/BFS) on the day of production (left) and 18 days after production, when no free liquids were observed (right).

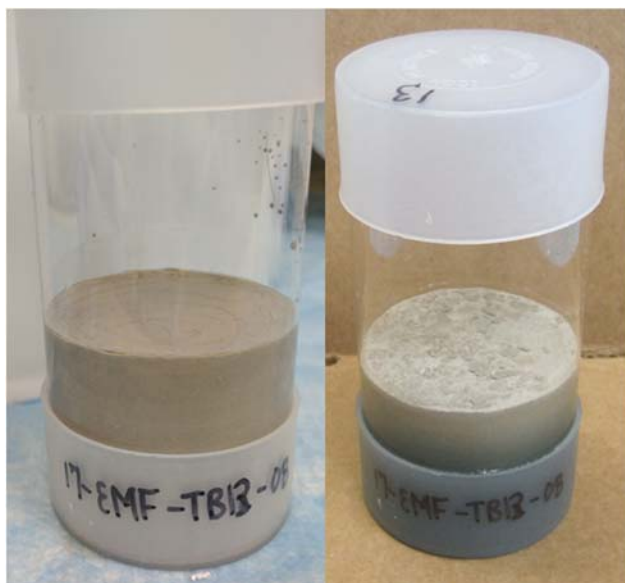


Figure A.13. Free liquid photos for TB13 (Simulant 5, Aquaset/BFS) on the day of production (left) and 18 days after production, when no free liquids were observed (right).

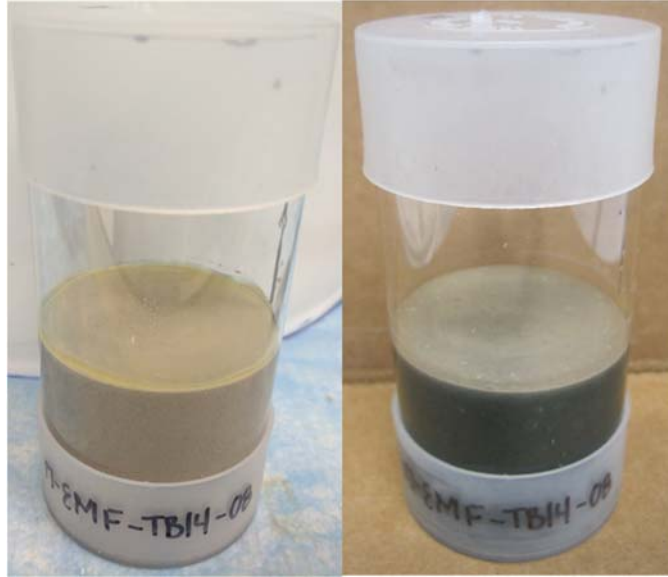


Figure A.14. Free liquid photos for TB14 (Simulant 6, Aquaset/BFS) on the day of production (left) and 14 days after production, when no free liquids were observed (right).

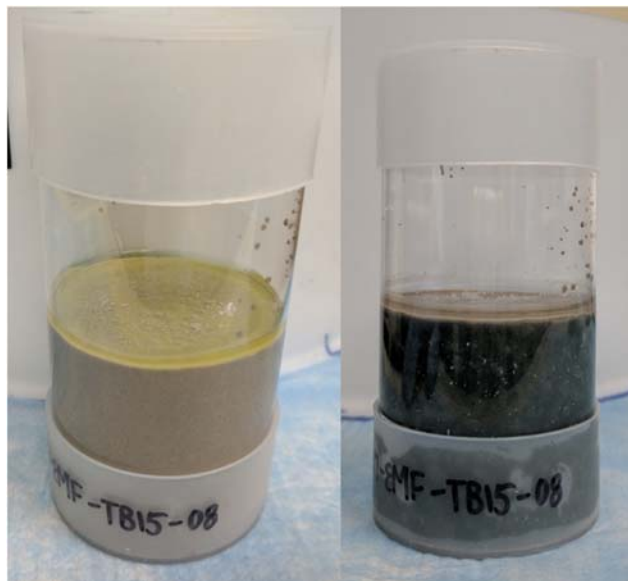


Figure A.15. Free liquid photos for TB15 (Simulant 7, Aquaset/BFS) on the day of production (left) and 18 days after production, when <1 vol% free liquids were observed (right).

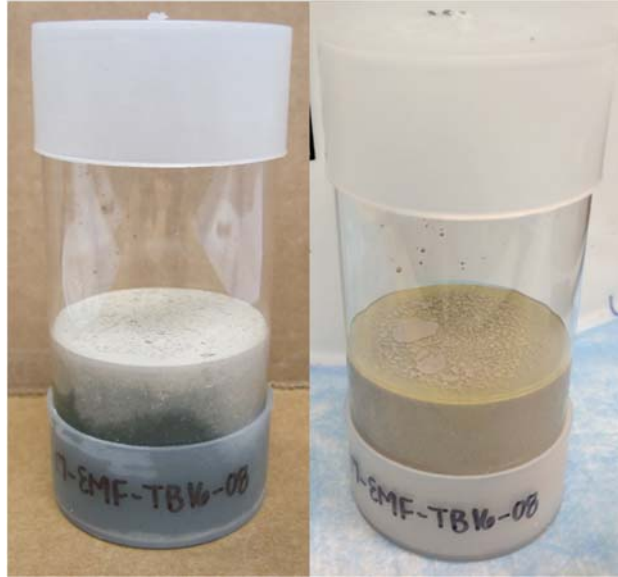


Figure A.16. Free liquid photos for TB16 (Simulant 8, Aquaset/BFS) on the day of production (left) and 14 days after production, when no free liquids were observed (right).

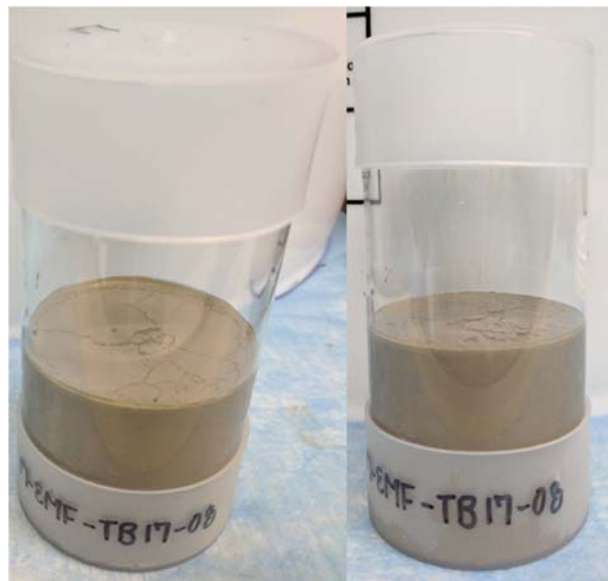


Figure A.17. Free liquid photos for TB17 (Simulant 1, ordinary portland cement [OPC]/BFS) on the day of production (left) and 5 days after production, when no free liquids were observed (right).

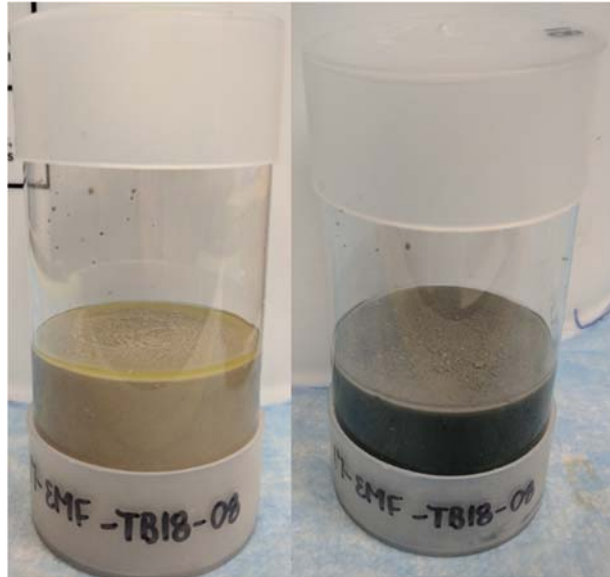


Figure A.18. Free liquid photos for TB18 (Simulant 2, OPC/BFS) on the day of production (left) and 5 days after production, when no free liquids were observed (right).

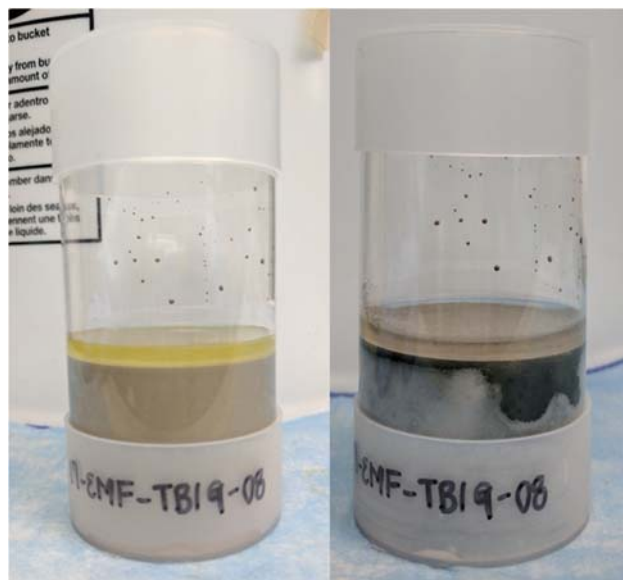


Figure A.19. Free liquid photos for TB19 (Simulant 3, OPC/BFS) on the day of production (left) and on the final observation day, 30 days after production, with free liquids still present (right).



Figure A.20. Free liquid photos for TB20 (Simulant 4, OPC/BFS) on the day of production (left) and 4 days after production, when no free liquids were observed (right).

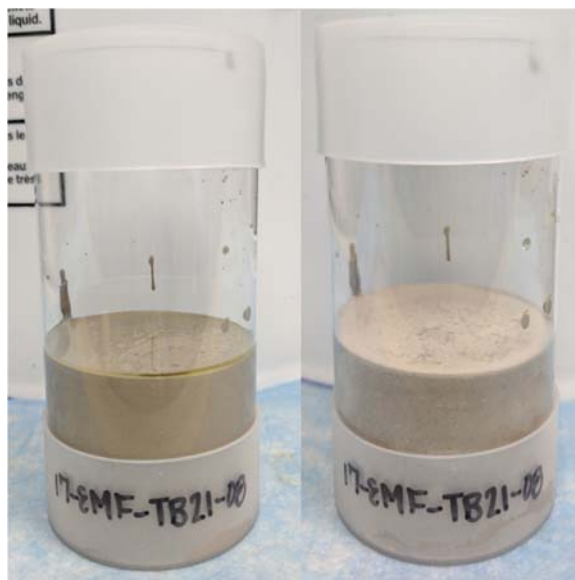


Figure A.21. Free liquid photos for TB21 (Simulant 5, OPC/BFS) on the day of production (left) and 3 days after production, when no free liquids were observed (right).

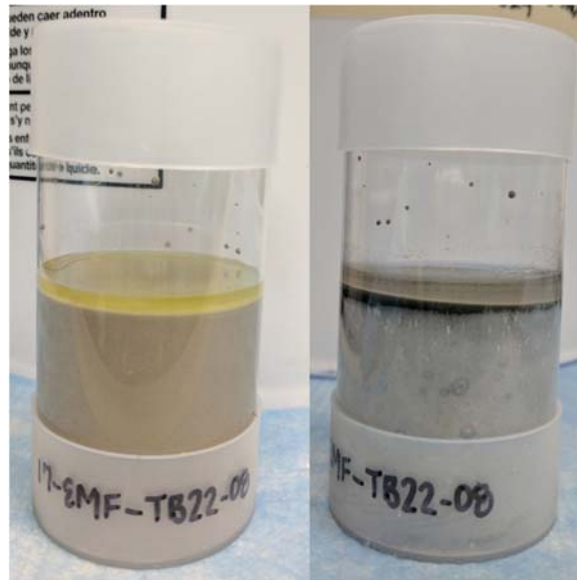


Figure A.22. Free liquid photos for TB22 (Simulant 6, OPC/BFS) on the day of production (left) and on the final observation day, 30 days after production, with free liquids still present (right).



Figure A.23. Free liquid photos for TB23 (Simulant 7, OPC/BFS) on the day of production (left) and 12 days after production, when <1 vol% free liquids were observed (right).

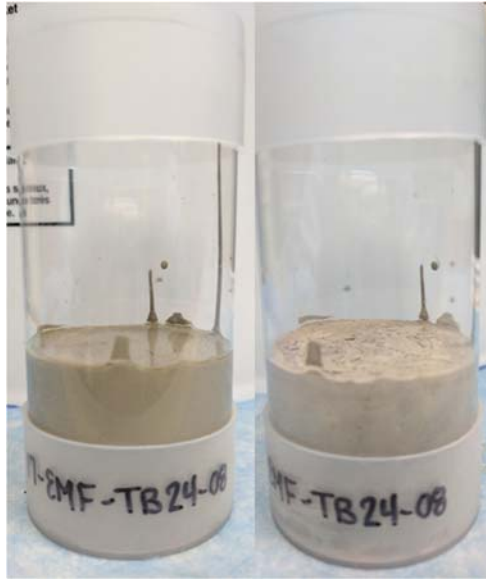


Figure A.24. Free liquid photos for TB24 (Simulant 8, OPC/BFS) day of production (left) and 4 days after production, when no free liquids were observed (right).

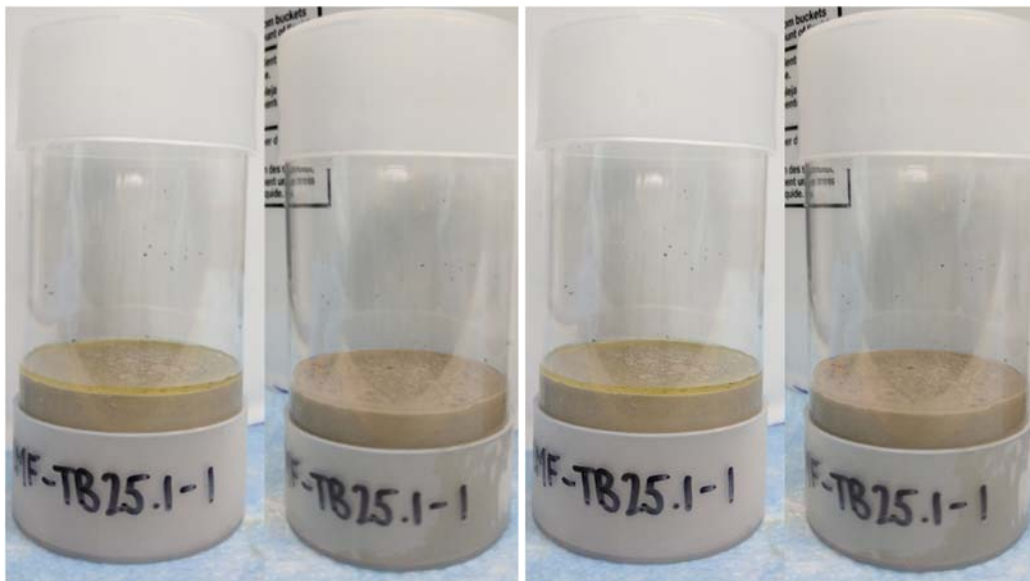


Figure A.25. Free liquid photos for TB25.1 (Avg Simulant, Cast Stone) on the day of production (left) and 3 days after production, when no free liquids were observed (right).

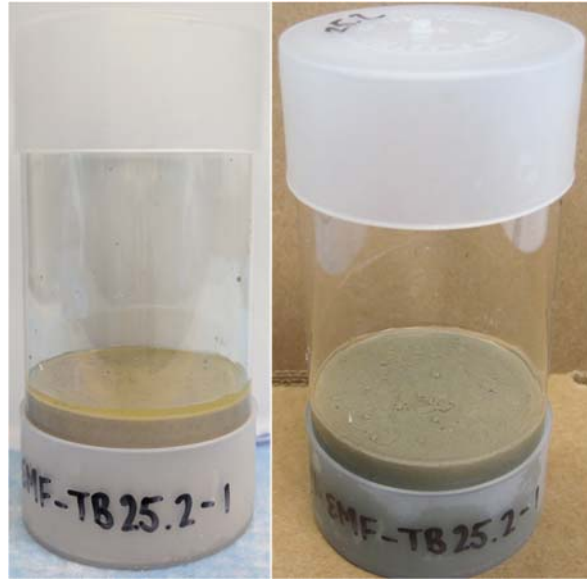


Figure A.26. Free liquid photos for TB25.2 (Avg Simulant, Cast Stone) on the day of production (left) and 8 days after production, when <1 vol% free liquids were observed (right).



Figure A.27. Free liquid photos for TB26.1a (Avg simulant, 10% HL, 18% OPC, 72% BFS) on the day of production (left) and 8 days after production, when <1 vol% free liquids were observed (right).

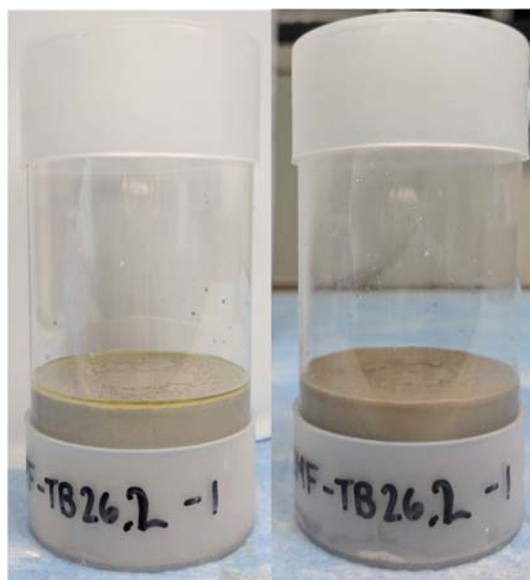


Figure A.28. Free liquid photos for TB26.2 (Avg simulant, 10% HL, 18% OPC, 72% BFS) on the day of production (left) and 3 days after production, when no free liquids were observed (right).

A.2 Composition Data for Dry Materials and Waste Forms after TCLP Testing

The composition of the dry ingredients used in this report was determined by solid digestion methods at Southwest Research Institute (Table A.1). To determine the composition of the monoliths after Toxicity Characteristic Leaching Procedure (TCLP) testing, solid digestion was performed, and the results are provided in Table A.2 (Cast Stone), Table A.3 (Aquaset/BFS), and Table A.4 (OPC/BFS).

Table A.1. Composition of Dry Ingredients

Constituent	Hydrated Lime (mg/kg)	OPC (mg/kg)	OPC (Westsik 2013) (µg/g)	Fly Ash (mg/kg)	Fly Ash (Westsik 2013) (µg/g)	BFS (mg/kg)	BFS (Westsik 2013) (µg/g)	Aquaset® II-GH (mg/kg)
Aluminum	1630	27,000	27,600	98,300	103,000	77,800	77,700	20,600
Antimony	0.987	53.7	<2,320	2.85	<2,320	0.533	<2,340	1.08
Arsenic	<1.48	37.4	<28.3	30.5	<28.3	<1.48	<28.6	9.03
Barium	13	602	492	5570	6,960	484	523	176
Beryllium	<0.493	0.708	-	2.88	-	8.81	-	0.556
Bismuth	<29.6	<29.6	-	<29.7	-	<29.5	-	<29.7
Boron	<976	<935	-	<903	-	<962	-	<903
Cadmium	<0.247	0.379	<4.67	1.16	<4.68	<0.246	<4.72	<0.246
Calcium	523,000	475,000	486,000	97,100	114,000	314,000	356,000	274,000
Chromium	<43.8	76.2	165	85.4	<65.0	<43.3	<65.6	<47.4
Cobalt	<0.493	23.8	-	17.6	-	<0.492	-	4.75
Copper	<0.493	254	242	118	<112	5.58	<113	17.7
Iron	841	22,600	27,800	41,900	52,700	6340	6,200	15,000

Constituent	Hydrated	OPC	OPC	Fly Ash	Fly Ash	BFS	BFS	Aquaset® II-GH
	Lime		(Westsik 2013)		(Westsik 2013)		(Westsik 2013)	
	(mg/kg)	(mg/kg)	(µg/g)	(mg/kg)	(µg/g)	(mg/kg)	(µg/g)	(mg/kg)
Lanthanum	1.92	8.66	-	44	-	44	-	12.8
Lead	<0.493	29.9	37.9	25.4	31.3	1.35	<17.9	7.19
Lithium	2.37	18.5	-	57.5	-	59.3	-	130
Magnesium	5570	5300	5,010	25,700	30,000	30,200	27,700	52,600
Manganese	26.2	699	614	598	557	1400	2,130	289
Mercury	<0.00988	<0.00986	<15.8	0.139	<15.8	<0.00971	<15.9	<0.00992
Molybdenum	<0.740	9.37	<31.1	9.12	<31.1	0.912	<31.4	1.25
Nickel	0.859	24.5	<484	48.3	<484	1.44	<488	9.09
Palladium	<24.7	<24.6	-	<24.7	-	<24.6	-	<24.8
Phosphorus	27.4	261	<3,080	1340	<3,080	83.6	<3110	286
Potassium	336	2550	<8,930	14,000	16,800	3850	<9010	6610
Selenium	<1.97	<1.97	<5,920	6.01	<5,920	<1.97	<5980	<1.97
Silicon	5000	91,700	110,000	214,000	270,000	141,000	181,000	131,000
Silver	<0.987	<0.985	1.79	<0.989	2.18	<0.984	<1.79	<0.984
Sodium	237	2250	<6,570	27,800	34,100	1550	<6630	3360
Strontium	376	1260	1,480	2930	3,730	466	670	903
Sulfur	195	13,200	14,000	3280	<11,100	13,500	23,800	5480
Thallium	<0.247	<0.246	-	1	-	0.282	-	0.257
Thorium	<19.7	<19.7	-	<19.8	-	<19.7	-	<19.8
Tin	<3.45	55.9	-	3.49	-	<3.44	-	<3.47
Titanium	85.1	1770	-	5750	-	2850	-	1000
Tungsten	<1.97	10.8	-	2.75	-	<1.97	-	2.81
Uranium	<197	<197	-	<198	-	<197	-	<198
Vanadium	1.77	72.9	-	176	-	20.2	-	23
Yttrium	5.59	13.9	-	39.6	-	63.6	-	9.39
Zinc	4.76	991	-	142	-	13.3	-	228
Zirconium	6.42	66.9	-	187	-	218	-	48.4

-: Not measured or not detected

Table A.2. Waste Form Composition after TCLP Testing, Cast Stone

Sample	17-EMF- TB1-04	17-EMF- TB2-02	17-EMF- TB3-02	17-EMF- TB4-02	17-EMF- TB5-02	17-EMF- TB6-02	17-EMF- TB7-02	17-EMF- TB8-02
Simulant	1	2	3	4	5	6	7	8
	(mg/kg)							
Aluminum	43,800	43,900	43,200	44,200	45,100	44,600	44,500	44,600
Antimony	4.09	4.19	4.17	4.08	4.08	4.11	4.11	4.17
Arsenic	77.3	76.8	79.9	79	80.7	80.5	79.7	80.8
Barium	1690	1680	1670	1720	1800	1750	1780	1790
Beryllium	3.49	3.48	3.63	3.61	3.56	3.54	3.58	3.58
Bismuth	<29.7	<29.6	<29.4	<29.6	<29.8	<29.6	<29.8	<29.2

Sample	17-EMF-TB1-04	17-EMF-TB2-02	17-EMF-TB3-02	17-EMF-TB4-02	17-EMF-TB5-02	17-EMF-TB6-02	17-EMF-TB7-02	17-EMF-TB8-02
Simulant	1	2	3	4	5	6	7	8
	(mg/kg)							
Boron	2830	<967	1070	1580	1890	<988	<781	1290
Cadmium	0.432	0.426	0.509	0.497	0.513	0.432	0.43	0.453
Calcium	137,000	138,000	134,000	139,000	136,000	140,000	139,000	138,000
Chromium	134	137	125	125	149	135	144	132
Cobalt	6.69	6.65	6.9	6.5	7.32	6.84	7.51	6.85
Copper	48.3	47.9	48.8	48.4	49	49	52.7	50.3
Iron	15,600	15,800	15,800	15,700	15,600	15,800	15,700	15,300
Lanthanum	25.9	26.4	26.4	26.6	25.8	26.2	26	26.3
Lead	10.2	10.2	10.1	10.5	10.1	9.97	9.95	10.2
Lithium	34.4	34.6	34.7	34.4	35	35.1	35	35.1
Magnesium	17,200	17,300	17,300	17,300	17,300	17,100	17,200	17,200
Manganese	636	641	641	639	639	631	635	634
Mercury	26.2	28	29.3	25.5	24.3	28.8	27.6	27.5
Molybdenum	3.56	3.33	3.77	3.88	3.68	3.24	3.89	3.73
Nickel	16.4	16.6	16.7	16.4	16.5	16.4	16.7	16.5
Palladium	<24.7	<24.7	<24.5	<24.7	<24.8	<24.7	<24.8	<24.4
Phosphorus	436	417	417	425	427	416	423	428
Potassium	5220	5260	5260	5180	5230	5270	5190	5220
Selenium	65.1	64.5	64.1	65.3	63.8	66.2	64.9	66.6
Silicon	115,000	113,000	111,000	112,000	114,000	114,000	114,000	113,000
Silver	<0.989	<0.987	<0.979	<0.988	<0.993	<0.987	<0.992	<0.975
Sodium	30,600	30,000	29,200	29,900	29,000	29,300	28,300	28,800
Strontium	1020	1020	1030	1040	1040	1030	1040	1040
Sulfur	6730	6810	6810	6290	10,300	10,300	9890	8810
Thallium	0.333	0.331	0.334	0.368	0.351	0.349	0.353	0.352
Thorium	<19.8	<19.7	<19.6	<19.8	<19.9	<19.7	<19.8	<19.5
Tin	3.55	<3.46	<3.43	<3.46	<3.48	<3.45	<3.47	<3.41
Titanium	2610	2600	2560	2640	2650	2640	2650	2640
Tungsten	6.34	6.51	12.1	3.83	13.1	5.31	13.9	4.59
Uranium	<198	<197	<196	<198	<199	<197	<198	<195
Vanadium	59.8	59.8	60.5	60.5	60.4	60.1	60.7	60.6
Yttrium	30.9	30.8	31.1	31.2	31.2	31.1	31.1	31.2
Zinc	337	241	282	344	341	270	297	339
Zirconium	124	123	122	123	123	123	124	124

Table A.3. Waste Form Composition after TCLP Testing, Aquaset/BFS

Sample	17-EMF-TB9-02	17-EMF-TB10-02	17-EMF-TB11-02	17-EMF-TB12-02	17-EMF-TB13-01	17-EMF-TB14-01	17-EMF-TB15-01	17-EMF-TB16-01
Simulant	1	2	3	4	5	6	7	8
	(mg/kg)	(mg/kg)	(mg/kg)	(mg/kg)	(mg/kg)	(mg/kg)	(mg/kg)	(mg/kg)
Aluminum	35,600	35,700	34,900	33,900	34,000	33,400	33,700	33,400
Antimony	0.716	0.693	0.637	1.14	1.21	1.13	1.14	1.1
Arsenic	68.9	70.4	66.4	70.3	73	71.6	72.1	72.5
Barium	285	282	279	246	261	248	249	243
Beryllium	4.75	4.81	4.33	4.62	4.49	4.55	4.49	4.43
Bismuth	<29.6	<29.8	<29.4	<29.9	<29.4	<29.5	<29.6	<29.5
Boron	2650	<963	1000	1510	1780	<946	<927	1190
Cadmium	<0.247	<0.246	0.252	0.343	0.339	0.268	0.25	0.256
Calcium	181,000	182,000	178,000	186,000	187,000	185,000	184,000	183,000
Chromium	113	117	108	112	119	127	131	122
Cobalt	1.39	0.984	0.94	1.56	1.33	1.51	1.26	1.64
Copper	7.37	6.21	6.07	8.99	8.45	8.33	7.99	8.38
Iron	5580	5730	5540	5470	5310	5380	5440	5430
Lanthanum	24.5	24.7	22.0	24.5	24.2	24.2	24.4	24.1
Lead	2.56	2.25	2.26	9.73	9.81	10.1	9.68	9.87
Lithium	46.8	47	47.2	46.7	46	46.4	46.5	45.7
Magnesium	23,000	23,100	23,000	18,900	18,600	18,700	19,000	18,500
Manganese	770	777	772	928	914	908	932	917
Mercury	26	29.7	29.9	26.9	27.6	27.8	27.6	27.9
Molybdenum	1.16	1.11	0.862	1.6	<0.736	1.27	<0.740	1.2
Nickel	2.54	2.57	2.49	2.99	2.28	2.39	2.11	2.32
Palladium	<24.7	<24.8	<24.5	<24.9	<24.5	<24.6	<24.7	<24.5
Phosphorus	78.7	95.8	74.3	89.5	87.8	89.7	82.9	82.2
Potassium	2820	2870	2830	2970	2960	2980	2960	2960
Selenium	62.1	63	58.3	64.3	63.8	66.5	66.6	65.2
Silicon	92,200	93,600	93,400	94,400	94,900	94,500	93,100	92,700
Silver	<0.987	<0.984	<0.981	<0.997	<0.981	<0.983	<0.987	<0.982
Sodium	23,900	23,600	22,300	22,700	22,200	22,200	20,700	22,000
Strontium	364	363	367	409	403	406	411	404
Sulfur	8800	8800	8740	11,700	15,700	15,700	15,400	14,200
Thallium	<0.247	<0.246	<0.245	0.259	0.251	0.262	0.26	0.246
Thorium	<19.7	<19.8	<19.6	<19.9	<19.6	<19.7	<19.7	<19.6
Tin	<3.46	<3.47	<3.43	<3.49	<3.43	<3.44	<3.45	<3.44
Titanium	1590	1600	1570	1530	1540	1510	1530	1520
Tungsten	10.2	5.13	4.76	11.5	5.25	9.09	3.93	10.7
Uranium	<197	<198	<196	<199	<196	<197	<197	<196
Vanadium	13.8	13.8	12.6	14.8	14.7	14.7	14.6	14.5
Yttrium	33.4	33.4	30.2	35.1	34.3	34.4	34.7	34.2
Zinc	282	179	206	298	296	158	265	289
Zirconium	116	119	106	114	112	113	114	111

Table A.4. Waste Form Composition after TCLP Testing, OPC/BFS

Sample	17-EMF-TB17-01	17-EMF-TB18-01	17-EMF-TB19-01	17-EMF-TB20-01	17-EMF-TB21-01	17-EMF-TB22-01	17-EMF-TB23-01	17-EMF-TB24-01
Simulant	1	2	3	4	5	6	7	8
	(mg/kg)							
Aluminum	34,600	34,900	33,900	34,400	36,200	36,400	36,200	36,300
Antimony	8.41	8.45	6.85	8.22	7.66	7.62	7.5	7.62
Arsenic	73.1	76.5	66.3	73.8	73.2	74.2	73	74.6
Barium	299	300	298	309	331	338	337	336
Beryllium	4.48	4.52	4.53	4.49	4.74	4.76	4.64	4.7
Bismuth	<29.2	<29.2	<29.7	<29.8	<29.7	<29.7	<29.3	<29.4
Boron	2630	<935	<970	1490	2020	<977	<981	1230
Cadmium	0.276	0.282	0.324	0.359	0.261	<0.248	<0.244	<0.245
Calcium	208,000	209,000	205,000	205,000	203,000	204,000	202,000	204,000
Chromium	132	162	123	126	124	127	128	127
Cobalt	3.69	3.82	3.54	3.75	3.41	3.65	3.4	3.57
Copper	38.2	39.7	37	38.5	35.7	36.7	40.3	37
Iron	6330	6350	5920	6100	6220	6240	6210	6350
Lanthanum	23.7	23.8	24.1	23.7	23.8	23.9	23.9	24
Lead	12.8	12.7	12.7	11.3	5.03	5.1	5.61	4.94
Lithium	31.6	31.9	30.9	31.9	32.7	32.6	32	32.4
Magnesium	12,400	12,800	12,100	13,100	16,800	16,700	16,400	16,900
Manganese	955	995	965	938	817	824	818	831
Mercury	24.7	27.3	29.5	21.8	26.6	28.4	28.4	28.2
Molybdenum	1.94	2.14	1.89	2.13	2.11	1.94	2.22	1.99
Nickel	4.02	7.47	4.06	4.43	4.24	4.62	6.11	4.36
Palladium	<24.3	<24.3	<24.8	<24.9	<24.7	<24.8	<24.4	<24.5
Phosphorus	85.9	84.7	92.7	88.8	79	77.9	80.3	81.7
Potassium	2450	2480	2470	2430	2310	2310	2290	2300
Selenium	63.9	65.4	61.4	66.3	62.1	65.4	63.6	64
Silicon	87,700	88,400	82,500	87,000	86,600	87,100	84,000	87,000
Silver	<0.973	<0.974	<0.985	<0.994	<0.989	<0.990	<0.977	<0.980
Sodium	23,900	23,400	22,400	23,000	22,300	22,300	20,900	21,800
Strontium	448	457	445	448	410	412	409	414
Sulfur	13,000	13,200	12,800	12,000	13,300	13,300	12,900	11,900
Thallium	<0.243	<0.243	<0.246	<0.249	<0.247	<0.248	<0.244	<0.245
Thorium	<19.5	<19.5	<19.8	<19.9	<19.8	<19.8	<19.5	<19.6
Tin	7.15	6.46	6.93	7.42	7.3	6.97	7.36	6.93
Titanium	1640	1650	1610	1640	1690	1700	1690	1700
Tungsten	5.25	6.71	3.01	5.68	4.59	6.41	5.85	7.42
Uranium	<195	<195	<198	<199	<198	<198	<195	<196
Vanadium	20.9	20.9	19.4	20.8	19.9	20.3	20	20.1
Yttrium	35.1	35.2	34.9	34.9	34	34.2	34	34.2
Zinc	385	295	313	379	371	294	340	377
Zirconium	116	115	113	117	120	122	122	123

Table A.5. Waste Form Composition after TCLP Testing: Avg Simulant, Cast Stone and HL Formulations

Sample	17-EMF-TB25.1-03	17-EMF-TB25.2-03	17-EMF-TB26.1a-03	17-EMF-TB26.2-03
Simulant	Avg	Avg	Avg	Avg
Formulation	Cast Stone	Cast Stone	HL, OPC, BFS	HL, OPC, BFS
	(mg/kg)	(mg/kg)	(mg/kg)	(mg/kg)
Aluminum	43,900	43,700	32,700	33,200
Antimony	3.73	3.86	6.66	6.11
Arsenic	11.8	11.2	5.08	4.94
Barium	1790	1800	307	299
Beryllium	3.47	3.43	4.24	4.25
Bismuth	<29.5	< 29.4	< 29.8	< 29.1
Boron	1350	1340	1250	1250
Cadmium	0.443	0.404	< 0.249	< 0.243
Calcium	136,000	135,000	213,000	218,000
Chromium	140	141	123	130
Cobalt	6.62	7.06	3.01	3.27
Copper	48.4	49	32.3	33
Iron	15,300	15,500	5550	5770
Lanthanum	26	25.6	21.8	21.5
Lead	10.4	10.5	4.77	4.8
Lithium	35.4	35.7	28.7	29.2
Magnesium	17,000	17,100	15,300	15,400
Manganese	644	656	737	747
Mercury	0.0595	0.0592	0.0292	< 0.00990
Molybdenum	3.82	4.39	1.71	1.74
Nickel	16.1	15.8	4.12	4.51
Palladium	<24.6	< 24.5	< 24.9	< 24.3
Phosphorus	445	435	75.3	67.8
Potassium	5500	5690	2060	2070
Selenium	<1.97	2.16	< 1.99	< 1.94
Silicon	113,000	114,000	77,400	78,500
Silver	<0.984	< 0.979	< 0.995	< 0.972
Sodium	30,000	30,700	22,200	22,400
Strontium	1040	1030	390	393
Sulfur	8240	8160	10,200	10,500
Thallium	0.385	0.391	< 0.249	< 0.243
Thorium	<19.7	< 19.6	< 19.9	< 19.4
Tin	4.07	4.01	6.4	6.14
Titanium	2570	2550	1520	1550
Tungsten	1.97	7.58	< 1.99	3.62
Uranium	<197	< 196	< 199	< 194
Vanadium	60.6	60.6	18.3	17.5
Yttrium	30.7	30.5	30.9	31.1
Zinc	335	342	357	363
Zirconium	124	125	108	107

A.3 Additional Results for Solution Concentrations of Cations and Anions from Environmental Protection Agency (EPA) Method 1315 Leach Tests

Table A.6. Concentrations of Major Anions, ⁹⁹Tc, and ¹²⁷I Measured in Leachates from EPA Method 1315 Tests. Cumulative release of ⁹⁹Tc and ¹²⁷I (%) are shown in parentheses.

Sample ID	Cl ⁻ (µg/mL)*		NO ₃ ⁻ (µg/mL)*		NO ₂ ⁻ (µg/mL)*		SO ₄ ⁻ (µg/mL)*		⁹⁹ Tc (µg/L)*		¹²⁷ I (µg/L)*	
	Result	EQL	Result	EQL	Result	EQL	Result	EQL	Result	EQL	Result	EQL
17-EMF-DI-BLK1-0.08d	2.47	1.25	ND	2.5	ND	2.5	ND	3.75	ND	0.0165	ND	0.063
17-EMF-DI-BLK1-1d	ND	1.25	ND	2.5	ND	2.5	ND	3.75	ND	0.0165	ND	0.063
17-EMF-DI-BLK1-2d	ND	1.25	ND	2.5	ND	2.5	ND	3.75	ND	0.0165	ND	0.063
17-EMF-DI-BLK1-7d	ND	1.25	ND	2.5	ND	2.5	ND	3.75	ND	0.0165	ND	0.063
17-EMF-DI-BLK1-14d	ND	1.25	ND	2.5	ND	2.5	ND	3.75	ND	0.0165	ND	0.063
17-EMF-DI-BLK1-28d	ND	1.25	ND	2.5	ND	2.5	ND	3.75	ND	0.0165	ND	0.063
17-EMF-DI-BLK1-42d	ND	1.25	ND	2.5	ND	2.5	ND	3.75	ND	0.0165	ND	0.063
17-EMF-DI-BLK1-49d	ND	1.25	ND	2.5	ND	2.5	ND	3.75	ND	0.0165	ND	0.063
17-EMF-DI-BLK1-63d	ND	1.25	ND	2.5	ND	2.5	ND	3.75	ND	0.0165	ND	0.063
17-EMF-DI-BLK2-0.08d	ND	1.25	ND	2.5	ND	2.5	ND	3.75	ND	0.0165	ND	0.063
17-EMF-DI-BLK2-1d	ND	1.25	ND	2.5	ND	2.5	ND	3.75	ND	0.0165	ND	0.063
17-EMF-DI-BLK2-2d	ND	1.25	ND	2.5	ND	2.5	ND	3.75	ND	0.0165	ND	0.063
17-EMF-DI-BLK2-7d	ND	1.25	ND	2.5	ND	2.5	ND	3.75	ND	0.0165	ND	0.063
17-EMF-DI-BLK2-14d	ND	1.25	ND	2.5	ND	2.5	ND	3.75	ND	0.0165	ND	0.063
17-EMF-DI-BLK2-28d	ND	1.25	ND	2.5	ND	2.5	ND	3.75	ND	0.0165	ND	0.063
17-EMF-DI-BLK2-42d	ND	1.25	ND	2.5	ND	2.5	ND	3.75	ND	0.0165	ND	0.063
17-EMF-DI-BLK2-49d	ND	1.25	ND	2.5	ND	2.5	ND	3.75	ND	0.0165	ND	0.063
17-EMF-DI-BLK2-63d	ND	1.25	ND	2.5	ND	2.5	ND	3.75	ND	0.0165	ND	0.063
17-EMF-TB27-1-0.08d	6.28	1.25	ND	2.5	2.66	2.5	5.32	3.75	0.98 (0.08)	0.165	3.1 (0.23)	0.126
17-EMF-TB27-1-1d	32.8	1.25	ND	2.5	14.2	2.5	25.9	3.75	6.15 (0.60)	0.165	16.7 (1.44)	0.126

Sample ID	Cl ⁻ (µg/mL)*		NO ₃ ⁻ (µg/mL)*		NO ₂ ⁻ (µg/mL)*		SO ₄ ⁻ (µg/mL)*		⁹⁹ Tc (µg/L)*		¹²⁷ I (µg/L)*	
	Result	EQL	Result	EQL	Result	EQL	Result	EQL	Result	EQL	Result	EQL
17-EMF-TB27-1-2d	17.9	1.25	ND	2.5	8.05	2.5	12.4	3.75	3.59 (0.90)	0.165	8.89 (2.09)	0.126
17-EMF-TB27-1-7d	54.4	1.25	ND	2.5	22.8	2.5	31.3	3.75	10.1 (1.74)	0.165	26.2 (4.00)	0.126
17-EMF-TB27-1-14d	38.8	1.25	ND	2.5	17.4	2.5	22.9	3.75	6 (2.24)	0.165	18.8 (5.36)	0.126
17-EMF-TB27-1-28d	44.2	1.25	ND	2.5	19.8	2.5	26.4	3.75	5.55 (2.71)	0.165	21.3 (6.91)	0.126
17-EMF-TB27-1-42d	26.8	1.25	ND	2.5	12.1	2.5	16.8	3.75	3.15 (2.97)	0.165	12.4 (7.82)	0.126
17-EMF-TB27-1-49d	10.7	1.25	ND	2.5	4.79	2.5	7.37	3.75	1.36 (3.08)	0.165	4.84 (8.17)	0.126
17-EMF-TB27-1-63d	19.3	1.25	ND	2.5	8.89	2.5	14.1	3.75	2.55 (3.30)	0.165	8.66 (8.80)	0.126
17-EMF-TB27-2-0.08d	11	1.25	ND	2.5	4.96	2.5	9.31	3.75	1.48 (0.12)	0.165	5.26 (0.38)	0.126
17-EMF-TB27-2-1d	34.6	1.25	ND	2.5	15	2.5	26.1	3.75	6.15 (0.64)	0.165	17.5 (1.65)	0.126
17-EMF-TB27-2-2d	15.3	1.25	ND	2.5	6.87	2.5	10	3.75	2.78 (0.87)	0.165	7.58 (2.20)	0.126
17-EMF-TB27-2-7d	54.5	1.25	ND	2.5	22.8	2.5	30.7	3.75	8.65 (1.59)	0.165	26 (4.09)	0.126
17-EMF-TB27-2-14d	38.4	1.25	ND	2.5	17.7	2.5	21.6	3.75	4.81 (1.99)	0.165	18.1 (5.40)	0.126
17-EMF-TB27-2-28d	44.6	1.25	ND	2.5	19.9	2.5	25.9	3.75	5.11 (2.42)	0.165	21 (6.92)	0.126
17-EMF-TB27-2-42d	28.1	1.25	ND	2.5	12.4	2.5	17	3.75	3.25 (2.69)	0.165	12.4 (7.82)	0.126
17-EMF-TB27-2-49d	11.9	1.25	ND	2.5	5.26	2.5	7.9	3.75	1.47 (2.81)	0.165	5.13 (8.20)	0.126
17-EMF-TB27-2-63d	20.1	1.25	ND	2.5	9	2.5	14.2	3.75	2.88 (3.05)	0.165	8.57 (8.82)	0.126
17-EMF-TB28-1-0.08d	2.37	1.25	ND	2.5	ND	2.5	ND	3.75	0.649 (0.05)	0.165	ND	0.126
17-EMF-TB28-1-1d	14.1	1.25	ND	2.5	7.74	2.5	ND	3.75	3.61 (0.34)	0.165	1.92 (0.15)	0.126

Sample ID	Cl ⁻ (µg/mL)*		NO ₃ ⁻ (µg/mL)*		NO ₂ ⁻ (µg/mL)*		SO ₄ ⁻ (µg/mL)*		⁹⁹ Tc (µg/L)*		¹²⁷ I (µg/L)*	
	Result	EQL	Result	EQL	Result	EQL	Result	EQL	Result	EQL	Result	EQL
17-EMF-TB28-1-2d	11.6	1.25	ND	2.5	6.57	2.5	ND	3.75	3.33 (0.61)	0.165	2.05 (0.29)	0.126
17-EMF-TB28-1-7d	38.9	1.25	ND	2.5	20.7	2.5	ND	3.75	9.05 (1.35)	0.165	3.67 (0.56)	0.126
17-EMF-TB28-1-14d	31	1.25	ND	2.5	17.5	2.5	ND	3.75	5.31 (1.77)	0.165	3.22 (0.79)	0.126
17-EMF-TB28-1-28d	60.6	1.25	ND	2.5	32.6	2.5	4.32	3.75	3.02 (2.02)	0.165	4.77 (1.13)	0.126
17-EMF-TB28-1-42d	34.7	1.25	ND	2.5	19.1	2.5	ND	3.75	0.995 (2.10)	0.165	3.16 (1.36)	0.126
17-EMF-TB28-1-49d	14.3	1.25	ND	2.5	8.14	2.5	ND	3.75	0.545 (2.14)	0.165	1.90 (1.50)	0.126
17-EMF-TB28-1-63d	23.2	1.25	ND	2.5	13.1	2.5	ND	3.75	0.984 (2.22)	0.165	2.94 (1.71)	0.126
17-EMF-TB28-2-0.08d	1.8	1.25	ND	2.5	ND	2.5	ND	3.75	0.466 (0.04)	0.165	ND	0.126
17-EMF-TB28-2-1d	13.8	1.25	ND	2.5	7.58	2.5	ND	3.75	3.8 (0.35)	0.165	2.01 (0.15)	0.126
17-EMF-TB28-2-2d	9.58	1.25	ND	2.5	5.38	2.5	ND	3.75	2.64 (0.56)	0.165	1.58 (0.27)	0.126
17-EMF-TB28-2-7d	35.8	1.25	ND	2.5	19.6	2.5	ND	3.75	8.28 (1.23)	0.165	3.45 (0.52)	0.126
17-EMF-TB28-2-14d	31.5	1.25	ND	2.5	17.9	2.5	ND	3.75	5.13 (1.65)	0.165	3.17 (0.75)	0.126
17-EMF-TB28-2-28d	42.9	1.25	ND	2.5	23.4	2.5	ND	3.75	3.18 (1.91)	0.165	3.89 (1.03)	0.126
17-EMF-TB28-2-42d	28.7	1.25	ND	2.5	15.7	2.5	ND	3.75	1.24 (2.01)	0.165	3.02 (1.25)	0.126
17-EMF-TB28-2-49d	11.5	1.25	ND	2.5	6.37	2.5	ND	3.75	0.574 (2.06)	0.165	1.83 (1.38)	0.126
17-EMF-TB28-2-63d	18.8	1.25	ND	2.5	10.4	2.5	ND	3.75	1.09 (2.14)	0.165	2.66 (1.57)	0.126

* Initial anion concentrations in the Avg simulant: Cl⁻ = 39,900 µg/mL, NO₃⁻ = 1410 µg/mL, NO₂⁻ = 17,000 µg/mL, and SO₄²⁻ = 24,000 µg/mL

Table A.7. Concentrations of Major Cations Measured in Leachates from EPA Method 1315 Tests (28-Day Cured Monoliths). EQL is estimated quantification limit; ND indicates “not detected”; cumulative release of Na (%) is shown in parentheses.

Sample ID	Al (µg/L)		Ca (µg/L)		Mg (µg/L)		K (µg/L)		Si (µg/L)		Na (µg/L)	
	Result	EQL	Result	EQL	Result	EQL	Result	EQL	Result	EQL	Result	EQL
17-EMF-DI-BLK1-0.08d	242	82.4	616	168	173	13.5	2650	806	ND	274	ND	223
17-EMF-DI-BLK1-1d	535	82.4	1430	168	211	13.5	ND	806	ND	274	ND	223
17-EMF-DI-BLK1-2d	ND	82.4	ND	168	ND	13.5	ND	806	ND	274	ND	223
17-EMF-DI-BLK1-7d	ND	82.4	ND	168	ND	13.5	ND	806	ND	274	ND	223
17-EMF-DI-BLK1-14d	ND	82.4	192	168	ND	13.5	ND	806	ND	274	ND	223
17-EMF-DI-BLK1-28d	ND	82.4	222	168	ND	13.5	ND	806	ND	274	ND	223
17-EMF-DI-BLK1-42d	ND	82.4	183	168	ND	13.5	ND	806	ND	274	ND	223
17-EMF-DI-BLK1-49d	ND	82.4	ND	168	ND	13.5	ND	806	ND	274	ND	223
17-EMF-DI-BLK1-63d	ND	82.4	191	168	ND	13.5	ND	806	ND	274	ND	223
17-EMF-DI-BLK2-0.08d	ND	82.4	ND	168	ND	13.5	ND	806	ND	274	ND	223
17-EMF-DI-BLK2-1d	ND	82.4	377	168	ND	13.5	ND	806	ND	274	ND	223
17-EMF-DI-BLK2-2d	ND	82.4	ND	168	ND	13.5	ND	806	ND	274	ND	223
17-EMF-DI-BLK2-7d	ND	82.4	ND	168	ND	13.5	ND	806	ND	274	ND	223
17-EMF-DI-BLK2-14d	ND	82.4	276	168	34.4	13.5	ND	806	275	274	ND	223
17-EMF-DI-BLK2-28d	ND	82.4	224	168	ND	13.5	ND	806	ND	274	ND	223
17-EMF-DI-BLK2-42d	ND	82.4	182	168	ND	13.5	ND	806	ND	274	ND	223
17-EMF-DI-BLK2-49d	ND	82.4	ND	168	ND	13.5	ND	806	ND	274	ND	223
17-EMF-DI-BLK2-63d	ND	82.4	175	168	ND	13.5	ND	806	ND	274	ND	223
17-EMF-TB27-1-0.08d	493	82.4	815	168	36.4	13.5	955	806	ND	274	14000 (0.36)	223
17-EMF-TB27-1-1d	3140	82.4	12200	168	28.7	13.5	3880	806	1030	274	64700 (2.03)	223
17-EMF-TB27-1-2d	1810	82.4	12400	168	84.5	13.5	2140	806	1270	274	33100 (2.89)	223
17-EMF-TB27-1-7d	4450	82.4	29900	168	107	13.5	5810	806	5900	274	94200 (5.32)	223
17-EMF-TB27-1-14d	3530	82.4	29300	168	153	13.5	3800	806	6150	274	75100 (7.26)	223

Sample ID	Al (µg/L)		Ca (µg/L)		Mg (µg/L)		K (µg/L)		Si (µg/L)		Na (µg/L)	
	Result	EQL	Result	EQL	Result	EQL	Result	EQL	Result	EQL	Result	EQL
17-EMF-TB27-1-28d	4300	82.4	35400	168	70.3	13.5	5060	806	7990	274	95300 (9.72)	223
17-EMF-TB27-1-42d	3300	82.4	29400	168	90.8	13.5	3150	806	6810	274	60600 (11.29)	223
17-EMF-TB27-1-49d	2090	82.4	20300	168	164	13.5	1490	806	4760	274	25900 (11.96)	223
17-EMF-TB27-1-63d	2740	82.4	27000	168	124	13.5	2260	806	6220	274	43400 (13.08)	223
17-EMF-TB27-2-0.08d	610	82.4	902	168	ND	13.5	1570	806	ND	274	23500 (0.61)	223
17-EMF-TB27-2-1d	3040	82.4	11200	168	25.5	13.5	4170	806	1170	274	66400 (2.31)	223
17-EMF-TB27-2-2d	1470	82.4	10900	168	69.1	13.5	1880	806	984	274	28000 (3.04)	223
17-EMF-TB27-2-7d	4400	82.4	29100	168	101	13.5	5900	806	5660	274	94400 (5.47)	223
17-EMF-TB27-2-14d	3650	82.4	29400	168	108	13.5	4130	806	6310	274	77400 (7.46)	223
17-EMF-TB27-2-28d	4120	82.4	33500	168	64.3	13.5	4930	806	7490	274	91300 (9.81)	223
17-EMF-TB27-2-42d	3500	82.4	30200	168	94.9	13.5	3500	806	7050	274	66500 (11.52)	223
17-EMF-TB27-2-49d	2260	82.4	20300	168	159	13.5	1510	806	4770	274	27800 (12.24)	223
17-EMF-TB27-2-63d	2970	82.4	28700	168	130	13.5	2450	806	6630	274	47200 (13.45)	223
17-EMF-TB28-1-0.08d	121	82.4	4310	168	ND	13.5	1230	806	ND	274	11000 (0.28)	223
17-EMF-TB28-1-1d	1590	82.4	28000	168	ND	13.5	4240	806	865	274	51900 (1.61)	223
17-EMF-TB28-1-2d	1830	82.4	29700	168	21.2	13.5	3380	806	1780	274	41300 (2.66)	223
17-EMF-TB28-1-7d	3520	82.4	56000	168	28.8	13.5	9550	806	4330	274	118000 (5.67)	223
17-EMF-TB28-1-14d	3070	82.4	54200	168	34.6	13.5	7040	806	4720	274	96300 (8.13)	223

Sample ID	Al (µg/L)		Ca (µg/L)		Mg (µg/L)		K (µg/L)		Si (µg/L)		Na (µg/L)	
	Result	EQL	Result	EQL	Result	EQL	Result	EQL	Result	EQL	Result	EQL
17-EMF-TB28-1-28d	3700	82.4	58900	168	22.4	13.5	11600	806	4910	274	164000 (12.32)	223
17-EMF-TB28-1-42d	3060	82.4	52700	168	25.6	13.5	7110	806	4800	274	97200 (14.80)	223
17-EMF-TB28-1-49d	2280	82.4	43000	168	41.3	13.5	2870	806	4260	274	41200 (15.85)	223
17-EMF-TB28-1-63d	2970	82.4	51400	168	33.8	13.5	4550	806	5140	274	66500 (17.55)	223
17-EMF-TB28-2-0.08d	134	82.4	3410	168	ND	13.5	1100	806	ND	274	9310 (0.24)	223
17-EMF-TB28-2-1d	1770	82.4	29200	168	ND	13.5	4300	806	995	274	52400 (1.58)	223
17-EMF-TB28-2-2d	1460	82.4	24300	168	21	13.5	2970	806	1420	274	35300 (2.49)	223
17-EMF-TB28-2-7d	3390	82.4	52500	168	30.6	13.5	9150	806	4210	274	110000 (5.31)	223
17-EMF-TB28-2-14d	2930	82.4	51900	168	33.1	13.5	6770	806	4410	274	93200 (7.70)	223
17-EMF-TB28-2-28d	3650	82.4	65200	168	21.1	13.5	9050	806	5010	274	125000 (10.91)	223
17-EMF-TB28-2-42d	3060	82.4	57200	168	26.5	13.5	5710	806	4890	274	78800 (12.93)	223
17-EMF-TB28-2-49d	2150	82.4	42000	168	43.7	13.5	2160	806	4070	274	32600 (13.76)	223
17-EMF-TB28-2-63d	2790	82.4	49200	168	45.5	13.5	3790	806	4970	274	53100 (15.13)	223

Table A.8. Results of Alkalinity, Ammonia, Electrical Conductivity (EC), Oxidation-Reduction Potential (E_h), and pH in Leachates from EPA Method 1315 Tests

Sample ID	pH	E_h (mV) ^(a)		EC (mS/cm)		Alkalinity (µg/mL)		Ammonia (mg/L)	
		Result	EQL	Result	EQL	Result	EQL	Result	EQL
17-EMF-DI-BLK1-0.08d	6.51	394	-1000	0.0109	0.0100	ND	23.5	ND	0.500
17-EMF-DI-BLK1-1d	6.56	270	-1000	ND	0.0100	ND	23.5	ND	0.500
17-EMF-DI-BLK1-2d	6.83	285	-1000	ND	0.0100	ND	23.5	ND	0.500
17-EMF-DI-BLK1-7d	6.36	279	-1000	ND	0.0100	ND	23.5	ND	0.500
17-EMF-DI-BLK1-14d	5.80	270	-1000	ND	0.0100	ND	23.5	ND	0.500
17-EMF-DI-BLK1-28d	6.78	278	-1000	ND	0.0100	ND	23.5	ND	0.500
17-EMF-DI-BLK1-42d	6.28	286	-1000	ND	0.0100	ND	23.5	ND	0.500
17-EMF-DI-BLK1-49d	7.80	192	-1000	ND	0.0100	ND	23.5	ND	0.500
17-EMF-DI-BLK1-63d	6.13	271	-1000	ND	0.0100	ND	23.5	ND	0.500
17-EMF-DI-BLK2-0.08d	5.98	365	-1000	ND	0.0100	ND	23.5	ND	0.500
17-EMF-DI-BLK2-1d	6.57	270	-1000	ND	0.0100	ND	23.5	ND	0.500
17-EMF-DI-BLK2-2d	6.20	304	-1000	ND	0.0100	ND	23.5	ND	0.500
17-EMF-DI-BLK2-7d	6.04	288	-1000	ND	0.0100	ND	23.5	ND	0.500
17-EMF-DI-BLK2-14d	5.87	282	-1000	ND	0.0100	ND	23.5	ND	0.500
17-EMF-DI-BLK2-28d	6.14	290	-1000	ND	0.0100	ND	23.5	ND	0.500
17-EMF-DI-BLK2-42d	6.07	297	-1000	ND	0.0100	ND	23.5	ND	0.500
17-EMF-DI-BLK2-49d	6.78	238	-1000	ND	0.0100	ND	23.5	ND	0.500
17-EMF-DI-BLK2-63d	6.15	276	-1000	ND	0.0100	ND	23.5	ND	0.500
17-EMF-TB27-1-0.08d	10.6	168	-1000	0.143	0.0100	24.6	23.5	ND	0.500
17-EMF-TB27-1-1d	11.2	-12.5	-1000	0.566	0.0100	865	23.5	ND	0.500
17-EMF-TB27-1-2d	11.1	-32.9	-1000	0.459	0.0100	65.2	23.5	ND	0.500
17-EMF-TB27-1-7d	11.4	-53.2	-1000	0.976	0.0100	162	23.5	ND	0.500
17-EMF-TB27-1-14d	11.5	-51.1	-1000	0.826	0.0100	155	23.5	ND	0.500
17-EMF-TB27-1-28d	11.6	-56.6	-1000	1.01	0.0100	181	23.5	ND	0.500
17-EMF-TB27-1-42d	11.5	-41.6	-1000	0.752	0.0100	159	23.5	ND	0.500
17-EMF-TB27-1-49d	11.2	-18.6	-1000	0.400	0.0100	94.5	23.5	ND	0.500
17-EMF-TB27-1-63d	11.3	-32.2	-1000	0.574	0.0100	122	23.5	ND	0.500
17-EMF-TB27-2-0.08d	10.6	139	-1000	0.165	0.0100	33.5	23.5	ND	0.500
17-EMF-TB27-2-1d	11.3	-12.8	-1000	0.579	0.0100	104	23.5	ND	0.500
17-EMF-TB27-2-2d	11.1	-31.5	-1000	0.451	0.0100	52.1	23.5	ND	0.500
17-EMF-TB27-2-7d	11.4	-54.0	-1000	1.02	0.0100	160	23.5	ND	0.500
17-EMF-TB27-2-14d	11.5	-53.2	-1000	0.850	0.0100	153	23.5	ND	0.500
17-EMF-TB27-2-28d	11.6	-55.8	-1000	1.03	0.0100	187	23.5	ND	0.500
17-EMF-TB27-2-42d	11.5	-44.8	-1000	0.748	0.0100	150	23.5	ND	0.500

Sample ID	pH	E_h (mV) ^(a)		EC (mS/cm)		Alkalinity ($\mu\text{g/mL}$)		Ammonia (mg/L)	
		Result	EQL	Result	EQL	Result	EQL	Result	EQL
17-EMF-TB27-2-49d	11.2	-20.8	-1000	0.407	0.0100	97.4	23.5	ND	0.500
17-EMF-TB27-2-63d	11.4	-34.9	-1000	0.606	0.0100	128	23.5	ND	0.500
17-EMF-TB28-1-0.08d	10.8	130	-1000	0.159	0.0100	35.2	23.5	ND	0.500
17-EMF-TB28-1-1d	11.6	-18.2	-1000	0.873	0.0100	159	23.5	ND	0.500
17-EMF-TB28-1-2d	11.5	-19.4	-1000	0.720	0.0100	142	23.5	ND	0.500
17-EMF-TB28-1-7d	11.8	-48.9	-1000	1.76	0.0100	395	23.5	ND	0.500
17-EMF-TB28-1-14d	11.9	-35.9	-1000	1.55	0.0100	350	23.5	ND	0.500
17-EMF-TB28-1-28d	12.0	-55.3	-1000	2.16	0.0100	367	23.5	ND	0.500
17-EMF-TB28-1-42d	12.0	-35.4	-1000	1.56	0.0100	300	23.5	ND	0.500
17-EMF-TB28-1-49d	11.6	-16.4	-1000	0.837	0.0100	182	23.5	ND	0.500
17-EMF-TB28-1-63d	11.7	-19.5	-1000	1.18	0.0100	240	23.5	ND	0.500
17-EMF-TB28-2-0.08d	10.7	115	-1000	0.135	0.0100	31.0	23.5	ND	0.500
17-EMF-TB28-2-1d	11.6	-20.8	-1000	0.876	0.0100	148	23.5	ND	0.500
17-EMF-TB28-2-2d	11.4	-15.0	-1000	0.620	0.0100	118	23.5	ND	0.500
17-EMF-TB28-2-7d	11.8	-46.0	-1000	1.62	0.0100	356	23.5	ND	0.500
17-EMF-TB28-2-14d	11.9	-36.8	-1000	1.49	0.0100	292	23.5	ND	0.500
17-EMF-TB28-2-28d	11.9	-28.0	-1000	1.77	0.0100	365	23.5	ND	0.500
17-EMF-TB28-2-42d	11.9	-28.4	-1000	1.38	0.0100	287	23.5	ND	0.500
17-EMF-TB28-2-49d	11.6	-17.3	-1000	0.743	0.0100	168	23.5	ND	0.500
17-EMF-TB28-2-63d	11.7	-19.4	-1000	1.04	0.0100	219	23.5	ND	0.500

(a) E_h values are not SHE corrected. Add +211 mV to SHE correct these values.

A.4 Cumulative Release Plots for ^{99}Tc , ^{127}I , and Na^+ from EPA Method 1315 Results Leach Tests

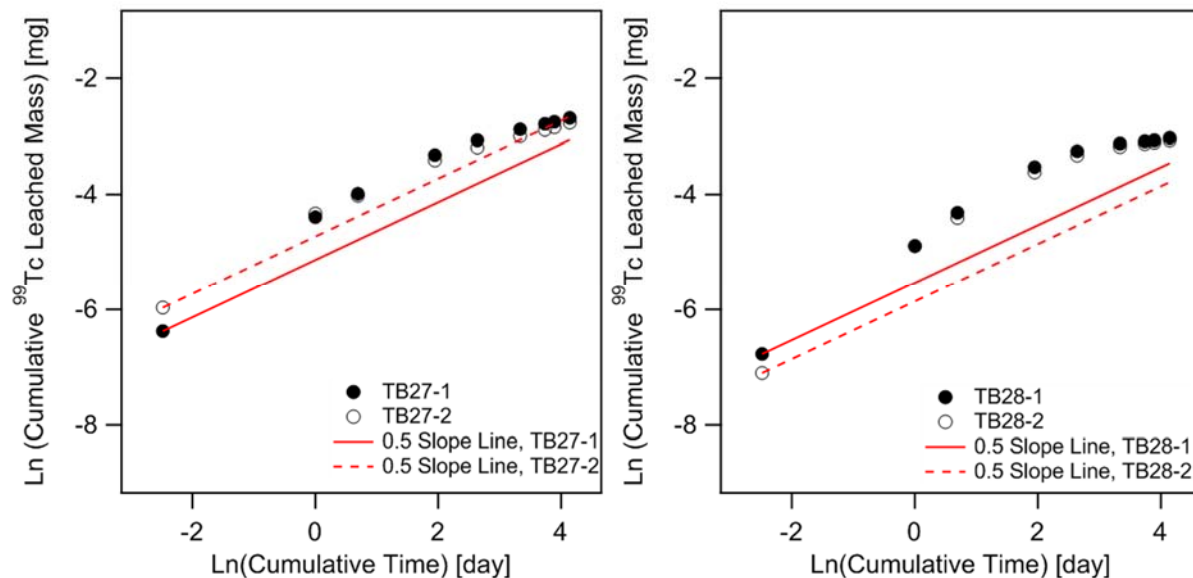


Figure A.29. Logarithm of the cumulative ^{99}Tc release plotted vs. the logarithm of cumulative time for monoliths leached for 63 days in deionized water (DIW) using EPA Method 1315 leach testing. The red line has a slope of 0.5 and models a diffusion controlled release mechanism.

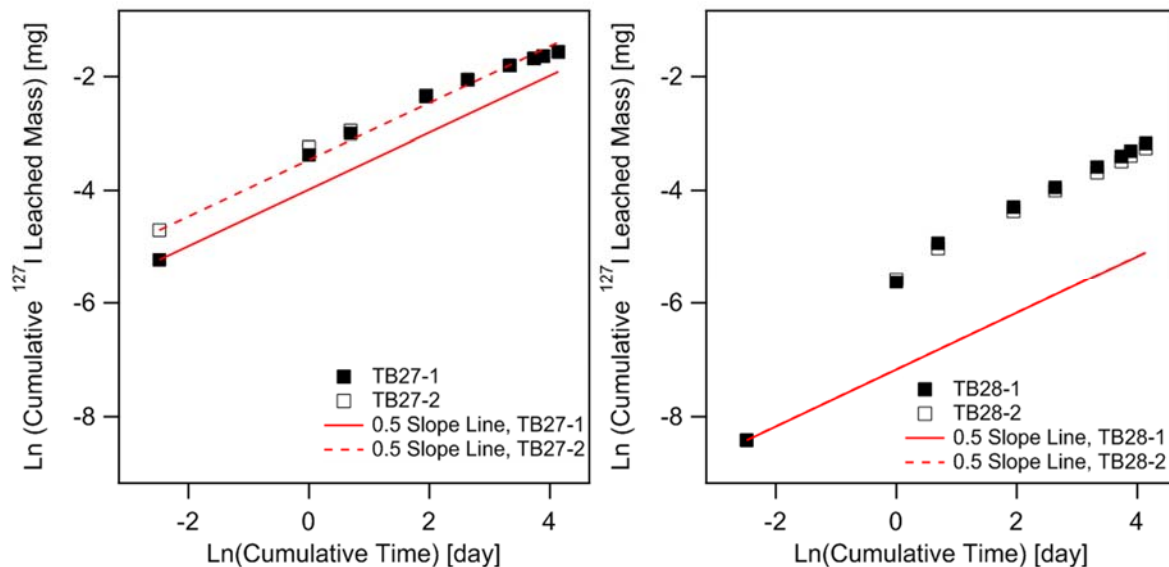


Figure A.30. Logarithm of the cumulative ^{127}I release plotted vs. the logarithm of cumulative time for monoliths leached for 63 days in DIW using EPA Method 1315 leach testing. The red line has a slope of 0.5 and models a diffusion controlled release mechanism.

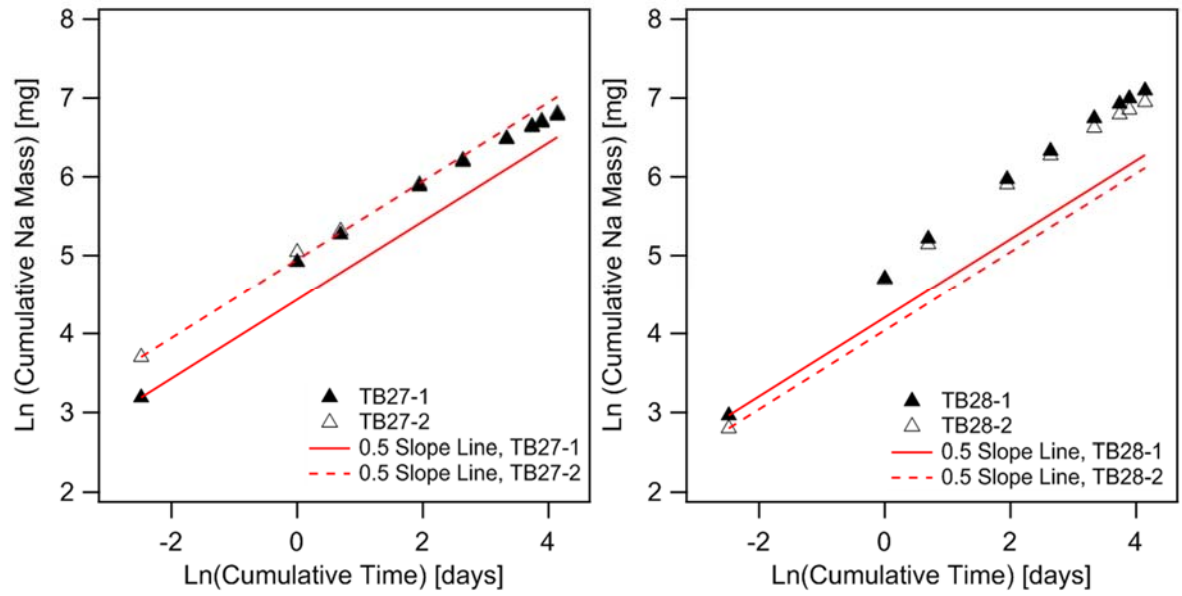


Figure A.31. Logarithm of the cumulative Na^+ release plotted vs. the logarithm of cumulative time for monoliths leached for 63 days in DIW using EPA Method 1315 leach testing. The red line has a slope of 0.5 and models a diffusion controlled release mechanism.

Distribution*

**No. of
Copies**

**No. of
Copies**

OFFSITE

ONSITE

Oak Ridge National Laboratory

EM Pierce

Pacific Northwest National Laboratory

M Asmussen

NK Qafoku

Savannah River National Laboratory

RL Russell

AD Cozzi

SA Saslow

G Flach

GL Smith

KM Fox

MMV Snyder

CC Herman

W Um

DI Kaplan

G Wang

CA Langton

JH Westsik, Jr.

DJ McCabe

BD Williams

RR Seitz

SB Yabusaki

Washington River Protection Solutions

Project File

EE Brown

Information Release (PDF)

SE Kelly

KP Lee (AREVA)

Ridha Mabrouki

PL Rutland

KH Subramanian

DJ Swanberg

JR Vitali

WRPS Documents-TOCVND@rl.gov

INTERA

R Andrews

M Apted

R Arthur

R Senger

*All distribution will be made electronically.



Pacific Northwest
NATIONAL LABORATORY

*Proudly Operated by **Battelle** Since 1965*

902 Battelle Boulevard
P.O. Box 999
Richland, WA 99352
1-888-375-PNNL (7665)

U.S. DEPARTMENT OF
ENERGY

www.pnnl.gov